Staff working paper / Document de travail du personnel—2026-33

Last updated: September 18, 2026

A New Approach to Estimating Portfolio-Balance Models of the Yield Curve

Antonio Diez de los Rios
Markets and Banking Department
Bank of Canada
adiez@bank-banque-canada.ca

DOI: https://doi.org/10.34989/swp-2026-33 | ISSN 1701-9397

A New Approach to Estimating Portfolio-Balance Models of the Yield Curve*

Antonio Diez de los Rios
Bank of Canada
diez@bankofcanada.ca

August 2026

Abstract

We show that the parameters of a broad class of portfolio-balance models can be recovered from estimates of Gaussian dynamic term structure models (GDTSMs) using a two-step estimator that bypasses the fixed-point problem that characterizes portfolio-balance models. Specifically, we develop a novel canonical representation of bond supply in terms of factor-mimicking portfolios, whose returns replicate the structural shocks to the pricing factors. We identify these structural shocks by assuming that each shock corresponds to a distinct, mutually exclusive dimension of bond-supply variation. Using U.S. Treasury yields and macroeconomic data, we show the recovered shocks admit interpretations as hedging-risk-premium, risk-bearing-capacity, and monetary-policy shocks.

JEL Classification: E43, E44, G12, H63
Keywords: government debt maturity structure, rational expectations equilibrium, structural shocks, term premia.

*I would like to thank Andreas Uthemann, Jonathan Witmer, and seminar participants at the Bank of Canada for their comments. Any remaining errors are my own. The views expressed in this paper are those of the author and do not necessarily reflect those of the Bank of Canada.

1 Introduction

Over the past two decades, central banks' large-scale asset purchases (LSAPs) have brought preferred-habitat and portfolio-balance models of the yield curve to the centre of modern macro-finance as a coherent framework for tracing how changes in the level and maturity of nominal government debt affect asset prices and macroeconomic outcomes.[1] Crucially, the same mechanisms that underpin LSAPs have become central again as public debt levels have risen (see, e.g., Hernández de Cos, 2025) and debt-management policies have become more active (see Miran and Roubini, 2024), renewing interest in how the maturity structure of government debt interacts with the financial markets' capacity to absorb it. Yet, estimating and identifying portfolio-balance supply effects from yields remains challenging.

Despite this renewed interest in bond supply-and-demand forces, most empirical yield-curve work in macro-finance still relies on Gaussian dynamic term structure models (GDTSMs) estimated on yields and macro data without modelling bond supply and demand explicitly (see, e.g., Ang and Piazzesi, 2003; Joslin, Le, and Singleton, 2013; Joslin, Priebsch, and Singleton, 2014; and Backus, Chernov, Zin, and Zviadadze, 2022). This dominance reflects the conceptual and practical advantages of GDTSMs. They characterize the joint distribution of yields (and, when applicable, macroeconomic variables), making them well-suited for likelihood-based inference and, therefore, provide a tractable framework for empirical work (see, e.g., Joslin, Singleton, and Zhu, 2011; hereafter JSZ). In fact, most of the empirical work on the portfolio-balance effects of LSAPs infers them from changes in the term-premium component of long-term bond yields around LSAP announcements, where term premia are estimated using GDTSMs (see, e.g., Gagnon et al., 2011; Christensen and Rudebusch, 2012; and Bauer and Rudebusch, 2014).

[1] In fact, central banks have repeatedly justified the use of LSAP programs by directly appealing to these theories of the yield curve (see, e.g., Williams, 2011; Yellen, 2011a; Yellen, 2011b; Stein, 2012; and Potter, 2013).

On the other hand, modern formulations of preferred-habitat and portfolio-balance models feature risk-averse arbitrageurs who absorb an increase in the supply of long-term nominal bonds only if compensated by higher expected returns (see Greenwood and Vayanos, 2014; and Vayanos and Vila, 2009, 2021; hereafter GV and VV).[2] However, this required compensation depends on the overall riskiness of the arbitrageurs' portfolio: the equilibrium riskiness depends on how strongly yields respond to absorb supply shocks, which, in turn, is pinned down by the required compensation. This feedback loop gives rise to a fixed-point problem that may admit multiple solutions or fail to converge, thereby weakening any one-to-one mapping from structural primitives to observed yields that underlies likelihood- or moment-based estimation. As a result, direct estimation of portfolio-balance models in yield-curve analysis has remained limited.

Motivated by these challenges in estimating portfolio-balance models of the yield curve, this paper presents a novel approach that exploits the observational equivalence between the portfolio-balance equilibrium and a GDTSM. Through this equivalence, we map GDTSM parameter estimates into portfolio-balance primitives, thereby bypassing the fixed-point problem and enabling tractable estimation of bond-supply parameters.

We make five contributions to the empirical yield-curve modelling literature. First, we introduce a general class of discrete-time portfolio-balance models and show that, as in Hamilton and Wu (2012b), its equilibrium yield dynamics are observationally equivalent to those of a GDTSM. The model features arbitrageurs with expected utility over real wealth and a stochastic supply of nominal government bonds that is affine in a set of state variables whose physical dynamics follow a structural vector autoregression (SVAR). Under the standard assumption that arbitrageurs are not too risk-averse and that the physical dynamics of the state variables are stationary, we provide conditions for the existence, uniqueness, and

[2] See Greenwood, Hanson, and Vayanos (2024) for a recent review of this literature.

stability of the equilibrium.

Second, we exploit the observational equivalence with GDTSMs and existence of a unique equilibrium to study the identification in this class of portfolio-balance models using the principle that if two different sets of portfolio-balance parameter values yield identical GDTSM parameters, the observed data cannot distinguish between them.[3] We show that, in the absence of additional restrictions, the model is generically underidentified. However, the identification of the parameters of the portfolio-balance model can be restored by assuming that a small number of factors drive the supply of nominal bonds and that the arbitrageurs' risk aversion is known.

In practice, this factor structure still leaves open how to interpret the supply factors and choose their loadings, since bond-supply specifications that imply the same prices of risk are observationally equivalent. We solve this by constructing factor-mimicking portfolios of bonds whose unexpected excess returns replicate the structural shocks driving the pricing factors, and setting the supply loadings equal to these portfolio weights. Importantly, this factor-mimicking specification provides a canonical representation of bond supply within each class of specifications that imply the same prices of risk.

Further, we show that imposing the orthogonality condition that each structural shock corresponds to a distinct, mutually exclusive dimension of bond-supply variation identifies the structural shocks in the SVAR. For example, consider a model with a "level" bond-supply shock that raises quantities broadly across maturities (an aggregate bond-supply shift) and a "slope" shock that changes the maturity composition of the outstanding debt (e.g., issuance tilts from short to long) while holding the aggregate bond supply fixed. In such a model, this "quantity" orthogonality condition would ensure that (i) innovations to the level factor change the aggregate supply of long-term bonds, holding fixed the differences in supply

[3] See, e.g., Hamilton and Wu (2012a), who apply this general econometric principle dating back to Fisher (1966) and Rothenberg (1971) to study the identification of GDTSMs.

across maturities, and (ii) innovations to the slope factor reallocate supply across maturities without changing the aggregate supply of long-term bonds.

Third, we translate the equivalence and identification results into a tractable two-step estimator. In the first step, we estimate a GDTSM by maximum likelihood to recover the physical and risk-neutral state dynamics using the JSZ approach. In the second step, we map the estimated GDTSM parameters into (i) portfolio-balance bond-supply parameters and (ii) the SVAR impact matrix implied by the portfolio-balance restrictions. As a result, this approach retains GDTSMs' empirical flexibility and computational simplicity while delivering estimates of the portfolio-balance model that are otherwise difficult to obtain directly.

Fourth, we implement our framework empirically using U.S. Treasury yields and macroeconomic data. We estimate a three-factor GDTSM and use the mapping between GDTSMs and portfolio-balance models to recover the model-implied dynamics of bond supply and structural shocks consistent with the observed yield curve. To anchor arbitrageurs' risk aversion, we calibrate it so that the model-implied price effects of large-scale asset purchases match the observed response of long-term yields to Federal Reserve asset purchase announcements.

Our estimates yield three economically interpretable shocks. The first shock resembles the hedging-risk-premium shock in Cieslak and Pang (2021): an aggregate demand shock that affects the long end of the curve more strongly than the short end, induces a positive correlation between the term premium and economic activity, and tends to take its most negative values during "flight-to-safety" episodes. The second shock resembles a risk-bearing-capacity shock similar to that in Gertler and Karadi (2011): an aggregate demand shock that affects the long end of the curve more strongly than the short end, but that instead induces a negative correlation between the term premium and economic activity, and tends to take its most negative realizations during periods of financial crisis in which term premia rise even as monetary policy eases. The third shock resembles a traditional monetary-policy shock (Christiano, Eichenbaum, and Evans, 1999). Importantly, we do not seem to identify any aggregate supply shock. We attribute this result to the fact that, over recent decades, the Federal Reserve has tended to respond much less strongly to aggregate supply-driven inflation (see Hofmann, Manea, and Mojon, 2024), thereby making aggregate supply-side shocks a less important risk for bondholders.

Finally, we use the recovered portfolio-balance parameters to decompose the sources of yield-curve fluctuations and the implied conduct of monetary policy in the U.S. Our variance decompositions show that the hedging-risk-premium shock largely drives movements in long-term yields and term premia. The short rate is primarily influenced by monetary policy and shocks to the financial intermediaries' risk-bearing capacity. Separately, exploiting the identified structural monetary-policy shock, we infer the Federal Reserve's monetary-policy rule implied by the term structure. Although imprecisely estimated, the implied rule suggests a systematic monetary-policy component that "looks through" short-term fluctuations in inflation but responds more than proportionally to changes in future inflation expectations.

Related Literature. Our paper is closely related to Hamilton and Wu (2012b), who demonstrate that portfolio-balance models may serve as a foundation for the specification of the affine price of risk in GDTSMs. We build on, and substantially extend, this insight in three ways. First, we establish observational equivalence for a more general class of discrete-time macro portfolio-balance models, restoring a well-defined mapping from primitives to yields, and provide the conditions under which the portfolio-balance equilibrium exists, is unique, and is stable. Second, we exploit this well-posed equilibrium to explicitly analyze identification, showing that the model is generically underidentified in the absence of additional structure and that economically motivated restrictions recover identification of the portfolio-balance parameters and structural shocks. Third, we derive a one-to-one mapping that allows portfolio-balance parameters to be recovered directly from standard GDTSM likelihood estimates via a tractable two-step procedure.

Our paper is also related to a small literature on empirical term-structure models that incorporate supply and demand factors. Li and Wei (2013), motivated by VV's preferred-habitat framework, estimate a GDTSM that augments standard yield-curve factors with Treasury and agency MBS supply factors. They then use the estimated model to quantify the term-premium effects of the Federal Reserve's LSAP programs. Relative to our approach, their strategy is reduced-form: bond supply enters the GDTSM as an additional state variable, rather than being pinned down by an explicit equilibrium mapping from supply primitives and arbitrageurs' demand to yields. Kaminska and Zinna (2020) estimate a structural term-structure model of U.S. real rates, in which arbitrageurs accommodate demand pressures from domestic and foreign official investors. More recently, Jansen, Li, and Schmid (2025) use a novel dataset of sector-level U.S. Treasury holdings to estimate maturity-specific demand functions and elasticities across different investors using the granular empirical estimation of Koijen and Yogo (2019), and integrate these into a VV model of the Treasury market with risk-averse arbitrageurs. Our paper instead asks how far one can go in estimating and structurally identifying a general class of portfolio-balance models using only yields and macro data, without observing bond quantities directly. This different objective makes our paper complementary to theirs. Importantly, a key implication of our identification exercise is that investor elasticities are not necessarily pinned down by the cross-section of yields alone, thereby providing a rationale for estimating them using a granular demand-based system that exploits bond holdings and time-series variation.

More broadly, our paper relates to the broader preferred-habitat and portfolio-balance literature on supply-and-demand forces in bond markets (Tobin, 1958, 1969; Modigliani and

Sutch, 1966; Vayanos and Vila, 2009, 2021; Greenwood and Vayanos, 2014), and to recent efforts to extend them beyond the baseline nominal government bond yield curve. King (2019) incorporates a zero lower bound (ZLB) on the short-term nominal rate into the VV framework. Greenwood, Hanson, and Liao (2018) and Hanson, Lucca, and Wright (2021) introduce slow-moving arbitrage into the portfolio-balance framework, which can strengthen the short-run price impact of supply shocks and generate stock–flow distinctions that matter for interpreting the effect of LSAP programs. He, Nagel, and Song (2022) and Hanson, Malkhozov, and Venter (2024) introduce balance-sheet costs to further limit arbitrageurs' ability to absorb bond-supply shocks. Jappelli, Pelizzon, and Subrahmanyam (2023) further extend the VV framework by introducing frictions in the repo market. Costain, Nuño, and Thomas (2025) explicitly introduce default risk into a VV-style model. Ray (2019) and Ray, Droste, and Gorodnichenko (2024) embed a VV preferred-habitat model of the yield curve within a New Keynesian macroeconomic model. Diez de los Rios (2025) proposes a portfolio-balance model in which both inflation and the yield curve are determined through an interest rule that satisfies the Taylor principle. Greenwood, Hanson, Stein, and Sunderam (2023) and Gourinchas, Ray, and Vayanos (2025) embed the portfolio-balance mechanism in an open-economy environment by linking term premia to exchange-rate dynamics and monetary-policy spillovers through currency risk premia.

Paper outline. Section 2 lays out the macro portfolio-balance model, introduces the state variables and bond-supply structure, characterizes equilibrium, and establishes the observational equivalence with GDTSMs. Section 3 develops the parameter mapping, identification restrictions, and two-step estimation procedure. Section 4 describes the data and the maximum-likelihood estimation of the GDTSM. Section 5 reports the recovered portfolio-balance parameters and interprets the identified structural shocks via impulse responses. Section 6 presents the variance decompositions. Section 7 derives and estimates the monetary-policy rule implied by the term structure. Section 8 concludes.

2 A Macro Portfolio-Balance Model of the Yield Curve

This section presents a portfolio-balance macro term-structure model similar to that in Diez de los Rios (2025), in which market-clearing between bond supply and demand jointly determines bond risk premia. We show that equilibrium excess returns and prices of risk depend on the exposure of the arbitrageurs' portfolio to the structural shocks and the term structure of bond supply. We then prove that the equilibrium bond dynamics can be recast as a GDTSM with affine prices of risk, providing a direct mapping between the portfolio-balance primitives and the familiar GDTSM parameters. This mapping is the key step that enables us to later recover the portfolio-balance parameters from GDTSM estimates.

2.1 State variables

We assume that the state of the economy is described by an $(M \times 1)$ vector of state variables, $\mathbf{x}_t$. The dynamic evolution of the state variables under the physical measure, $\mathbb{P}$, is given by a Gaussian SVAR(1) process:

$$\mathbf{x}_{t+1} = \mathbf{\Phi}_{x0} + \mathbf{\Phi}_{xx}\mathbf{x}_t + \mathbf{\Sigma}_x \boldsymbol{\eta}_{t+1}, \tag{2.1}$$

where, to guarantee the stationarity of the dynamics of the pricing factors, the eigenvalues of $\mathbf{\Phi}_{xx}$ lie inside the unit circle in the complex plane. Further, we assume that $\mathbf{\Sigma}_x$ is non-singular and that $\boldsymbol{\eta}_{t+1} \sim iid\ N(0, \mathbf{I}_M)$ where $\mathbf{I}_M$ is the $(M \times M)$ identity matrix. To simplify the notation, we will often replace $\mathbf{\Sigma}_x \boldsymbol{\eta}_{t+1}$ by the reduced-form shocks $\boldsymbol{\varepsilon}_{x,t+1}$ below. Consequently, we have that $\boldsymbol{\varepsilon}_{x,t+1} \sim iid\ N(0, \mathbf{\Omega}_{xx})$, where $\mathbf{\Omega}_{xx} = \mathrm{Var}_t(\boldsymbol{\varepsilon}_{x,t+1}) = \mathbf{\Sigma}_x \mathbf{\Sigma}_x'$ is a symmetric positive definite matrix.

Note that, since structural shocks can, in principle, affect more than one variable, we do not necessarily restrict $\mathbf{\Sigma}_x$ to be lower triangular (i.e., a recursive identification of the structural shocks using a Cholesky decomposition). Indeed, we show below that our portfolio-balance model imposes additional restrictions that identify the M^2 elements of the matrix $\mathbf{\Sigma}_x$.

2.2 Macroeconomic variables

Similar to Backus, Chernov, Zin, and Zviadadze (2022; hereafter BCZZ), we further assume that the rate of inflation prevailing in the economy between time $t-1$ and t, π_t, and the rate of growth of aggregate real output g_t are both affine functions of the vector of state variables:

$$\pi_t = p_{x0} + \mathbf{p}_x' \mathbf{x}_t, \tag{2.2}$$

$$g_t = g_{x0} + \mathbf{g}_x' \mathbf{x}_t, \tag{2.3}$$

where $\pi_t = \log(P_t/P_{t-1})$ and P_t denotes the price level in the economy, and where $g_t = \log(Y_t/Y_{t-1})$, and Y_t is the level of real output.

Note that since $\mathbf{x}_t$ is stationary, both inflation and output growth are assumed to be stationary as well (though they can be highly persistent).

2.3 Assets

Short-term nominal bond. Let $B_t^{(1)}$ be the nominal price (i.e., in dollars) at time t of a one-period zero-coupon bond, $b_t^{(1)} \equiv \log[B_t^{(1)}]$ be its log price, and $i_t = -b_t^{(1)}$ be the short-term nominal interest rate in this economy, which we assume to be affine in the vector of state variables:

$$i_t = \delta_{x0} + \boldsymbol{\delta}_x' \mathbf{x}_t. \tag{2.4}$$

The one-period zero-coupon bond pays one dollar at time $t+1$. Therefore, its real gross return from t to $t+1$ is given by $R_{t+1}^{(1)} = \frac{1}{B_t^{(1)}} \times \frac{P_t}{P_{t+1}}$, which in log form can be expressed as $r_{t+1}^{(1)} \equiv \log\left[R_{t+1}^{(1)}\right] = i_t - \pi_{t+1}$, while its log excess return over the short-term real interest rate, r_t, from time t to $t+1$ is given by

$$rx_{t+1}^{(1)} = i_t - \pi_{t+1} - r_t. \tag{2.5}$$

Note that, even though the nominal and real short-term interest rates are known at time t, one-period nominal bonds are risky because inflation is stochastic. Specifically, nominal bonds suffer a real loss when inflation (unexpectedly) increases.

In addition to the one-period nominal bond, we further assume that arbitrageurs can invest in a set of n-period (default-free) nominal zero-coupon bonds with maturities $n = 2, \ldots, N$. Consistent with the notation for the one-period nominal bond, we denote the nominal price (i.e., in dollars) at time t of an n-period nominal zero-coupon bond that pays 1 dollar at date $t+n$ by $B_t^{(n)}$, its log price by $b_t^{(n)} \equiv \log B_t^{(n)}$, and its (log) yield by $y_t^{(n)} \equiv -b_t^{(n)}/n$. Specifically, let the gross real return on the n-period nominal zero-coupon bond be $R_{t+1}^{(n)} = \frac{B_{t+1}^{(n-1)}}{B_t^{(n)}} \times \frac{P_t}{P_{t+1}}$ for $n = 1, \ldots, N$, where $B_{t+1}^{(0)} = 1$ given that a nominal one-period zero-coupon bond pays 1 dollar at date $t+1$.

The log real return on the n-period nominal zero-coupon bond is given by $r_{t+1}^{(n)} \equiv \log\left[R_{t+1}^{(n)}\right] = b_{t+1}^{(n-1)} - b_t^{(n)} - \pi_{t+1}$, for $n = 1, \ldots, N$, while its log excess return over the short-term real interest rate from time t to $t+1$ is

$$rx_{t+1}^{(n)} = b_{t+1}^{(n-1)} - b_t^{(n)} - \pi_{t+1} - r_t, \qquad \text{for } n = 1, \ldots, N. \tag{2.6}$$

Note that equation (2.6) collapses to equation (2.5) in the previous section for the case of $n = 1$ given that $b_{t+1}^{(0)} = 0$ and $i_t \equiv -b_t^{(1)}$.

Similar to one-period nominal bonds, nominal long-term bonds are subject to inflation risk in that the holder of a nominal long-term bond suffers a capital loss in real terms when inflation increases. In addition, nominal long-term bonds are subject to interest-rate risk because they suffer a capital loss if short-term nominal interest rates rise unexpectedly (even if inflation remains constant).

We also define the log nominal return on the n-period nominal zero-coupon bond in excess of the short-term nominal interest rate:

$$\widetilde{rx}_{t+1}^{(n)} = b_{t+1}^{(n-1)} - b_t^{(n)} - i_t, \qquad \text{for } n = 2, \ldots, N, \tag{2.7}$$

where the log nominal return on the n-period nominal zero-coupon bond in excess of the short-term nominal interest rate satisfies $\widetilde{rx}_{t+1}^{(n)} = rx_{t+1}^{(n)} - rx_{t+1}^{(1)}$. Moreover, taking expectations on (2.7) yields a difference equation which can be iterated forward to obtain the traditional decomposition of the yield of the n-period nominal zero-coupon bond into an expectations and a term-premium component:

$$y_t^{(n)} = \underbrace{\frac{1}{n}\left[\sum_{k=0}^{n-1} \mathrm{E}_t\left(i_{t+k}\right)\right]}_{\text{Expectations component}} + \underbrace{\frac{1}{n}\left[\sum_{k=0}^{n-1} \mathrm{E}_t\left(\widetilde{rx}_{t+k+1}^{(n-k)}\right)\right]}_{\text{Term premium}}. \tag{2.8}$$

The first term in equation (2.8) is the average path of expected future nominal short rates, while the second term is the (nominal) term premium.

Specifically, we assume that the log bond prices are affine functions of the state variables, $\mathbf{x}_t$:

$$b_t^{(n)} = -b_{x0}^{(n)} - \mathbf{b}_x^{(n)\prime}\mathbf{x}_t \qquad \text{for } n = 1, \ldots, N, \tag{2.9}$$

and therefore the zero-coupon bond yields are also affine in the state variables:

$$y_t^{(n)} = a_{x0}^{(n)} + \mathbf{a}_x^{(n)\prime}\mathbf{x}_t \qquad \text{for } n = 1, \ldots, N, \tag{2.10}$$

with $a_{x0}^{(n)} = b_{x0}^{(n)}/n$ and $\mathbf{a}_x^{(n)} = \mathbf{b}_x^{(n)}/n$.

Short-term real interest rate. Finally, and in line with our log-linear specification, we assume that the real short-term interest rate, r_t, is related to the set of state variables through the following affine relationship:

$$r_t = \rho_{x0} + \boldsymbol{\rho}_x' \mathbf{x}_t. \tag{2.11}$$

Our specification nests different cases, such as (i) a constant real short-term interest rate, (ii) a Gaussian AR(1) process, or (iii) the possibility that the short real rate depends on all or a subset of the state variables driving the economy and financial markets.

2.4 Arbitrageurs

As in GV, we assume that the government issues nominal bonds, and that arbitrageurs and other investors trade them. We assume that arbitrageurs choose a portfolio allocation over nominal bonds that maximizes their expected utility given their real wealth. Specifically, we assume that arbitrageurs have power utility with a (constant) coefficient of relative risk aversion γ. Therefore, the arbitrageurs' portfolio choice problem can be expressed as

$$\max_{\left\{d_t^{(n)}\right\}_{n=1}^N} \frac{\mathrm{E}_t W_{t+1}^{1-\gamma} - 1}{1-\gamma}, \tag{2.12}$$

where $d_t^{(n)}$ is the portfolio weight in the nominal n-period zero-coupon bond and W_{t+1} denotes the arbitrageurs' real wealth at time $t+1$. Let $\mathrm{E}_t[\cdot]$ denote the conditional expectation operator given the information available at time t.

The arbitrageurs' real wealth evolves across time according to the following budget constraint:

$$\frac{W_{t+1}}{W_t} = R_{t+1}^{(p)} = \sum_{n=1}^N d_t^{(n)} R_{t+1}^{(n)} + \left[1 - \sum_{n=1}^N d_t^{(n)}\right] R_{t+1}^{(r)}, \tag{2.13}$$

where $R_{t+1}^{(p)}$ is the gross real return on the arbitrageurs' portfolio, and $R_{t+1}^{(r)} \equiv \exp(r_t)$ is the gross real return from investing in the short-term real bond. Note that the portfolio weight invested in the real one-period bond is given by $d_t^{(r)} = 1 - \sum_{n=1}^N d_t^{(n)}$.

Following Campbell and Viceira (2002), we solve the arbitrageurs' portfolio choice problem by assuming that the gross return on the arbitrageurs' portfolio, $R_{t+1}^{(p)}$, is conditionally lognormal (an assumption that we will verify below), which implies that the arbitrageurs' real wealth at time $t+1$ is conditionally lognormal as well. Specifically, approximating the portfolio return in (2.13) using a second-order Taylor approximation and taking derivatives with respect to the portfolio weights, $\mathbf{d}_t = \left[d_t^{(1)}, d_t^{(2)}, \ldots, d_t^{(N)}\right]'$, we arrive at the following first-order condition for the arbitrageurs' portfolio choice problem:

$$\mathrm{E}_t rx_{t+1}^{(n)} + \frac{1}{2}\mathrm{Var}_t\left[rx_{t+1}^{(n)}\right] = \gamma \sum_{j=1}^{N} \mathrm{Cov}_t\left[rx_{t+1}^{(n)}, rx_{t+1}^{(j)}\right] d_t^{(j)} \qquad \text{for } n = 1, \ldots, N, \tag{2.14}$$

when specialized to the case of the excess return on the n-period zero-coupon bond.[4] Note that this solution is equivalent to the multiple-asset mean-variance solution once we convert from log returns to simple returns.[5]

2.5 Bond supply

We model the supply of nominal long-term government bonds, net of other investors' demand, as an affine function of the state variables, $\mathbf{x}_t$. Specifically, we assume that the value (in real terms) of the net supply at time t of a nominal bond with maturity n available to the arbitrageur is given by $s_t^{(n)} W_t$, where

$$s_t^{(n)} = s_{x0}^{(n)} + \mathbf{s}_x^{(n)\prime} \mathbf{x}_t, \qquad \text{for } n = 2, \ldots, N. \tag{2.15}$$

Once more, our specification nests different cases, such as (i) a constant supply of nominal bonds, (ii) the case that the net supply of nominal bonds available to the arbitrageurs is exogenous, price-inelastic, and described by a one-factor model (see GV), and (iii) the case that there is a preferred-habitat sector with demand functions that are linear and decreasing

[4] Campbell and Viceira (2002) note that this Taylor approximation is exact in continuous time, given that higher-order terms converge to zero over shorter and shorter time intervals.

[5] As in the case of the portfolio-balance models of GV, VV, and Greenwood, Hanson, and Liao (2018), the arbitrageurs trade off mean against variance in the portfolio return. However, in our setup, the relevant mean return for arbitrageurs with power utility is the mean simple return (as in Campbell and Viceira, 2002). See Diez de los Rios (2025) for a detailed derivation of the arbitrageurs' portfolio choice problem.

in the (log) price of the nominal bond (see VV).[6]

For simplicity and expositional ease, we further assume that the one-period real bond is in zero net supply and that there is no preferred-habitat sector for this bond: $s_t^{(r)} = \overline{s}^{(r)} = 0$.[7]

Finally, we assume that the central bank can control the supply of nominal short-term bonds such that, in equilibrium, nominal short-term interest rates are consistent with the short-term interest rate in equation (2.4).

2.6 Equilibrium

As in VV, GV, and Greenwood, Hanson, and Liao (2018), we solve for a rational-expectations solution to the model. Specifically, we solve for the endogenous real short-term rate and nominal bond price equilibrium processes that are consistent with:

1. the inflation process given by equation (2.2)
2. the nominal short rate in equation (2.4),
3. equilibrium in the nominal bond market (i.e., $d_t^{(n)} = s_t^{(n)}$ for all $n = 2, \ldots, N$), and
4. equilibrium in the real bond market (i.e., $d_t^{(r)} = 0$).

2.6.1 Excess returns on nominal zero-coupon bonds

We start by substituting the expressions for the inflation rate, the (log) bond prices, and the real short-term rate in equations (2.2), (2.9), and (2.11) into the excess-return equations

[6] Specifically, consider the case that log bond prices are affine in the set of state variables, $b_t^{(n)} = -b_{x0}^{(n)} - \mathbf{b}_x^{(n)'}\mathbf{x}_t$ as we conjecture above (cf. equation 2.10). If we then assume, as in VV, that (i) the nominal bonds are in zero net supply and that (ii) the demand for the n-period nominal bond coming from the preferred-habitat sector is linear and decreasing in the log bond price, $d_{PH,t}^{(n)} = \alpha_0^{(n)} + \alpha_b^{(n)} b_t^{(n)}$ with $\alpha_b^{(n)} < 0$, we have that $s_{x0}^{(n)} = -\alpha_0^{(n)} + \alpha_b^{(n)} b_{x0}^{(n)}$ and $\mathbf{s}_x^{(n)} = \alpha_b^{(n)} \mathbf{b}_x^{(n)}$. Note that, while we have assumed that the intercepts in the demand of the preferred-habitat sector are constant, the residual supply available to the arbitrageur, $s_t^{(n)}$, would remain affine if we assume that this intercept is also affine in $\mathbf{x}_t$.

[7] This is consistent with the fact that Treasury Inflation-Protected Securities (TIPS) are issued in the U.S. with maturities of 5, 10, and 30 years. Moreover, and consistent with the assumption that $\overline{s}^{(r)}$ is small in practice, we note that TIPS only account for approximately 9% of the outstanding amount of U.S. Treasury securities by the end of 2018 (see `https://www.sifma.org/resources/research/fixed-income-chart/`).

for the nominal zero-coupon bonds in equation (2.6). Specifically, we have that the log real return from investing in the nominal n-period zero-coupon bond, for $n = 1, \ldots, N$, in excess of the real short-term rate satisfies:

$$\begin{aligned} rx_{t+1}^{(n)} = &\left\{ b_{x0}^{(n)} - \left[p_{x0} + b_{x0}^{(n-1)} \right] - \left[\mathbf{p}_x + \mathbf{b}_x^{(n-1)} \right]' \mathbf{\Phi}_{x0} - \rho_{x0} \right\} \\ &+ \left\{ \mathbf{b}_x^{(n)\prime} - \left[\mathbf{p}_x + \mathbf{b}_x^{(n-1)} \right]' \mathbf{\Phi}_{xx} - \boldsymbol{\rho}_x' \right\} \mathbf{x}_t \\ &- \left[\mathbf{p}_x + \mathbf{b}_x^{(n-1)} \right]' \boldsymbol{\varepsilon}_{x,t+1}. \end{aligned} \tag{2.16}$$

Notice that the exposure of the real return on the nominal long-term bond to the reduced-form innovations to the state variables, $\boldsymbol{\varepsilon}_{x,t+1} = \mathbf{\Sigma}_x \boldsymbol{\eta}_{t+1}$, has two components. First, nominal long-term bonds are exposed to inflation risk, as captured by inflation loadings on the state variables, $\mathbf{p}_x$. In addition, as described above, nominal long-term bonds (i.e., $n = 2, \ldots, N$) are also exposed to interest-rate risk, which is captured by the term $\mathbf{b}_x^{(n-1)}$.

Importantly, note that since $\boldsymbol{\varepsilon}_{x,t+1}$ is conditionally normally distributed, the log returns on the nominal bonds in excess of the real short-term interest rates are conditionally normal as well. Therefore, since the arbitrageurs' log portfolio return is, conditional on the information available at time t, a linear combination of the log excess returns on the nominal bonds, the log portfolio return is also conditionally normal as initially assumed.

2.6.2 Arbitrageurs' first-order condition

Using the nominal bond excess return in equation (2.16) to compute the variance-covariance terms in (2.14), we can solve the arbitrageurs' optimization problem:

Lemma 1. *Under the affine conjecture (2.9), the arbitrageurs' first-order condition (2.14) implies that*

$$\mathrm{E}_t rx_{t+1}^{(n)} + \frac{1}{2} \mathrm{Var}_t \left[rx_{t+1}^{(n)} \right] = - \left[\mathbf{p}_x + \mathbf{b}_x^{(n-1)} \right]' \mathbf{\Sigma}_x \boldsymbol{\lambda}_{x,t} \qquad \text{for } n = 1, \ldots, N, \tag{2.17}$$

where

$$\boldsymbol{\lambda}_{x,t} = \gamma \mathbf{\Sigma}_x' \sum_{j=1}^{N} \left\{ - \left[\mathbf{p}_x + \mathbf{b}_x^{(j-1)} \right] d_t^{(j)} \right\}. \tag{2.18}$$

Equation (2.17) implies that the expected excess return from investing in the nominal bonds, corrected by a Jensen's inequality term, is equal to the (inner) product of the sensitivity of the excess returns on the nominal bonds to the structural shocks, $-\left[\mathbf{p}_x + \mathbf{b}_x^{(n-1)}\right]' \boldsymbol{\Sigma}_x$, and a price of risk term, $\boldsymbol{\lambda}_{x,t}$. Specifically, we have that (i) $\boldsymbol{\lambda}_{x,t}$ captures the expected excess return per unit of sensitivity demanded by arbitrageurs as compensation for being exposed to the fundamental shocks, $\boldsymbol{\eta}_{t+1}$, (ii) consistent with the notion of the absence of arbitrage, this compensation per unit of factor sensitivity is the same for all nominal bonds, and (iii), the price of risk $\boldsymbol{\lambda}_{x,t}$ depends on the overall sensitivity of the arbitrageurs' portfolio to that factor: $\boldsymbol{\Sigma}_x' \sum_{j=1}^{N} \left\{-\left[\mathbf{p}_x + \mathbf{b}_x^{(j-1)}\right] d_t^{(j)}\right\}$. Consequently, the riskier the arbitrageurs' portfolio is, the higher the compensation (per unit of factor sensitivity) they demand for holding it.

2.6.3 Solution of the model

Similar to models in GV and VV, the absence of arbitrage does not impose restrictions on the prices of risk in $\boldsymbol{\lambda}_{x,t}$. Once more, we will follow these authors and determine the prices of risk that are consistent with market clearing in the bond markets. In equilibrium, we have that

$$d_t^{(n)} W_t = s_t^{(n)} W_t \qquad \text{for } n = 2, \ldots, N, \tag{2.19}$$

$$d_t^{(r)} W_t = 0. \tag{2.20}$$

Note that, since the portfolio weight in the real one-period bond is $d_t^{(r)} = 1 - \sum_{n=1}^{N} d_t^{(n)}$, the arbitrageurs' equilibrium allocation to the short-term nominal bond is $d_t^{(1)} = 1 - \sum_{n=2}^{N} s_t^{(n)}$.[8]

Substituting $rx_{t+1}^{(n)}$ from equation (2.16) and the market clearing conditions in equations

[8] This is Walras's law for the bond market. The budget constraint in equation (2.13) implies that $\sum_{n=1}^{N} d_t^{(n)} + d_t^{(r)} = 1$, while the market clearing conditions in equations (2.19) and (2.20) impose $d_t^{(n)} = s_t^{(n)}$ for $n = 2, \ldots, N$ and $d_t^{(r)} = 0$. The market for one-period nominal bonds then clears automatically, $s_t^{(1)} = d_t^{(1)}$, with the central bank supplying the residual amount of short-term nominal bonds. Consequently, the net supply of nominal bonds available to the arbitrageurs satisfies the accounting identity $\sum_{n=1}^{N} s_t^{(n)} = 1$, which we use in Section 5 to compute the weighted-average maturity of the arbitrageurs' bond portfolio, $\text{WAM}_t = \sum_{n=1}^{N} n\, s_t^{(n)}$.

(2.19) and (2.20) into the first-order condition of the arbitrageurs' portfolio choice problem in equation (2.17), we find a set of N affine equations in $\mathbf{x}_t$. Further, by setting the constant terms and linear terms in $\mathbf{x}_t$ to zero, we can find the coefficients for the equilibrium real short-term rate, ρ_{x0} and $\boldsymbol{\rho}_x$, and a set of difference equations defining the equilibrium bond loadings $\left\{b_{x0}^{(n)}, \mathbf{b}_x^{(n)\prime}\right\}_{n=1}^{N}$. The next theorem collects the results.

Theorem 1. *The parameters of the real short-term rate are given by*

$$\boldsymbol{\rho}_x' = \boldsymbol{\delta}_x' - \mathbf{p}_x'\boldsymbol{\Phi}_{xx}^{\mathbb{Q}} \tag{2.21}$$

$$\rho_{x0} = \delta_{x0} - p_{x0} - \mathbf{p}_x'\boldsymbol{\Phi}_{x0}^{\mathbb{Q}} + \frac{1}{2}\mathbf{p}_x'\boldsymbol{\Omega}_{xx}\mathbf{p}_x \tag{2.22}$$

while the equilibrium bond price loadings, $\left\{b_{x0}^{(n)}, \mathbf{b}_x^{(n)\prime}\right\}_{n=1}^{N}$, *satisfy the following set of difference equations*

$$\mathbf{b}_x^{(n)\prime} = \mathbf{b}_x^{(n-1)\prime}\boldsymbol{\Phi}_{xx}^{\mathbb{Q}} + \boldsymbol{\delta}_x' \tag{2.23}$$

$$b_{x0}^{(n)} = b_{x0}^{(n-1)} + \mathbf{b}_x^{(n-1)\prime}(\boldsymbol{\Phi}_{x0}^{\mathbb{Q}} - \boldsymbol{\Omega}_{xx}\mathbf{p}_x) - \frac{1}{2}\mathbf{b}_x^{(n-1)\prime}\boldsymbol{\Omega}_{xx}\mathbf{b}_x^{(n-1)} + \delta_{x0} \tag{2.24}$$

for $n = 1, \ldots, N$, *with initial conditions given by* $b_{x0}^{(0)} = 0$ *and* $\mathbf{b}_x^{(0)} = \mathbf{0}$, *and where* $\boldsymbol{\Phi}_{x0}^{\mathbb{Q}}$ *and* $\boldsymbol{\Phi}_{xx}^{\mathbb{Q}}$ *satisfy*

$$\boldsymbol{\Phi}_{xx}^{\mathbb{Q}} = \boldsymbol{\Phi}_{xx} + \gamma\boldsymbol{\Omega}_{xx}\sum_{j=2}^{N}\left[\mathbf{b}_x^{(j-1)}\mathbf{s}_x^{(j)\prime}\right], \tag{2.25}$$

$$\boldsymbol{\Phi}_{x0}^{\mathbb{Q}} = \boldsymbol{\Phi}_{x0} + \gamma\boldsymbol{\Omega}_{xx}\left\{\mathbf{p}_x + \sum_{j=2}^{N}\left[\mathbf{b}_x^{(j-1)}s_{x0}^{(j)}\right]\right\}. \tag{2.26}$$

Furthermore, provided that the eigenvalues of $\boldsymbol{\Phi}_{xx}$ *lie inside the unit circle and* γ *is below a threshold* $\overline{\gamma}$, *equation (2.25) admits a unique solution within a closed ball* $\|\boldsymbol{\Phi}_{xx}^{\mathbb{Q}}\| \leq \rho < 1$, *where* $\|\cdot\|$ *denotes the operator norm induced by a Lyapunov rotation of the pricing factors. The implied risk-neutral dynamics are stationary, in the sense that all the eigenvalues of* $\boldsymbol{\Phi}_{xx}^{\mathbb{Q}}$ *lie inside the unit circle in the complex plane.*

We note that equations (2.23) and (2.24) are reminiscent of the standard zero-coupon bond pricing recursions in a standard GDTSM. This similarity echoes the findings of Hamilton and Wu (2012b), who demonstrate that portfolio-balance models may serve as a foundation for the specification of the affine price of risk in GDTSMs. Our results broaden the scope of their work by showing that the equilibrium dynamics of the real short-term rate, as determined by the parameters in (2.21) and (2.22), are also consistent with a Gaussian affine term structure model. We formalize this equivalence in the following theorem.

Theorem 2. *The equilibrium parameters of the real short-term rate, as defined in equations (2.21) and (2.22), along with the equilibrium bond price loadings from equations (2.23) and (2.24), are consistent with a Gaussian affine term structure model in which the real SDF is defined by*

$$\log M_{t+1} = -r_t - \frac{1}{2}\boldsymbol{\lambda}'_{x,t}\boldsymbol{\lambda}_{x,t} - \boldsymbol{\lambda}'_{x,t}\boldsymbol{\eta}_{t+1}, \tag{2.27}$$

while the nominal SDF is defined by

$$\log M^{\$}_{t+1} = -i_t - \frac{1}{2}\boldsymbol{\lambda}^{\$\prime}_{x,t}\boldsymbol{\lambda}^{\$}_{x,t} - \boldsymbol{\lambda}^{\$\prime}_{x,t}\boldsymbol{\eta}_{t+1}, \tag{2.28}$$

where the processes for inflation, π_t, and the nominal short-term rate, i_t are given by equations (2.2) and (2.4) respectively. Further, the prices of risk of the real SDF coincide with those in the arbitrageurs' FOC in equation (2.18) evaluated at the market clearing conditions (2.19) and (2.20):

$$\boldsymbol{\lambda}_{x,t} = \boldsymbol{\lambda}_{x0} + \boldsymbol{\lambda}_{x}\mathbf{x}_t, \tag{2.29}$$

with

$$\boldsymbol{\lambda}_{x0} = \boldsymbol{\Sigma}_x^{-1}(\boldsymbol{\Phi}_{x0} - \boldsymbol{\Phi}^{\mathbb{Q}}_{x0}) = -\gamma\boldsymbol{\Sigma}'_x\left\{\mathbf{p}_x + \sum_{j=2}^{N}\left[\mathbf{b}_x^{(j-1)}s_{x0}^{(j)}\right]\right\}, \tag{2.30}$$

$$\boldsymbol{\lambda}_{x} = \boldsymbol{\Sigma}_x^{-1}(\boldsymbol{\Phi}_{xx} - \boldsymbol{\Phi}^{\mathbb{Q}}_{xx}) = -\gamma\boldsymbol{\Sigma}'_x\sum_{j=2}^{N}\left[\mathbf{b}_x^{(j-1)}\mathbf{s}_x^{(j)\prime}\right], \tag{2.31}$$

while the prices of risk of the nominal SDF satisfy

$$\boldsymbol{\lambda}^{\$}_{x,t} = \boldsymbol{\lambda}^{\$}_{x0} + \boldsymbol{\lambda}^{\$}_{x}\mathbf{x}_t, \tag{2.32}$$

with $\boldsymbol{\lambda}^{\$}_{x0} = \boldsymbol{\lambda}_{x0} + \boldsymbol{\Sigma}'_x \mathbf{p}_x$ *and* $\boldsymbol{\lambda}^{\$}_{x} = \boldsymbol{\lambda}_x$.

Theorem 2 naturally gives rise to two risk-neutral pricing measures. Let $\mathbb{Q}$ denote the risk-neutral measure induced by the real SDF M_{t+1} in (2.27). Under this measure, the state vector follows

$$\mathbf{x}_{t+1} = \boldsymbol{\Phi}^{\mathbb{Q}}_{x0} + \boldsymbol{\Phi}^{\mathbb{Q}}_{xx}\mathbf{x}_t + \boldsymbol{\Sigma}_x \boldsymbol{\eta}^{\mathbb{Q}}_{t+1}, \tag{2.33}$$

where $\boldsymbol{\eta}^{\mathbb{Q}}_{t+1} \sim iid\, N(0, \mathbf{I}_M)$, which allows us to interpret $\boldsymbol{\Phi}^{\mathbb{Q}}_{xx}$ and $\boldsymbol{\Phi}^{\mathbb{Q}}_{x0}$ in the bond pricing equations (2.25) and (2.26) as the parameters driving the state variable dynamics under the real risk-neutral measure, $\mathbb{Q}$ implied by the portfolio-balance model.

On the other hand, let $\mathbb{Q}^{\$}$ denote the risk-neutral measure induced by the nominal SDF $M^{\$}_{t+1}$ in (2.28), under which

$$\mathbf{x}_{t+1} = \boldsymbol{\Phi}^{\mathbb{Q}^{\$}}_{x0} + \boldsymbol{\Phi}^{\mathbb{Q}^{\$}}_{xx}\mathbf{x}_t + \boldsymbol{\Sigma}_x \boldsymbol{\eta}^{\mathbb{Q}^{\$}}_{t+1}, \tag{2.34}$$

where $\boldsymbol{\eta}^{\mathbb{Q}^{\$}}_{t+1} \sim iid\, N(0, \mathbf{I}_M)$ and $\boldsymbol{\Phi}^{\mathbb{Q}^{\$}}_{x0} = \boldsymbol{\Phi}^{\mathbb{Q}}_{x0} - \boldsymbol{\Omega}_{xx}\mathbf{p}_x$ and $\boldsymbol{\Phi}^{\mathbb{Q}^{\$}}_{xx} = \boldsymbol{\Phi}^{\mathbb{Q}}_{xx}$. In particular, the nominal bond pricing recursions in equations (2.23) and (2.24) coincide with those one would obtain by solving $B^{(n)}_t = \mathrm{E}^{\mathbb{Q}^{\$}}_t \left[\exp\left(-\sum_{k=0}^{n-1} i_{t+k}\right)\right]$ where $\mathrm{E}^{\mathbb{Q}^{\$}}_t$ denotes the conditional expectation under the nominal risk-neutral measure used to price nominal payoffs.

2.6.4 Uniqueness of the equilibrium

Importantly, the solution to the equilibrium bond loadings in equation (2.23) requires solving the fixed-point problem $\boldsymbol{\Phi}^{\mathbb{Q}}_{xx} = \mathbf{T}(\boldsymbol{\Phi}^{\mathbb{Q}}_{xx})$ in equation (2.25). Specifically, we have that in equation (2.23) the nominal bond loadings, $\left\{\mathbf{b}^{(n)}_x\right\}_{n=1}^{N}$, depend on $\boldsymbol{\Phi}^{\mathbb{Q}}_{xx}$, but in equation (2.25) the autocorrelation matrix of the state variables under $\mathbb{Q}$ depends on $\left\{\mathbf{b}^{(n)}_x\right\}_{n=1}^{N}$. This feedback loop occurs because, when arbitrageurs are risk averse ($\gamma \neq 0$), the equilibrium price of risk, $\boldsymbol{\lambda}_{x,t}$, depends on the overall sensitivity of the arbitrageurs' portfolio to the state variables, $\sum_{j=1}^{N}\left\{-\left[\mathbf{p}_x+\mathbf{b}_x^{(j-1)}\right]s_t^{(j)}\right\}$, which depends on the bond factor loadings themselves.

In models with stochastic bond supply, such as ours, this type of circularity can generate self-fulfilling beliefs and multiple equilibria, given that the perceived riskiness of absorbing supply shocks is itself endogenous to the equilibrium price impact of those shocks (see, e.g., VV, GV, and Greenwood, Hanson, and Liao 2018). Intuitively, if arbitrageurs believe that bond-supply shocks will have a large impact on yields, the bonds are perceived as riskier. Consequently, arbitrageurs demand a large increase in yields to absorb a positive supply shock, making the high sensitivity of yields self-fulfilling. On the other hand, if arbitrageurs believe that yields will be less sensitive to supply shocks, the bonds are perceived as less risky, and arbitrageurs thus demand a smaller increase in yields to compensate them for the same bond-supply shock. An equilibrium may even fail to exist if arbitrageurs are too risk-averse (i.e., $\gamma \geq \overline{\gamma}$) because a positive bond-supply shock can trigger a yield response so large that it raises the perceived riskiness of holding bonds, increasing the compensation demanded to hold those bonds, and thus inducing an even larger yield response. In this case, the feedback between beliefs and prices is destabilizing, and the fixed-point mapping in equation (2.25) fails to converge to a finite equilibrium.

This potential non-existence, together with the possibility of multiple equilibria when an equilibrium does exist, poses a fundamental challenge for the identification and estimation of portfolio-balance models. In particular, absent any further (equilibrium-selection) restrictions, portfolio-balance models might fail to satisfy the standard coherency condition that requires a well-defined, one-to-one mapping from structural primitives into equilibrium outcomes: for a given parameter vector, equilibrium outcomes may be undefined (if there is no equilibrium) or set-valued (when there are multiple equilibria). As a result, for a given set of parameters, likelihoods or moment conditions might not be uniquely pinned down, a situation closely related to the identification and estimation of discrete games of complete information with multiple Nash equilibria studied in Bajari, Hong, and Ryan (2010).

In this paper, we overcome this problem by showing that, provided the physical dynamics of the state variables are stationary and arbitrageurs are not too risk-averse ($\gamma < \overline{\gamma}$), the equilibrium exists, is unique within the region covered by our contraction argument, and is stable. Specifically, we show in the appendix that when all the eigenvalues of $\mathbf{\Phi}_{xx}$ lie inside the unit circle in the complex plane and $\gamma < \overline{\gamma}$, the mapping for the fixed-point problem $\mathbf{\Phi}_{xx}^{\mathbb{Q}} = \mathbf{T}(\mathbf{\Phi}_{xx}^{\mathbb{Q}})$ in equation (2.25) is a contraction within a closed ball $\|\mathbf{\Phi}_{xx}^{\mathbb{Q}}\| \leq \rho < 1$.[9] Consequently, using Banach contraction mapping theorem we have that $\mathbf{\Phi}_{xx}^{\mathbb{Q}} = \mathbf{T}(\mathbf{\Phi}_{xx}^{\mathbb{Q}})$ admits a unique solution $\mathbf{\Phi}_{xx}^{\mathbb{Q}*}$, and this solution is stable in the sense that, for any initial guess $\mathbf{\Phi}_{xx}^{\mathbb{Q}(0)}$ in this ball, the Picard iteration $\mathbf{\Phi}_{xx}^{\mathbb{Q}(n+1)} = \mathbf{T}(\mathbf{\Phi}_{xx}^{\mathbb{Q}(n)})$ converges to $\mathbf{\Phi}_{xx}^{\mathbb{Q}*}$. Note that the convergence of the Picard iteration within the ball implies that, similar to Greenwood, Hanson, and Liao (2018), the solution we select is stable in the sense that it is robust to small perturbations in arbitrageurs' beliefs regarding the equilibrium. Solutions outside the ball are the self-fulfilling equilibria described above, in which arbitrageurs believe that bond-supply shocks will have a large impact on yields and the equilibrium response to those shocks validates their belief.

Our selection therefore prunes those solutions and restores the coherency condition: for a given set of structural parameters, the model delivers exactly one equilibrium. The coherency condition and the observational equivalence established in Theorem 2 together deliver a well-defined mapping between the structural parameters of the portfolio-balance model and those of the implied GDTSM. This mapping underlies the identification strategy developed

[9] This can be seen intuitively in the limit as γ approaches zero. In this case, a continuity argument suggests that the mapping for the fixed-point problem in equation (2.25) becomes a contraction as both sides of this equation converge to $\mathbf{\Phi}_{xx}$ when $\gamma \to 0$.

in the next section, where we show how the portfolio-balance parameters can be recovered from estimated GDTSM parameters and propose a new estimation approach based on this equivalence.

3 Recovering the Portfolio-Balance Parameters from GDTSM Estimates

Similar to Hamilton and Wu (2012a), who discuss the identification of GDTSMs, we can exploit the mapping from the portfolio-balance model parameters to the GDTSM parameters in equations (2.25) and (2.26) to infer the parameters of the portfolio-balance model from estimates of the GDTSM. In the previous section, we showed the conditions under which there is a unique mapping between the portfolio-balance and GDTSM parameters. However, identifying the portfolio-balance parameters further requires that the mapping be one-to-one: if two different portfolio-balance parameter values yield identical GDTSM parameters, the observed data cannot distinguish between them.

In this section, we show that without structure, the portfolio-balance model is underidentified. However, under the assumption that the nominal bond supply can be represented in terms of M (factor-mimicking) orthogonal portfolios of nominal bonds whose unexpected returns perfectly replicate $\boldsymbol{\eta}_t$, the innovations to the state variables in equation (2.1), it is possible to recover the parameters driving the dynamics of supply factors as well as the parameters of the structural impact matrix, $\boldsymbol{\Sigma}_x$. Finally, we propose a two-step estimation approach that recovers the uniquely identified structural shocks and bond supply parameters from the GDTSM's estimated parameters.

3.1 Identification of the bond supply parameters

We begin by discussing the identification of the parameters that govern the (residual) supply of nominal bonds in equation (2.15). Note that, on the bond-supply side, the portfolio-balance structure feeds into the GDTSM exclusively through the risk-neutral dynamics. Specifically, we have that the total number of restrictions implied by equations (2.25) and (2.26) is $(M^2 + M)$, given that both $\mathbf{\Phi}^{\mathbb{Q}}_{x0}$ and $\mathbf{\Phi}^{\mathbb{Q}}_{xx}$ have dimensions $(M \times 1)$ and $(M \times M)$, respectively.

In contrast, the number of free parameters in the portfolio-balance model includes the risk-aversion parameter γ, the intercept terms of the supply process $\left\{s^{(n)}_{x0}\right\}_{n=2}^{N}$ for each bond maturity, and the loading parameters $\left\{\mathbf{s}^{(n)}_{x}\right\}_{n=2}^{N}$. This yields $1 + (N-1) + (N-1)M$ free parameters. Given that the number of bonds under consideration, N, is usually substantially larger than the number of factors, M, we have that the number of free parameters exceeds the number of restrictions implied by equations (2.25) and (2.26). Consequently, without additional assumptions, the portfolio-balance model is generally underidentified.

Factor structure in the nominal bond supply. We address this lack of identification by assuming, as in GV and VV, that a small number of supply factors drives the supply of nominal bonds of different maturities.

Formally, we impose the following assumptions.

Assumption 1. *The bond supply process has a factor structure:*

$$s^{(n)}_t = s^{(n)}_{\beta 0} + \mathbf{s}^{(n)\prime}_{\beta} \boldsymbol{\beta}_t \qquad \textit{for } n = 2, \ldots, N, \tag{3.1}$$

where $\boldsymbol{\beta}_t$ is a $(M \times 1)$ vector of bond supply factors that is an affine transformation of the underlying set of factors $\mathbf{x}_t$:

$$\boldsymbol{\beta}_t = \boldsymbol{\beta}_{x0} + \boldsymbol{\beta}_x \mathbf{x}_t. \tag{3.2}$$

Assumption 2. *The relative risk aversion parameter, γ, and the set of supply factor loadings $\left\{s^{(n)}_{\beta 0}, \mathbf{s}^{(n)}_{\beta}\right\}_{n=2}^{N}$ are either known or known functions of the GDTSM parameters of the model.*

Under Assumption 1, the supply of each maturity is driven by the supply factors $\boldsymbol{\beta}_t$, which summarize the dimensions of nominal bond supply that matter for the arbitrageurs' portfolio decisions. The coefficients $\left\{s_{\beta 0}^{(n)}, \mathbf{s}_{\beta}^{(n)}\right\}_{n=2}^{N}$ describe how each maturity loads onto these supply factors, while $\boldsymbol{\beta}_{x0}$ and $\boldsymbol{\beta}_x$ control how bond supply comoves with the pricing factors $\mathbf{x}_t$. Assumption 2 fixes γ and the cross-sectional loadings $\left\{s_{\beta 0}^{(n)}, \mathbf{s}_{\beta}^{(n)}\right\}_{n=2}^{N}$, so the only unknown bond supply parameters are the $M^2 + M$ entries of $\boldsymbol{\beta}_{x0}$ and $\boldsymbol{\beta}_x$, thus effectively reducing the dimensionality of the portfolio-balance parameter space.

Specifically, substituting equations (3.1) and (3.2) into (2.25) and (2.26) reveals the following linear one-to-one mapping between the parameters of the portfolio-balance model and the GDTSM:

$$\boldsymbol{\Phi}_{x0}^{\mathbb{Q}} = \boldsymbol{\Phi}_{x0} + \gamma \boldsymbol{\Omega}_{xx} \left[\mathbf{p}_x + \sum_{j=2}^{N} \mathbf{b}_x^{(j-1)} s_{\beta 0}^{(j)}\right] + \gamma \boldsymbol{\Omega}_{xx} \left[\sum_{j=2}^{N} \mathbf{b}_x^{(j-1)} \mathbf{s}_{\beta}^{(j)\prime}\right] \boldsymbol{\beta}_{x0}, \tag{3.3}$$

$$\boldsymbol{\Phi}_{xx}^{\mathbb{Q}} = \boldsymbol{\Phi}_{xx} + \gamma \boldsymbol{\Omega}_{xx} \left[\sum_{j=2}^{N} \mathbf{b}_x^{(j-1)} \mathbf{s}_{\beta}^{(j)\prime}\right] \boldsymbol{\beta}_x. \tag{3.4}$$

Note that, in this case, the total number of restrictions implied by equations (3.3) and (3.4) is exactly $(M^2 + M)$, which coincides with the number of free parameters in $\boldsymbol{\beta}_{x0}$ and $\boldsymbol{\beta}_x$. Consequently, under an additional rank condition to ensure that $\gamma \boldsymbol{\Omega}_{xx} \sum_{j=2}^{N} \mathbf{b}_x^{(j-1)} \mathbf{s}_{\beta}^{(j)\prime}$ is invertible (i.e., it has full rank), both $\boldsymbol{\beta}_{x0}$ and $\boldsymbol{\beta}_x$ can be uniquely recovered from the GDTSM parameters.

Absent further restrictions, the cross-section of yields does not generally identify maturity-specific supply (or demand) elasticities once the model allows as many bond-supply factors as state variables. To see the issue, suppose that in addition to bond-supply factors $\boldsymbol{\beta}_t$, which shift the quantity of bonds arbitrageurs must absorb, the net supply of the n-period bond also responds elastically to its own price, for example, because preferred-habitat investors adjust holdings in response to price changes: $s_t^{(n)} = s_{\beta 0}^{(n)} + \mathbf{s}_{\beta}^{(n)\prime} \boldsymbol{\beta}_t + s_b^{(n)} b_t^{(n)}$. In this case, the maturity-specific elasticities, $\left\{s_b^{(n)}\right\}_{n=2}^{N}$, introduce $N-1$ additional portfolio-balance parameters without a corresponding increase in the number of GDTSM parameters recoverable from yields alone. As a result, recovering maturity-specific elasticities within a portfolio-balance model typically requires either (i) additional information beyond yields or (ii) auxiliary restrictions that are, in practice, hard to justify and risk being arbitrary. Our framework thus provides a rationale for estimating elasticities in a granular demand-based system that exploits bond holdings and time-series variation to separately discipline investors' demand responses as in Jansen, Li, and Schmid (2025). These authors use sector-level U.S. Treasury holdings data within the demand-system methodology of Koijen and Yogo (2019) to estimate maturity-specific demand functions and elasticities, and then integrate those estimates into a VV-style model with risk-averse arbitrageurs. In contrast, our focus is on what can be identified and estimated from yields (and macro variables) alone using the GDTSM-based mapping; integrating these tools with a holdings-based demand system to jointly discipline elasticities and equilibrium pricing is a natural extension that we leave for future work.

Still, the fact that elasticities are not separately identified from yields does not mean that the model cannot generate empirically relevant, maturity-specific "localized" supply effects of the type often associated with elastic supply/demand. As noted by VV, with multiple risk factors, supply shocks that originate at different maturities affect arbitrageurs' exposures to the underlying risk factors in different ways, and changes in each bond supply factor exposure have different relative effects across maturities. As a result, demand (or supply) effects become more localized: shocks concentrated in short (long) maturities have more pronounced effects on short (long) yields, even when supply enters through a low-dimensional factor structure.

Supply factor loadings and factor-mimicking portfolios. This factor structure in the supply of nominal bonds still leaves open the question of how the supply factors $\boldsymbol{\beta}_t$ should be interpreted and how to choose the loadings $\left\{\mathbf{s}_{\beta}^{(n)}\right\}_{n=2}^{N}$ in practice. To connect these supply factors to economically meaningful objects, we propose constructing portfolios of bonds with unexpected excess returns that match the structural shocks driving the state variables.

Specifically, define the sequence of the factor-mimicking portfolio weights $\left\{\boldsymbol{\omega}^{(n)}\right\}_{n=2}^{N}$ as

$$\boldsymbol{\omega}^{(n)} = -\boldsymbol{\Sigma}_x^{-1}\left[\sum_{j=2}^{N}\mathbf{b}_x^{(j-1)}\mathbf{b}_x^{(j-1)\prime}\right]^{-1}\mathbf{b}_x^{(n-1)}, \quad n = 2, \ldots, N. \tag{3.5}$$

and note that

$$\sum_{n=2}^{N}\boldsymbol{\omega}^{(n)}\left[\widetilde{rx}_{t+1}^{(n)} - \mathrm{E}_t\widetilde{rx}_{t+1}^{(n)}\right] = \sum_{n=2}^{N}\boldsymbol{\omega}^{(n)}\left[-\mathbf{b}_x^{(n-1)\prime}\boldsymbol{\Sigma}_x\boldsymbol{\eta}_{t+1}\right] = \boldsymbol{\eta}_{t+1}, \tag{3.6}$$

where, as a reminder, $\widetilde{rx}_{t+1}^{(n)} = rx_{t+1}^{(n)} - rx_{t+1}^{(1)} = b_{t+1}^{(n-1)} - b_t^{(n)} - i_t$ represents the log nominal return on the n-period nominal zero-coupon bond in excess of the short-term nominal interest rate as defined in equation (2.7), and $\boldsymbol{\eta}_{t+1}$ represents the structural shock in the SVAR(1) in equation (2.1). That is, the innovations to the excess returns on the portfolios of nominal bonds with weights $\left\{\boldsymbol{\omega}^{(n)}\right\}_{n=2}^{N}$ are exactly equal to the structural shocks driving the state variables.

We now tie the supply factors to these portfolios by setting the supply factor loadings equal to the factor-mimicking weights:

$$\mathbf{s}_{\beta}^{(n)} = \boldsymbol{\omega}^{(n)} \quad \text{for } n = 2, \ldots, N. \tag{3.7}$$

In this way, each of the individual supply factors in the vector $\boldsymbol{\beta}_t$ measures the supply of structural risk that arbitrageurs are exposed to, in that an increase in the supply of the factor-mimicking portfolios directly corresponds to an increase in the exposure of the arbitrageurs' portfolio to the individual structural shocks in $\boldsymbol{\eta}_t$.[10]

[10]The representation of the bond supply as exposures to the structural shocks connects to the fiscal-insurance literature on government debt management, in which the maturity structure is the technology through which the government chooses its exposure to the economy's shocks. Angeletos (2002) shows that a portfolio of noncontingent bonds of different maturities can replicate the complete-markets allocation

Further, we assume that

$$s_{\beta 0}^{(n)} = 0 \quad \text{for } n = 2, \ldots, N, \tag{3.8}$$

which implies $s_{\beta 0}^{(1)} = 1$ given that $s_{\beta 0}^{(1)} = 1 - \sum_{n=2}^{N} s_{\beta 0}^{(n)}$. Therefore, this assumption implies that $\left\{ s_{\beta 0}^{(n)} \right\}_{n=2}^{N}$ can be viewed as a portfolio that is fully invested in the nominal short-term bond (i.e., the reference rate when computing the excess returns, $\widetilde{rx}_{t+1}^{(n)}$). Consequently, we have that under equations (3.7) and (3.8), the supply of bonds with different maturities can be represented as a linear combination of the supply of the M fundamental risks in the economy and the supply of the one-period nominal bond.

This representation of bond supply is, in fact, reminiscent of Huberman, Kandel, and Stambaugh (1987), in which M factor-mimicking portfolios and the riskless asset span the priced payoff space. The portfolios with weights $\left\{ \boldsymbol{\omega}^{(n)} \right\}_{n=2}^{N}$ span the priced dimensions of bond supply, since they replicate the structural shocks $\boldsymbol{\eta}_t$, and the one-period nominal bond plays the role of the reference asset. Bond supply therefore affects the yield curve only through the quantities $\boldsymbol{\beta}_t$ of the M factor-mimicking portfolios that arbitrageurs absorb.

This specification also collapses the equilibrium relation to a linear system and yields a transparent link between the bond supply factors, $\boldsymbol{\beta}_t$, and the prices of risk in the GDTSM, $\boldsymbol{\lambda}_{x,t}$. Substituting equations (3.7) and (3.8) into equations (3.3) and (3.4), and using the identity $\boldsymbol{\Omega}_{xx} \sum_{j=2}^{N} \mathbf{b}_x^{(j-1)} \mathbf{s}_\beta^{(j)\prime} = -\boldsymbol{\Sigma}_x$, we can write the risk-neutral autocorrelation relation as

$$\boldsymbol{\Phi}_{xx}^{\mathbb{Q}} = \boldsymbol{\Phi}_{xx} - \gamma \boldsymbol{\Sigma}_x \boldsymbol{\beta}_x, \tag{3.9}$$

which is linear in $\boldsymbol{\Phi}_{xx}^{\mathbb{Q}}$. Solving this relation, together with its counterpart for the constant, for $\boldsymbol{\beta}_{x0}$ and $\boldsymbol{\beta}_x$ delivers the following proposition:

precisely because bond prices at different maturities respond differently to shocks. Guibaud, Nosbusch, and Vayanos (2013) study the optimal maturity structure of government debt in a preferred-habitat model, while Bhandari, Evans, Golosov, and Sargent (2017) characterize optimal debt management when the government's portfolio is risky. Viewed through this lens, the supply factors $\boldsymbol{\beta}_t$ capture the amount of exposure to the structural shocks that the government supplies to the arbitrageurs.

Proposition 1. *Under the factor-mimicking normalization in equations (3.7) and (3.8), we have that*

$$\boldsymbol{\beta}_{x0} = \frac{1}{\gamma}\boldsymbol{\Sigma}_x^{-1}\left(\boldsymbol{\Phi}_{x0} - \boldsymbol{\Phi}_{x0}^{\mathbb{Q}}\right) + \boldsymbol{\Sigma}_x'\mathbf{p}_x = \frac{1}{\gamma}\boldsymbol{\lambda}_{x0} + \boldsymbol{\Sigma}_x'\mathbf{p}_x, \tag{3.10}$$

$$\boldsymbol{\beta}_{x} = \frac{1}{\gamma}\boldsymbol{\Sigma}_x^{-1}\left(\boldsymbol{\Phi}_{xx} - \boldsymbol{\Phi}_{xx}^{\mathbb{Q}}\right) = \frac{1}{\gamma}\boldsymbol{\lambda}_{x}. \tag{3.11}$$

Importantly, under the factor-mimicking choice $\mathbf{s}_\beta^{(n)} = \boldsymbol{\omega}^{(n)}$, recovering the parameters that drive the supply factors $\boldsymbol{\beta}_t$ does not require solving the fixed-point problem of Theorem 1, nor, consequently, that γ be sufficiently low. Because equation (3.9) is linear, the equilibrium exists and is unique for any $\gamma > 0$, and recovering $\boldsymbol{\beta}_t$ reduces to inverting this same linear relation. That inversion requires only that $\boldsymbol{\Sigma}_x$ be invertible, which holds because $\boldsymbol{\Sigma}_x$ is non-singular. The factor-mimicking weights in equation (3.5) must also be well defined, which requires the factor loadings $\left\{\mathbf{b}_x^{(n-1)}\right\}_{n=2}^{N}$ to span $\mathbb{R}^M$; this holds under the canonical GDTSM of Section 4.[11]

Note that setting the supply factor loadings equal to the factor-mimicking weights is a normalization rather than a restriction. To see this, let an affine bond supply specification be the collection of intercepts and loadings $\left\{s_{x0}^{(n)}, \mathbf{s}_x^{(n)}\right\}_{n=2}^{N}$ in equation (2.15), and let two such specifications be observationally equivalent when, holding the state variables and the remaining parameters of the model fixed, they support the same equilibrium. Then, by equations (2.25) and (2.26), a supply specification enters the equilibrium only through the two aggregates $\sum_{j=2}^{N}\mathbf{b}_x^{(j-1)}s_{x0}^{(j)}$ and $\sum_{j=2}^{N}\mathbf{b}_x^{(j-1)}\mathbf{s}_x^{(j)\prime}$, which measure the exposure to the structural shocks that bond supply loads onto the arbitrageurs' portfolio. The following proposition

[11]The spanning condition is implied by the canonical GDTSM of Section 4, and is therefore not an additional restriction on the model. In that representation, the short rate loads on every latent factor, $\boldsymbol{\delta}_z = \mathbf{1}_M$, and $\boldsymbol{\Phi}_{zz}^{\mathbb{Q}} = \mathrm{diag}(\boldsymbol{\phi}_{zz}^{\mathbb{Q}})$ is diagonal, so that iterating the loading recursion in equation (2.23) gives $b_{z,i}^{(n)} = \left[1 - (\phi_{zz,i}^{\mathbb{Q}})^n\right] / \left[1 - \phi_{zz,i}^{\mathbb{Q}}\right]$. Each latent factor therefore decays at its own rate under $\mathbb{Q}$ and traces out its own pattern of loadings across maturities, and because we assume in Section 4 that the eigenvalues in $\boldsymbol{\phi}_{zz}^{\mathbb{Q}}$ are distinct, these M patterns are linearly independent. The same is then true of $\left\{\mathbf{b}_x^{(n-1)}\right\}_{n=2}^{N}$, since the two representations are related by a non-singular affine transformation of the factors, which preserves rank.

characterizes the equivalence classes that these aggregates induce and the position of the factor-mimicking specification within them.

Proposition 2. *Consider two affine bond supply specifications, A and B, both affine in the same vector of state variables* $\mathbf{x}_t$ *as in equation (2.15),*

$$s_{A,t}^{(n)} = s_{A,x0}^{(n)} + \mathbf{s}_{A,x}^{(n)\prime}\mathbf{x}_t, \qquad s_{B,t}^{(n)} = s_{B,x0}^{(n)} + \mathbf{s}_{B,x}^{(n)\prime}\mathbf{x}_t, \qquad \textit{for } n = 2, \ldots, N, \tag{3.12}$$

and hold the remaining parameters of the model fixed. Then:

(i) Specifications A and B are observationally equivalent if and only if they load the arbitrageurs' portfolio with the same exposure to the structural shocks:

$$\sum_{j=2}^{N} \mathbf{b}_x^{(j-1)} s_{A,x0}^{(j)} = \sum_{j=2}^{N} \mathbf{b}_x^{(j-1)} s_{B,x0}^{(j)}, \tag{3.13}$$

$$\sum_{j=2}^{N} \mathbf{b}_x^{(j-1)} \mathbf{s}_{A,x}^{(j)\prime} = \sum_{j=2}^{N} \mathbf{b}_x^{(j-1)} \mathbf{s}_{B,x}^{(j)\prime}, \tag{3.14}$$

where $\left\{\mathbf{b}_x^{(n)}\right\}_{n=1}^{N}$ *are the bond price loadings of the equilibrium that both specifications support. Equivalently, A and B are observationally equivalent if and only if they imply the same prices of risk,* $\boldsymbol{\lambda}_{x0}$ *and* $\boldsymbol{\lambda}_x$*.*

(ii) Each equivalence class contains exactly one factor-mimicking specification, that is, exactly one specification satisfying equations (3.7) and (3.8). Its supply factor parameters, $\boldsymbol{\beta}_{x0}$ *and* $\boldsymbol{\beta}_x$*, are given by equations (3.10) and (3.11).*

(iii) Substituting equations (3.7) and (3.8) into equations (3.1) and (3.2), we find that the factor-mimicking specification of a given class has intercepts $\boldsymbol{\omega}^{(n)\prime}\boldsymbol{\beta}_{x0}$ *and loadings* $\boldsymbol{\beta}_x'\boldsymbol{\omega}^{(n)}$*. Any other specification* $\left\{s_{x0}^{(n)}, \mathbf{s}_x^{(n)}\right\}_{n=2}^{N}$ *in that class differs from it by a reallocation of supply across maturities that carries no exposure to the structural shocks:*

$$\sum_{j=2}^{N} \mathbf{b}_x^{(j-1)} \left[s_{x0}^{(j)} - \boldsymbol{\omega}^{(j)\prime}\boldsymbol{\beta}_{x0}\right] = \mathbf{0}, \qquad \sum_{j=2}^{N} \mathbf{b}_x^{(j-1)} \left[\mathbf{s}_x^{(j)} - \boldsymbol{\beta}_x'\boldsymbol{\omega}^{(j)}\right]' = \mathbf{0}. \tag{3.15}$$

Such reallocations leave the prices of risk, and hence every bond price, unchanged.

The normalization we impose on bond supply is reminiscent of a familiar feature of GDTSMs. Gaussian term structure models are observationally equivalent under affine transformations of the factors (Dai and Singleton, 2000), so their estimation relies on a normalization, such as the canonical representation of Joslin, Singleton, and Zhu (2011) that we adopt for the GDTSM. Proposition 2 delivers an analogous invariance on the supply side: for a given set of pricing factors, bond supply is observationally equivalent under reallocations of quantities across maturities that leave the arbitrageurs' exposure to the structural shocks unchanged. The factor-mimicking specification is the normalization that selects one member of each class.

Specifically, Proposition 2 delimits what the yield curve can and cannot say about bond supply. Part (i) says that the yield curve identifies bond supply only through the amount of structural risk for arbitrageurs to absorb. Two specifications that load the same exposure onto the arbitrageurs' portfolio command the same compensation, and hence the same prices of risk and the same yields, however differently they spread that exposure across maturities. Within each class, the factor-mimicking specification is the natural representative: its supply factors measure the quantities of the M portfolios that replicate the structural shocks, and part (ii) shows that every class contains exactly one of them, with the parameters recovered in Proposition 1. What the normalization sets aside is the content of part (iii). Any reallocation of supply across maturities whose factor exposures cancel leaves every bond price untouched, and yet it changes the bonds that arbitrageurs actually hold, including the weighted-average maturity of their portfolio. Such reallocations exist because there are more maturities than factors, so what yields identify is the risk that bond supply delivers, not the maturity composition that delivers it. Note that this is the cross-sectional counterpart of the elasticity result above: pinning down the composition requires the holdings data that a granular demand system such as Jansen, Li, and Schmid (2025) exploits.

3.2 Identification of the structural shocks

We now turn to the identification of the structural impact matrix, $\mathbf{\Sigma}_x$. In this case, note that the estimation of the GDTSM delivers an estimate of the reduced-form covariance matrix $\mathbf{\Omega}_{xx} = \mathbf{\Sigma}_x \mathbf{\Sigma}_x'$, which only identifies $M(M+1)/2$ entries of the M^2 unknown elements of $\mathbf{\Sigma}_x$.[12]

We identify $\mathbf{\Sigma}_x$ by exploiting the structure provided by the portfolio-balance model. When the supply factor loadings equal the factor-mimicking weights, $\mathbf{s}_\beta^{(n)} = \boldsymbol{\omega}^{(n)}$, they depend on $\mathbf{\Sigma}_x$, so we can select $\mathbf{\Sigma}_x$ by restricting the loadings. Specifically, we require that each structural shock be associated with a distinct, mutually exclusive risk-supply dimension, so that variation in the supply of one factor-mimicking portfolio does not mechanically reallocate supply into the other factor-mimicking portfolios.

Consider, for example, two stylized supply factors, the supply-side analogs of the level and slope of the yield curve. A level factor raises the supply of every long-term bond by the same amount, i.e., $s_{\beta_l}^{(n)} = 1$ for $n = 2, \ldots, N$: it shifts the supply-by-maturity schedule up in parallel, changing the aggregate supply of long-term bonds while leaving its shape (the differences between the supply of two long-term bonds with different maturities) unchanged. A slope factor shifts supply from shorter to longer maturities, $\sum_{n=2}^N s_{\beta_s}^{(n)} = 0$: it changes the shape of the schedule while leaving the aggregate supply of long-term bonds unchanged. Note that, since the constant level loadings collapse the sum to the slope factor's effect on the aggregate, their loadings are orthogonal:

$$\sum_{n=2}^{N} s_{\beta_l}^{(n)} s_{\beta_s}^{(n)} = \sum_{n=2}^{N} s_{\beta_s}^{(n)} = 0,$$

That is, neither factor reallocates supply into the other's dimension: a slope innovation leaves the aggregate supply of long-term bonds untouched, and a level innovation leaves the

[12]Specifically, $\mathbf{\Sigma}_x$ is only identified up to an orthonormal rotation matrix $\mathbf{Q}$, where $\mathbf{Q}\mathbf{Q}' = \mathbf{I}_M$, because any rotated matrix $\mathbf{\Sigma}_x\mathbf{Q}$ also satisfies $\mathbf{\Omega}_{xx} = \mathbf{\Sigma}_x\mathbf{Q}\left(\mathbf{\Sigma}_x\mathbf{Q}\right)'$.

shape of the schedule untouched.

Motivated by this level and slope supply example, we impose that the supply factor loadings are mutually orthogonal across factors. Specifically, for any two supply factors j and k, the impact on the supply of factor-mimicking portfolio k from a unit change in the supply of factor-mimicking portfolio j is $\sum_{n=2}^{N} s_{\beta_k}^{(n)} s_{\beta_j}^{(n)}$.[13] Therefore, to ensure that each structural shock is associated with a distinct, mutually exclusive risk-supply dimension, we impose:

Assumption 3. *The supply factor loadings are mutually orthogonal across factors:*

$$\sum_{n=2}^{N} s_{\beta_j}^{(n)} s_{\beta_k}^{(n)} = 0 \quad \textit{for all } j \neq k. \tag{3.16}$$

Consequently, since we set the supply factor loadings $\left\{\mathbf{s}_{\beta}^{(n)}\right\}_{n=2}^{N}$ equal to the weights of the factor-mimicking portfolios, and these portfolio weights depend on the structural impact matrix $\mathbf{\Sigma}_x$, the orthogonality condition in (3.16) imposes $M(M-1)/2$ restrictions on $\mathbf{\Sigma}_x$, thereby pinning down the rotation and delivering a unique $\mathbf{\Sigma}_x$.

To be more specific, let $\mathbf{B} = \sum_{n=2}^{N} \mathbf{b}_x^{(n-1)} \mathbf{b}_x^{(n-1)\prime}$ where, provided that $N-1 \geq M$, $\mathbf{B}$ is positive definite given that the factor loadings $\left\{\mathbf{b}_x^{(n-1)}\right\}_{n=2}^{N}$ span $\mathbb{R}^M$, as established above. Therefore, under the assumption that the supply factor loadings are equal to the weights of the factor-mimicking portfolios, we can write $\mathbf{s}_{\beta}^{(n)} = \boldsymbol{\omega}^{(n)} = -\mathbf{\Sigma}_x^{-1}\mathbf{B}^{-1}\mathbf{b}_x^{(n-1)}$. Consequently,

$$\sum_{n=2}^{N} \mathbf{s}_{\beta}^{(n)} \mathbf{s}_{\beta}^{(n)\prime} = \mathbf{\Sigma}_x^{-1}\mathbf{B}^{-1}(\mathbf{\Sigma}_x^{-1})'. \tag{3.17}$$

Thus the orthogonality restriction (3.16) is equivalent to requiring that $\mathbf{\Sigma}_x^{-1}\mathbf{B}^{-1}(\mathbf{\Sigma}_x^{-1})'$ is diagonal which, in turn, is satisfied when $\mathbf{\Sigma}_x'\mathbf{B}\mathbf{\Sigma}_x$ is diagonal. Together with $\mathbf{\Omega}_{xx} = \mathbf{\Sigma}_x\mathbf{\Sigma}_x'$, this yields exactly M^2 equations for the M^2 unknown elements of $\mathbf{\Sigma}_x$.

[13] Because the supply factor loadings equal the factor-mimicking weights, the loading $s_{\beta_k}^{(n)}$ is both the response of maturity-n supply to factor k and the weight that factor-mimicking portfolio k places on maturity n. A unit increase in the supply of factor-mimicking portfolio j raises the supply of maturity n by $s_{\beta_j}^{(n)}$, so its total effect on the supply of factor-mimicking portfolio k is the sum of these changes weighted by that portfolio's holdings, $\sum_{n=2}^{N} s_{\beta_k}^{(n)} s_{\beta_j}^{(n)}$.

A convenient way to implement these restrictions is to use the eigendecomposition of a suitably scaled version of $\mathbf{B}$. Let $\boldsymbol{\Omega}_{xx}^{1/2}$ denote the symmetric square root of $\boldsymbol{\Omega}_{xx}$, and define $\widetilde{\mathbf{B}} = \boldsymbol{\Omega}_{xx}^{1/2}\mathbf{B}\boldsymbol{\Omega}_{xx}^{1/2}$. Let $\mathbf{U}$ be the orthonormal matrix whose columns are the eigenvectors of $\widetilde{\mathbf{B}}$ such that $\mathbf{U}'\widetilde{\mathbf{B}}\mathbf{U}$ is a diagonal matrix collecting the eigenvalues of $\widetilde{\mathbf{B}}$, provided these eigenvalues are distinct. Then, setting

$$\boldsymbol{\Sigma}_x = \boldsymbol{\Omega}_{xx}^{1/2}\mathbf{U}, \tag{3.18}$$

immediately implies

$$\boldsymbol{\Sigma}_x\boldsymbol{\Sigma}_x' = \boldsymbol{\Omega}_{xx}^{1/2}\mathbf{U}\mathbf{U}'\boldsymbol{\Omega}_{xx}^{1/2} = \boldsymbol{\Omega}_{xx}, \tag{3.19}$$

since $\mathbf{U}$ is orthonormal, and

$$\boldsymbol{\Sigma}_x'\mathbf{B}\boldsymbol{\Sigma}_x = \mathbf{U}'\boldsymbol{\Omega}_{xx}^{1/2}\mathbf{B}\boldsymbol{\Omega}_{xx}^{1/2}\mathbf{U} = \mathbf{U}'\widetilde{\mathbf{B}}\mathbf{U}, \tag{3.20}$$

which is diagonal by construction, as required.

Intuitively, the solution (3.18) selects the unique rotation of the structural impact matrix (up to column signs and the order of the shocks), in which each structural shock is associated with a unique, independent supply factor. In our empirical implementation, we resolve the sign indeterminacy by normalizing each column of $\boldsymbol{\Sigma}_x$ to have a positive diagonal element, so that the signs reported for the structural impact matrix and for the impulse responses follow from this convention.

Importantly, Assumption 3 places no discipline on how the structural shocks move inflation, output growth, or the short-term interest rate, and therefore offers no a priori guarantee that they admit an economic interpretation. Yet, the shocks that we recover do. Specifically, we show in Section 5.3 below that the impulse responses of the three recovered shocks resemble those of the hedging-risk-premium shock of Cieslak and Pang (2021), a risk-bearing-capacity shock similar to that in Gertler and Karadi (2011), and the monetary-policy shock of Christiano, Eichenbaum, and Evans (1999).

3.3 Two-step estimation procedure

The one-to-one mapping between the parameters of the portfolio-balance model and the GDTSM in equations (3.3) and (3.4) thus suggests the following two-step estimation approach.

1. Estimate the parameters of the GDTSM using standard methods, for example, by maximum likelihood as in Joslin, Singleton, and Zhu (2011).[14] Then, using these estimates of $\widehat{\delta}_{x0}$, $\widehat{\boldsymbol{\delta}}_x$, $\widehat{\mathbf{p}}_x$, $\widehat{\boldsymbol{\Phi}}_{x0}$, $\widehat{\boldsymbol{\Phi}}_{xx}$, $\widehat{\boldsymbol{\Omega}}_{xx}$, $\widehat{\boldsymbol{\Phi}}^{\mathbb{Q}}_{x0}$, and $\widehat{\boldsymbol{\Phi}}^{\mathbb{Q}}_{xx}$ obtain estimates of the bond price loadings $\left\{\widehat{\mathbf{b}}^{(n)}_x\right\}_{n=1}^{N}$. Compute the matrix $\widehat{\mathbf{B}} = \sum_{n=2}^{N} \widehat{\mathbf{b}}^{(n-1)}_x \widehat{\mathbf{b}}^{(n-1)\prime}_x$.

2. Then recover the estimate of the structural impact matrix, $\widehat{\boldsymbol{\Sigma}}_x$, and, for a given value of γ, the estimates of the bond supply factor parameters $\widehat{\boldsymbol{\beta}}_{x0}$ and $\widehat{\boldsymbol{\beta}}_x$, through the following equations:

$$\widehat{\boldsymbol{\Sigma}}_x = \widehat{\boldsymbol{\Omega}}^{1/2}_{xx}\widehat{\mathbf{U}}, \tag{3.21}$$

$$\widehat{\boldsymbol{\beta}}_{x0} = \frac{1}{\gamma}\widehat{\boldsymbol{\Sigma}}^{-1}_x\left(\widehat{\boldsymbol{\Phi}}_{x0} - \widehat{\boldsymbol{\Phi}}^{\mathbb{Q}}_{x0}\right) + \widehat{\boldsymbol{\Sigma}}'_x\widehat{\mathbf{p}}_x, \tag{3.22}$$

$$\widehat{\boldsymbol{\beta}}_{x} = \frac{1}{\gamma}\widehat{\boldsymbol{\Sigma}}^{-1}_x\left(\widehat{\boldsymbol{\Phi}}_{xx} - \widehat{\boldsymbol{\Phi}}^{\mathbb{Q}}_{xx}\right), \tag{3.23}$$

   where $\widehat{\mathbf{U}}$ is the orthonormal matrix whose columns are the eigenvectors of $\widehat{\boldsymbol{\Omega}}^{1/2}_{xx}\widehat{\mathbf{B}}\widehat{\boldsymbol{\Omega}}^{1/2}_{xx}$.

Standard errors for $\widehat{\boldsymbol{\beta}}_{x0}$, $\widehat{\boldsymbol{\beta}}_x$, and $\widehat{\boldsymbol{\Sigma}}_x$ can be calculated using the Delta method.[15]

Note that risk aversion plays a limited role in this recovery. The estimate of the structural impact matrix in equation (3.21) is constructed from the GDTSM estimates alone and does not depend on γ. The same is therefore true of the estimated structural shocks, their impulse

[14] Alternatively, one could use the minimum-chi-square estimation approach introduced by Hamilton and Wu (2012a), the linear regression approach introduced in Adrian, Crump, and Moench (2013), or the asymptotic least squares estimation approach introduced by Diez de los Rios (2015) as alternatives to maximum likelihood estimation of the parameters of the GDTSM.

[15] The Delta method requires that $\widehat{\boldsymbol{\Sigma}}_x$ be a differentiable function of the GDTSM parameter estimates, which is guaranteed by the condition imposed in equation (3.18). When the eigenvalues of $\widetilde{\mathbf{B}}$ are distinct, each of its eigenvectors is uniquely determined up to sign and varies differentiably with the entries of $\widetilde{\mathbf{B}}$, and hence with the GDTSM parameters.

responses, and every object built from them, including the variance decompositions of Section 6 and the implied monetary-policy rule of Section 7. Risk aversion enters only the recovery of the bond supply parameters. Still, the slope coefficients in equation (3.23) scale by $1/\gamma$, so their signs and statistical significance do not depend on γ. Only the intercept in equation (3.22), which combines a term in $1/\gamma$ with a term that does not, varies non-trivially with the calibrated value.

4 Baseline Estimation of the GDTSM

We begin by fitting a three-factor GDTSM to U.S. Treasury yields and macroeconomic data to obtain a reduced-form description of the term structure that is suitable for our mapping exercise. The state vector is constructed from the first three principal components of zero-coupon yields spanning maturities from three months to thirty years, which capture the familiar level, slope, and curvature factors documented in the literature. We then estimate the GDTSM by maximum likelihood using the canonical approach of Joslin, Singleton, and Zhu (2011), which treats these principal components as observed factors and separates the estimation of physical and risk-neutral dynamics. The estimated model matches the cross-section and time-series of yields with small pricing errors and exhibits economically sensible dynamics for both yields and macro variables, providing the baseline GDTSM, whose parameters we map into the portfolio-balance structure.

4.1 Yields and macro data

Our dataset comprises end-of-quarter observations from March 1986 (1986Q1) to June 2025 (2025Q2) on zero-coupon bond yields for maturities of three and six months and one, two, three, five, seven, ten, fifteen, twenty, and thirty years. Specifically, we use Treasury bill rates from the Federal Reserve Board's H.15 release for the three- and six-month bond yields. We obtain longer-maturity yields from the Gürkaynak, Sack, and Wright (2007) database.

As documented in the literature (Litterman and Scheinkman, 1991), the first three principal components (PCs) of U.S. government bond yields account for over 99% of the cross-sectional variation in yields. They are traditionally interpreted as level, slope, and curvature factors (see Figure 1). Specifically, note that an increase in the first PC of the yield curve raises all yields, thereby raising the level of the yield curve. An increase in the second PC of the yield curve raises short yields and lowers long yields, flattening (or even inverting) the yield curve. Finally, an increase in the third PC increases very short- and very long-term yields but lowers medium-term yields, increasing the curvature of the yield curve.

We measure (core) inflation as the change in the (log) Consumer Price Index (CPI) for All Urban Consumers (All Items Less Food and Energy in U.S. City Average) between the last month of the quarter and the last month of the previous quarter. CPI data are obtained from the Bureau of Labor Statistics. Similarly, we measure output growth as the quarterly change in the (log) Real Gross Domestic Product, obtained from the National Income and Product Accounts.[16]

4.2 Maximum likelihood estimation of GDTSMs

We start by estimating an $M = 3$ factor GDTSM on our sample of eleven zero-coupon bond yields by maximum likelihood (ML) using the approach of Joslin, Singleton, and Zhu (2011). Specifically, we follow these authors in (i) working with bond state variables that are linear combinations (i.e., portfolios) of the yields themselves, $\mathbf{x}_t = \mathbf{W}'\mathbf{y}_t$ where $\mathbf{W}$ is a full-rank matrix of weights and $\mathbf{y}_t = [y_t^{(1)}, y_t^{(2)}, y_t^{(4)}, \ldots, y_t^{(80)}, y_t^{(120)}]'$ is a vector collecting these yields, whose maturities are measured in quarters (so that $y_t^{(120)}$ is the thirty-year yield), and (ii)

[16] To mitigate the unusually large swings in economic growth during the COVID-19 period (when annualized real growth swung from about -30% in 2020Q2 to $+30\%$ in 2020Q3), we replace these two observations with a three-quarter moving average centred on each point. Results are qualitatively the same in the absence of this outlier adjustment.

further assuming that $\mathbf{x}_t$ is observed perfectly. In our case, $\mathbf{W}$ is selected such that $\mathbf{x}_t$ coincides with the first three principal components of the yields used in the estimation.

In particular, JSZ show that, under the assumption of stationarity under $\mathbb{Q}$, any GDTSM is observationally equivalent to a canonical model with $i_t = \mathbf{1}'_M \mathbf{z}_t$, where $\mathbf{1}_M$ is an $(M \times 1)$ vector of ones, and the state variables $\mathbf{z}_t$ are latent and follow the following VAR process under the $\mathbb{Q}$-measure:

$$\mathbf{z}_{t+1} = \mathbf{\Phi}^{\mathbb{Q}}_{z0} + \mathbf{\Phi}^{\mathbb{Q}}_{zz} \mathbf{z}_t + \boldsymbol{\varepsilon}^{\mathbb{Q}}_{z,t+1}, \tag{4.1}$$

where $k^{\mathbb{Q}\$}_{\infty}$ is the first and only nonzero element of $\mathbf{\Phi}^{\mathbb{Q}}_{z0}$ (that is, $\mathbf{\Phi}^{\mathbb{Q}}_{z0,1} = k^{\mathbb{Q}\$}_{\infty}$ and $\mathbf{\Phi}^{\mathbb{Q}}_{z0,j} = 0$ for $j = 2, \ldots, M$), the matrix $\mathbf{\Phi}^{\mathbb{Q}}_{zz}$ is in ordered real Jordan form with relevant elements (i.e., eigenvalues) collected in the vector $\boldsymbol{\phi}^{\mathbb{Q}}_{zz}$, the reduced-form innovations satisfy $\boldsymbol{\varepsilon}^{\mathbb{Q}}_{z,t+1} \sim iid\, N(0, \mathbf{\Omega}_{zz})$, and $\mathbf{z}_t$ follows an unrestricted VAR(1) process under the historical measure, $\mathbb{P}$. Specifically, we follow the literature and assume that the eigenvalues of $\mathbf{\Phi}^{\mathbb{Q}}_{zz}$ are real, distinct, and less than one in absolute value, and, consequently, we have that $\mathbf{\Phi}^{\mathbb{Q}}_{zz} = \mathrm{diag}(\boldsymbol{\phi}^{\mathbb{Q}}_{zz})$.

By further noticing that $\mathbf{x}_t = \mathbf{W}'\mathbf{y}_t = \mathbf{W}'(\mathbf{a}_{z0} + \mathbf{a}_z \mathbf{z}_t)$ where $\mathbf{a}_{z0}$ and $\mathbf{a}_z$ are the constant and factor bond loadings implied by the JSZ canonical model bond pricing, and using results on invariant transformations of affine term structure models (see Dai and Singleton, 2000, and appendix), JSZ show that any GDTSM that uses state variables that are linear combinations of yields, $\mathbf{x}_t = \mathbf{W}'\mathbf{y}_t$, must satisfy

$$\boldsymbol{\delta}'_x = \mathbf{1}'_M \mathbf{D}^{-1}, \qquad \delta_{x0} = -\boldsymbol{\delta}'_x \mathbf{c}, \tag{4.2}$$

$$\mathbf{\Phi}^{\mathbb{Q}}_{xx} = \mathbf{D}\mathrm{diag}(\boldsymbol{\phi}^{\mathbb{Q}}_{zz})\mathbf{D}^{-1}, \qquad \mathbf{\Phi}^{\mathbb{Q}}_{x0} = (\mathbf{I} - \mathbf{\Phi}^{\mathbb{Q}}_{xx})\mathbf{c} + \mathbf{D}\mathbf{\Phi}^{\mathbb{Q}}_{z0}, \tag{4.3}$$

where $\mathbf{c} = \mathbf{W}'\mathbf{a}_{z0}$ and $\mathbf{D} = \mathbf{W}'\mathbf{a}_z$. As a result, the risk-neutral dynamics of the yield curve (and therefore, the cross-section of interest rates) are entirely determined by (a) $k^{\mathbb{Q}\$}_{\infty}$, the first and only nonzero element of $\mathbf{\Phi}^{\mathbb{Q}}_{z0}$; (b) $\boldsymbol{\phi}^{\mathbb{Q}}_{zz}$, the speed of mean reversion of the state variables under $\mathbb{Q}$; and (c) $\mathbf{\Omega}_{xx}$, the covariance matrix of the innovations from the VAR. On the other hand, the VAR dynamics under $\mathbb{P}$ for the observed factors, $\mathbf{x}_t = \mathbf{W}'\mathbf{y}_t$, remain unrestricted.

Given this separation between risk-neutral and physical dynamics, and the VAR dynamics remaining unrestricted, JSZ propose the following two-step estimator. In the first step, they estimate $\boldsymbol{\Phi}_{x0}$ and $\boldsymbol{\Phi}_{xx}$ by OLS, given that, since the VAR dynamics are unrestricted, OLS recovers the estimates of the conditional mean (Zellner, 1962). In the second step, they estimate the remaining parameters of the model ($k_{\infty}^{\mathbb{Q}\$}$, $\boldsymbol{\phi}_{zz}^{\mathbb{Q}}$, $\boldsymbol{\Omega}_{xx}$) via numerical maximization of the likelihood function taking as given the $\mathbb{P}$-dynamics estimates obtained in the first step. Consequently, JSZ report improved convergence and speed of ML estimation over other canonical representations. Further details on the estimation approach are available in the appendix.

4.3 GDTSM parameter estimates

Yields dynamics. Table 1 summarizes the results from the ML estimation of the GDTSM. In panel a, we present the results of estimating the VAR dynamics for the state variables in equation (2.1). We note that most of the off-diagonal elements of $\boldsymbol{\Phi}_{xx}$ are not statistically significant, as the coefficient of the lagged curvature factor on the slope is the only off-diagonal element of $\boldsymbol{\Phi}_{xx}$ that is statistically different from zero. In contrast, most of the off-diagonal elements of $\boldsymbol{\Omega}_{xx}$ are statistically significant, except for the covariance between the (reduced-form) innovations to the slope and curvature factors.

Panel b presents estimates of the parameters driving the dynamics of the state variables under the risk-neutral measure. In line with previous results in the literature, the dynamics of the state variables under the risk-neutral measure are more persistent than under the physical measure, in that the largest element of $\boldsymbol{\phi}_{zz}^{\mathbb{Q}}$, i.e., the dominant eigenvalue of $\boldsymbol{\Phi}_{xx}^{\mathbb{Q}}$, is larger than the corresponding eigenvalue of $\boldsymbol{\Phi}_{xx}$. In particular, the largest eigenvalue of $\boldsymbol{\Phi}_{xx}^{\mathbb{Q}}$ is very close to one (0.9975), a feature needed to replicate the level factor that characterizes the term structure of U.S. Treasury bond yields. That this eigenvalue lies inside the unit circle is consistent with the stationarity of the risk-neutral dynamics implied by Theorem 1. Further, the eigenvalues of $\mathbf{\Phi}_{xx}^{\mathbb{Q}}$ are all very precisely estimated due to the cross-equation restrictions imposed by the no-arbitrage conditions on the cross-section of interest rates, which we fit with a root mean square pricing error (RMSPE) of less than ten basis points.

Macro dynamics. Finally, panels c and d display the coefficients for both inflation and output growth with respect to the state variables. Specifically, we find that the level factor has a positive and statistically significant effect on both inflation and growth. In addition, both the slope and curvature factors drive inflation dynamics, whereas their effects on output growth are not statistically different from zero.

5 Portfolio-Balance Parameters: Empirical Results

In this section, we use the estimated baseline GDTSM parameters to recover the portfolio-balance model parameters of the U.S. yield curve using the framework discussed in Section 3. Specifically, we calibrate the arbitrageurs' relative risk aversion, γ, to match the price effects of the Federal Reserve's pre-pandemic LSAP supply shocks. We then present our estimated structural impact matrix, $\mathbf{\Sigma}_x$, which we use, together with the remaining parameters that drive the dynamics of the state variables, to recover the set of (estimated) structural shocks, analyze their time-series behaviour, and label them (as hedging-risk-premium, risk-bearing-capacity, and monetary-policy shocks). Finally, we combine the calibrated risk aversion with the estimated structural impact matrix to recover the bond-supply parameters $\boldsymbol{\beta}_{x0}$ and $\boldsymbol{\beta}_x$, which, by Proposition 1, also deliver the prices of the structural risks and thus a reading of how the supply of and the compensation for each fundamental risk vary with the state of the yield curve.

5.1 Calibration of arbitrageurs' relative risk aversion

Similar to Diez de los Rios (2025), we calibrate the arbitrageurs' relative risk aversion coefficient, γ, to match the price effects of the Federal Reserve's pre-pandemic LSAP supply shocks. Specifically, as in Vayanos and Vila (2021), we model central bank purchases of nominal bonds as a change $\Delta s_{x0}^{(n)}$ in the intercept of the (relative) amount of bonds with maturity n supplied to the arbitrageurs at time t (see equation 2.15). Furthermore, we assume that this supply shock (i) is unanticipated, (ii) takes place at time zero, (iii) can be well approximated by a one-factor model, and (iv) reverts deterministically to zero at a rate of ϕ_β:

$$\Delta s_{x0}^{(n)} = s_\beta^{(n)} \Delta\overline{\beta}\phi_\beta^t, \qquad \text{for } n = 1, \ldots, N, \tag{5.1}$$

where the coefficient $s_\beta^{(n)}$ measures the sensitivity of the supply to changes in the (deterministic) factor $\overline{\beta}$.

The following proposition collects the impact of such an increase on bond prices.

Proposition 3. *The impact on the nominal bond prices due to the change in the supply of government bonds given by equation (5.1) satisfies*

$$\Delta b_t^{(n)} = -b_\beta^{(n)} \Delta\overline{\beta}\phi_\beta^t, \tag{5.2}$$

where

$$b_\beta^{(n)} = b_\beta^{(n-1)}\phi_\beta + \gamma \mathbf{b}_x^{(n-1)\prime}\mathbf{\Omega}_{xx}\sum_{j=1}^{N}\left[\mathbf{b}_x^{(j-1)} + \mathbf{p}_x\right] s_\beta^{(j)} \qquad \textit{for } n = 1, \ldots, N, \tag{5.3}$$

where the recursion is initialized with $b_\beta^{(0)} = 0$.

Note that we have estimates for $\mathbf{b}_x^{(n)}$, $\mathbf{p}_x$, and $\mathbf{\Omega}_{xx}$ from the estimation of the baseline GDTSM. Therefore, to use equation (5.3) to calibrate the arbitrageurs' relative risk aversion, we will need to make additional assumptions on (i) the sensitivity of the bond supply to changes in the (deterministic) QE factor $s_\beta^{(n)}$, (ii) the persistence of the QE factor, ϕ_β, and (iii) the size of the QE shock, $\Delta\overline{\beta}$. We now discuss our specific choices in more detail.

Sensitivity of the bond supply to changes in the QE factor. Regarding the sensitivity of the supply to changes in the (deterministic) factor $\overline{\beta}$, we follow Greenwood, Hanson, and Vayanos (2015) and King (2019) and assume that the sequence $\left\{s_\beta^{(n)}\right\}_{n=1}^{N}$ satisfies:

$$s_\beta^{(n)} = 1 - \frac{2n}{N+1}, \tag{5.4}$$

Since $\sum_{n=1}^{N} s_\beta^{(n)} = 0$, we have that this specification for $s_\beta^{(n)}$ implies that the Quantitative Easing purchases reduce the amount of long-term bonds and increase the amount of short-term bonds in equal measure. That is, changes in $\overline{\beta}$ do not alter the total value of bonds available to the arbitrageurs but affect only the weighted-average maturity of their portfolio.[17] Specifically, we have that equation (5.4) implies that the impact on the weighted-average maturity, ΔWAM_t, due to the change in the supply of government bonds given by equation (5.1) is

$$\Delta\text{WAM}_t = \Delta\overline{\beta}\phi_\beta^t \sum_{j=1}^{N} j s_\beta^{(j)}. \tag{5.5}$$

Persistence of the QE factor. Second, following King (2019), we set $\phi_\beta = 0.9608$ to match plausible market expectations regarding the persistence of the Fed's LSAP bond-supply shocks. As noted by King (2019), this value is chosen to match Carpenter et al.'s (2015) finding that market participants expected the Fed's balance sheet to normalize by August 2020, implying an LSAP shock half-life of approximately 4.3 years.

[17]Note that only the weighted sum $\sum_{j=1}^{N} \mathbf{b}_x^{(j-1)} s_\beta^{(j)}$ enters in equation (5.3). Consequently, as noted by King (2019), the exact specification of the individual supply factor loadings, $s_\beta^{(n)}$, is not of first-order importance for the pricing of bonds, as long as it can capture the variation in the duration of the portfolio that the arbitrageur needs to hold.

Size of the QE shock. Finally, we calibrate $\Delta\overline{\beta}$ to ensure that the effect at time zero of the supply shock in equation (5.1) reduces the weighted-average maturity of the portfolio of bonds that arbitrageurs are required to hold by 6.8 quarters (1.7 years). This choice reflects the decline in the weighted-average duration of U.S. Treasury debt resulting from the Federal Reserve's pre-pandemic LSAP programs, as documented by Greenwood, Hanson, Rudolph, and Summers (2016).

Calibrated relative risk aversion. Given these assumptions and the estimates of the GDTSM presented above, and following Greenwood, Hanson, and Vayanos (2015), we choose the arbitrageurs' relative risk-aversion coefficient, γ, to match the price effects of LSAP supply shocks. As noted by Greenwood, Hanson, Rudolph, and Summers (2016), the cumulative reduction of ten-year bond equivalents available to investors due to the LSAP programs implemented between late 2008 and mid-2014 was roughly \$3 trillion. Furthermore, Williams' (2014) summary of QE studies suggests that an LSAP announcement of a \$600 billion purchase of ten-year bond equivalents reduced ten-year yields by between 15 and 25 basis points. Thus, using the midpoint of this range, the total price impact on ten-year yields from all pre-pandemic LSAP announcements is 1%. Specifically, with $\gamma = 16$, we can replicate the result that the effect of a 1.7-year reduction in the weighted-average maturity of the arbitrageurs' portfolio of government bonds is 1%. This calibrated value is somewhat large relative to the range of 1 to 10 typically assumed in the macro-finance literature. That range, however, describes the relative risk aversion of a representative household, whereas the marginal investor in our model is a specialized arbitrageur who absorbs the net supply of long-term government bonds and bears its interest-rate risk, for whom a higher coefficient is natural. Still, it remains substantially smaller than the $\gamma = 100$ used by Hamilton and Wu (2012b).[18]

[18]The price impact in equation (5.3) is linear in γ, while the weighted-average-maturity target used to calibrate $\Delta\overline{\beta}$ does not depend on γ. The implied yield effect therefore scales linearly with risk aversion, so the calibration maps transparently to any alternative value: for the same 1.7-year maturity reduction,

5.2 Structural impact matrix estimate

We now present estimates of the structural shock impact matrix. Panel a of Table 2 presents the estimates of $\mathbf{\Sigma}_x$ obtained by rotating the estimate of $\mathbf{\Omega}_{xx}$ obtained in the GDTSM baseline estimation in the previous section using equation (3.18). Note that, as established in Section 3.3, this estimate does not depend on the calibrated risk aversion; it is a function of the GDTSM estimates alone. The structural shocks and impulse responses analyzed below therefore inherit this independence. We find that all the entries of $\mathbf{\Sigma}_x$ are statistically significant and, consequently, our estimate of $\mathbf{\Sigma}_x$ is neither lower triangular (as implied by a Cholesky-style identification approach) nor symmetric. In fact, the entries above the diagonal of $\mathbf{\Sigma}_x$ are all positive, while the entries below the diagonal are all negative.

Direct inspection of the estimated entries of $\mathbf{\Sigma}_x$ does not reveal any meaningful economic interpretation of the identified shocks. For this reason, we now turn to label the three structural shocks by inspecting the time-series dynamics of the estimated shocks, as well as their impulse-response functions for the yields and macroeconomic variables.

5.3 Impulse-response functions and labelling of the shocks

Figure 2 displays the estimated structural shocks, $\hat{\boldsymbol{\eta}}_{t+1} = \hat{\mathbf{\Sigma}}_x^{-1}\left(\mathbf{x}_{t+1} - \hat{\mathbf{\Phi}}_{x0} - \hat{\mathbf{\Phi}}_{xx}\mathbf{x}_t\right)$, and Figures 3, 4, and 5 present the impulse-response functions of the variables in the model to a one-standard-deviation increase in each one of these shocks.

Before examining the characteristics of each of the three structural shocks, we advance that our approach identifies the following three shocks: a hedging-risk-premium shock (as in Cieslak and Pang, 2021), a risk-bearing-capacity shock (as in Gertler and Karadi, 2011), and a monetary-policy shock (as in Christiano, Eichenbaum, and Evans, 1999). These three shocks have the characteristics of aggregate demand shocks, in which inflation and output

$\gamma = 10$ implies a yield effect of 62.5 basis points.

growth move in the same direction (see, e.g., Blanchard and Quah, 1989). Interestingly, none of these three shocks has the characteristics of an aggregate supply shock, which typically affects inflation and output growth in opposite directions. Because the structural shocks are recovered entirely from bond-yield data, our approach recovers only the shocks that move the yield curve, namely those spanned by the pricing factors; our analysis of inflation therefore concerns its spanned component. Aggregate supply shocks transmit only weakly to yields: over recent decades, the Federal Reserve has responded much less strongly to supply-driven inflation (see Hofmann, Manea, and Mojon, 2024), so these shocks pass only faintly into the expected path of the short rate, and hence into bond yields. Their weak transmission also makes aggregate supply shocks, at most, a minor and weakly priced component of yield-curve risk, which is why they do not emerge among our three structural shocks.[19]

Hedging-risk-premium shock (#1). The impulse responses of the first shock are displayed in Figure 3. On impact, a one-standard-deviation increase in the first shock immediately and unambiguously raises both inflation and output growth. Over the short run (1–4 quarters) and the medium run (5–8 quarters), the responses for both variables remain positive but begin a gradual decline. The effects of this shock, however, are highly persistent, remaining positive even at longer horizons (9–40 quarters).

The short-term nominal interest rate also rises immediately upon impact, but unlike inflation and output growth, it follows a hump-shaped trajectory. In the short run, the nominal short rate continues to increase as monetary policy "leans against" the inflationary

[19] A model with four pricing factors uncovers a shock with aggregate-supply characteristics, but the identification of this shock is fragile. Recall that, by equation (3.18), the rotation is unique only if the eigenvalues of $\widetilde{\mathbf{B}}$ are distinct, which holds at three factors, where the eigenvalues of $\widetilde{\mathbf{B}}$ are 1.18, 8.19×10^{-3}, and 2.97×10^{-5}, so that consecutive eigenvalues differ by more than two orders of magnitude. On the other hand, with four factors the eigenvalues are 0.586, 1.17×10^{-2}, 3.07×10^{-3}, and 4.95×10^{-5}, so that two of them differ by a factor of only about four, against factors above fifty for the other pairs. This proximity leaves $\mathbf{\Sigma}_x$ potentially weakly identified. Given this finding, and that the fourth factor explains only an additional 0.08% of the cross-sectional variation in yields, we interpret the aggregate-supply shock found at four factors as confirmation that aggregate supply risk is, at most, a minor and weakly priced component of the yield curve.

pressures. The response peaks roughly six to eight quarters after the shock and then declines gradually, remaining positive in the medium and long run, consistent with the shock's strong persistence. This delayed hump is consistent with a deliberate interest-rate smoothing motive by the Federal Reserve, through which the central bank spreads a series of smaller interest rate hikes over several quarters rather than implementing a large increase (thereby adjusting its stance while limiting volatility in interest rates). Decomposing the nominal short-term rate reveals that (i) the expected-inflation component jumps on impact but drifts down gradually; (ii) the real short rate increases by more than the contemporaneous rise in expected inflation, implying a monetary-policy tightening in terms of the real rates; and (iii) the contribution of the inflation risk premium is practically negligible. Collectively, these features are consistent with a systematic, smoothed monetary-policy reaction function that raises real rates in response to an expansionary, inflationary impulse: a defining attribute of an aggregate demand shock.

Consistent with this aggregate-demand interpretation, a positive shock induces a broad-based rise in nominal bond yields across the maturity spectrum. The rise in yields is front-loaded but long-lived, and it is more pronounced for long-term bond yields, resulting in a temporary steepening of the nominal yield curve. Decomposing long-term yields into their expectations and term-premium component reveals two distinct channels: (i) an upward revision to the expected path of the policy rate, and (ii) a contemporaneous increase in the compensation investors demand for holding nominal bonds.

The expectations component of nominal bond yields rises on impact because the shock lifts the expected path of the short-term nominal rate. As discussed above, the monetary-policy response is gradual, with the central bank deliberately spreading rate hikes over several quarters, and this expectation of a smoothed tightening is reflected in the average path of future short-term nominal rates. The contribution of the expectations component is largest for shorter maturities and diminishes as maturity increases. This pattern is consistent with the transitory nature of the shock: although persistent, its effects fade over the long horizon, limiting the influence on the medium- and long-term expectations that dominate 10- and 30-year yields.

The term premium also rises on impact and remains persistently elevated. Unlike the expectations component, its contribution to the total yield response increases with maturity. Importantly, the response of the term premium is positively correlated with output growth (i.e., procyclical). Interpreted through the portfolio-balance lens, positive realizations of the shock (when term premia rise) are associated with conditions in which investors rotate out of safe assets (reducing the demand for nominal bonds) or with markets needing to absorb greater bond supply (potentially due to fiscal expansions). Conversely, negative realizations of the shock (when term premia fall) can coincide with flight-to-safety episodes (increasing demand for nominal bonds) or with central bank purchases that reduce the duration risk investors must bear.

This correlation pattern is reminiscent of the hedging-risk-premium shock identified by Cieslak and Pang (2021). These authors estimate a VAR on daily yield changes and daily log stock returns and identify a hedging-risk-premium shock using sign restrictions by imposing that this shock affects the term-premium component of long-term yields more strongly than that of short-term yields, and that this shock induces a positive comovement between yields and growth (which they proxy by stock returns). Although our shock is recovered under an entirely different identification strategy (a quantity-orthogonality restriction on bond supply), its response pattern satisfies both of Cieslak and Pang's identifying restrictions.

Moreover, a narrative reading of the time series of the estimated shock on the top panel of Figure 2 further reinforces the interpretation of the first shock as a hedging-risk-premium shock.[20] The most negative realization occurred in 2011Q3, when the United States faced the debt-ceiling crisis culminating in S&P's first-ever downgrade of U.S. sovereign debt on August 5, 2011, followed shortly thereafter by the Federal Reserve's announcement of its Maturity Extension Program on September 21 (a $400 billion maturity-swap designed to lengthen the duration of the Fed's Treasury holdings). Both developments are consistent with a compression of term premia, as investors sought refuge in safe assets while the Fed simultaneously removed duration risk from the market.[21]

The second-most negative shock realization occurred in 2008Q4, at the height of the global financial crisis. During this quarter, the U.S. government enacted the Troubled Asset Relief Program (TARP) on October 3, the Fed announced its first large-scale asset-purchase program (QE1) on November 25, involving purchases of GSE and MBS debt, and cut the funds rate to 0–0.25% on December 16. Similarly, in 2020Q1, the onset of COVID-19 prompted two emergency rate cuts (on March 3 and March 15), a return to the zero lower bound, and renewed large-scale asset purchases, with the FOMC committing on March 23 to buy Treasuries and agency MBS "in the amounts needed" to restore market functioning. These measures again reduced the amount of debt the market needed to absorb, compressing term premia and yielding the third most negative shock value. Other episodes in the negative tail of the shock distribution include the Savings and Loan crisis, which reached its height with the federal seizure of Lincoln Savings and Loan (1989Q2), and the Black Monday crash of October 19, 1987 (1987Q4). Notably, the most positive realization of the shock occurred in 1987Q3, indicating that the Black Monday stock market crash was preceded by a period

[20] The estimated shocks are innovations dated at the end of each quarter, so their alignment with historical episodes reflects what was unanticipated as of the quarter's close rather than the calendar timing of the events.

[21] Although the downgrade should, in principle, have raised U.S. borrowing costs, it instead triggered a flight to safety into U.S. Treasuries: yields fell rather than rose, as global investors moved capital into dollar-denominated sovereign debt despite the reduction in its credit rating (an outcome widely cited as evidence of the enduring role of U.S. government securities as the world's benchmark safe asset and the U.S. dollar as the pre-eminent reserve currency). See `https://www.marketwatch.com/story/us-treasury-yields-fall-despite-downgrade-2011-08-08`.

of reduced demand for government bond assets and higher term premia as investors shifted towards riskier holdings.

On the other side, the positive tail of the shock distribution seems to align with news of fiscal expansions and elevated bond issuance. The second most positive shock realization in 2021Q1 coincided with the signing of the American Rescue Plan Act on March 11, 2021, amid large fiscal stimulus and substantial Treasury issuance to support the post-pandemic recovery. Similarly, a large positive spike in 2009Q2, with a smaller one in 2009Q1, corresponds to the fiscal push associated with the American Recovery and Reinvestment Act signed on February 17, 2009, designed to counteract the global financial crisis. A further notable spike occurs in 2016Q4, coinciding with the U.S. presidential election (November 8, 2016) and the widely discussed "reflation trade," during which markets priced expectations of larger deficits and infrastructure spending.

Risk-bearing-capacity shock (#2). Similar to the hedging-risk-premium shock, a one-standard-deviation increase in the second shock raises inflation and output growth on impact, with responses that remain positive over the short and medium run and decay only gradually at longer horizons (Figure 4). The short-term nominal rate rises immediately and follows a hump-shaped path, reflecting a policy reaction that raises real rates by more than expected inflation from the second quarter onward. The expectations components of longer-maturity yields rise because the expected path of the policy rate shifts up. The impact on the inflation risk premium in the nominal short rate is negligible. Again, these features are broadly consistent with the dynamics of an aggregate-demand shock and are similar to those observed for the hedging-risk-premium shock.

The main distinguishing feature between the second structural shock and the hedging-risk-premium shock is that term premia fall on impact at the ten- and thirty-year maturities but are essentially unchanged at the two-year maturity. This results in the net yield response being stronger at the short end of the curve: the two-year yield rises the most, the ten-year yield increases only modestly, and the thirty-year yield declines slightly. The immediate consequence is a flattening of the nominal yield curve. This flattening is in sharp contrast to the hedging-risk-premium shock, in which term premia rise, and the yield curve temporarily steepens. Importantly, unlike in the hedging-risk-premium shock, the term-premium response here is countercyclical, declining as economic activity rises.

Interpreted through the portfolio-balance lens, this shock aligns with a Gertler and Karadi (2011) shock that varies intermediaries' risk-bearing capacity and investors' risk appetite, thereby altering the required compensation for holding long-duration nominal bonds. Negative realizations capture financial crisis-style episodes in which balance-sheet constraints tighten, market intermediation weakens, and term premia, especially at the long end, rise even as growth softens and policy eases. Positive realizations correspond to expansion phases with ample risk capacity and orderly market functioning, during which the required compensation for holding long-duration assets falls even while the expected policy path shifts upward.

Consistent with this interpretation, the time series of the second structural shock, displayed in the middle panel of Figure 2, exhibits large negative realizations clustered around episodes of acute financial stress: that is, episodes in which the risk-bearing capacity of financial intermediaries is impaired, and investors require additional compensation for holding duration risk. Specifically, we find that the most negative value for the second structural shock occurs in 2008Q1, as the first phase of the Global Financial Crisis crystallized. After months of funding strain, the U.K. government nationalized Northern Rock (February 22, 2008), a salient signal of the banking system's fragility. In the United States, market pressure on Bear Stearns escalated despite Fed liquidity provision (March 14), culminating in its acquisition by JPMorgan the following weekend and the creation of Maiden Lane to warehouse illiquid assets. These events are consistent with a sudden tightening of intermediary balance-sheet constraints and heightened risk aversion.

A similarly large negative realization appears in 2001Q3, which included the financial market repercussions of the September 11 attacks as markets remained closed for several days, reopened to sharp declines, and the Federal Reserve cut its policy rate as part of a broad effort to stabilize funding and payments. Again, this pattern is consistent with a sudden deterioration in risk-bearing capacity and an increase in term premia even if the expectations component of yields fell with policy easing. Additional negative spikes align with earlier stress episodes: the dissolution of the Soviet Union (1991Q4) and the subsequent European currency turmoil (1992Q2–Q3), including the U.K.'s forced exit from the ERM, both of which tightened global funding conditions; the Long-Term Capital Management collapse (1998Q3), which directly impaired dealer intermediation; and the corporate-governance shocks surrounding WorldCom's accounting revelations and bankruptcy alongside the passage of Sarbanes–Oxley (2002Q2–Q3). In each case, narratives point to binding balance-sheet constraints or investors' confidence declines that raise term premia while the expectations component declines as contemporaneous monetary policy eases.

On the other side of the distribution, positive realizations align with expansionary phases in which expectations of a higher policy path coexist with subdued term premia at the long end of the yield curve. The most positive risk-bearing-capacity shock occurred in 2022Q1, when the Federal Reserve ended net asset purchases in early March and delivered its first rate increase since 2018 in mid-March. With the Fed's balance sheet still exceptionally large at that time and market functioning orderly, the expected path of the short rate shifted up. At the same time, the required compensation for holding long-duration nominal bonds remained compressed: exactly the combination that yields a front-loaded rise in short and intermediate maturities and a relatively contained movement in the long end of the yield curve. A second illustrative case spans the Mexican peso crisis. Although the peso devaluation was announced on December 20, 1994, the broader "Tequila" effects propagated well into 1995Q1. Our identification records 1994Q4 as an expansionary-expectations phase, consistent with firming policy-rate expectations and low term premia, followed by a sharp negative realization in 1995Q1 as the crisis unfolded, risk tolerance receded, and the compensation demanded for bearing duration risk rose.

Importantly, the characteristics of our risk-bearing-capacity shock also resemble those of the common-risk-premium shock identified in Cieslak and Pang (2021): a shock that affects the term-premium component of long-term yields more strongly than that of short-term yields, yet induces a negative correlation between the term premium and economic activity. These authors attribute this shock to the discount rate risk premium that drives the common component of the compensation demanded by both stock and bond investors. Our risk-bearing-capacity shock exhibits the same pattern: a stronger effect on long-term bond premia and negative comovement between the term premium and economic activity, as in Cieslak and Pang's (2021) common-risk-premium shock. While we do not pursue this research avenue further, our results thus seem to suggest a relationship between the shocks to the common discount rate risk premium demanded by stock and bond investors and the risk-bearing capacity of financial intermediaries.

Monetary-policy shock (#3). Finally, we present the impulse responses related to a one-standard-deviation increase in the third identified shock in Figure 5. On impact, both inflation and output growth decline, with output growth falling by somewhat more than inflation. In addition, the magnitudes of the declines are much smaller in absolute value than those of the other two shocks, and the effects are more short-lived. Specifically, we find that the impulse responses return to baseline by roughly the tenth quarter. Further, when comparing the behaviour of the short-term nominal interest rate with that of the previous two shocks, we note that (i) the nominal short rate jumps sharply on impact without the delayed, hump-shaped adjustment consistent with the gradual policy reaction to an expansionary impulse observed under the hedging-risk-premium and risk-bearing-capacity shocks, and (ii) this shock is negatively correlated with inflation and output growth. In fact, this pattern of an immediate, front-loaded rate increase coinciding with contractions in inflation and activity suggests a monetary-policy-tightening interpretation of this shock (i.e., Christiano, Eichenbaum, and Evans, 1999).

Again, we corroborate the interpretation of the shock through a narrative approach (bottom panel of Figure 2): large negative shock realizations coincide with recessions or financial crisis episodes, during which monetary policy eases to cushion the downturn. The pattern is evident around the early-1990s recession, the dot-com bust of the early 2000s, the Great Recession (2008–09), the COVID-19 collapse in 2020, and the 1987Q4 "Black Monday" crash.

Interestingly, the estimated shocks corresponding to the 2022–24 Federal Reserve tightening cycle illustrate how our identification strategy can separate the estimated monetary-policy stance from the monetary-policy rate level. We estimate the 2022Q1 shock to be strongly negative even as the Federal Reserve delivered its first post-pandemic rate increase of 25 basis points on March 16 and signalled further hikes alongside plans to shrink its balance sheet. We assess this negative (expansionary) shock to be consistent with markets judging that, given the inflation backdrop, a larger initial hike was probably warranted. In fact, contemporary market commentary emphasized the slow pivot from crisis-era accommodation and discussed whether the Fed was "behind the curve" heading into liftoff.[22] Subsequent commentary continued to characterize the Fed's policy as catching up to price

[22]See, e.g., El-Erian (2022).

pressures throughout 2022. As inflation remained elevated, the Fed accelerated with four successive 75-basis-point hikes (June, July, September, November) and a 50-basis-point hike in December, a sequence that our estimates record as contractionary monetary shocks (making the 2022Q4 estimate the most positive shock in the sample). Notably, 2023Q1 also ranks among the most positive policy shocks in the sample, despite corresponding to only two 25-basis-point increases (February 1 and March 22), reflecting the information content of communication and guidance—re-anchoring expectations towards a higher-for-longer path even as the step size slowed. Overall, this sequence of shocks fits the "late-then-catch-up" narrative discussed in Bordo, Cochrane, and Taylor (2023, 2024): an initially insufficient move relative to inflation conditions, followed by outsized hikes and accelerated balance-sheet normalization that surprised to the hawkish side.

5.4 Bond supply parameter estimates

Having calibrated γ and estimated $\boldsymbol{\Sigma}_x$, we recover the bond-supply parameters $\boldsymbol{\beta}_{x0}$ and $\boldsymbol{\beta}_x$ from equations (3.22) and (3.23). By Proposition 1, these supply loadings are also, up to the positive scaling $1/\gamma$, the prices of the corresponding structural risks. Panel b of Table 2 therefore reports, at once, how the supply of and the compensation required for each fundamental risk vary with the level, slope, and curvature of the yield curve. This joint reading is unavailable in a reduced-form GDTSM, which pins down the total price of interest-rate risk but not its allocation across economically distinct shocks. That allocation depends on the rotation $\boldsymbol{\Sigma}_x$, which the quantity-orthogonality restriction recovers from the economics of bond supply. Note that risk aversion enters $\boldsymbol{\beta}_x$ only through the positive factor $1/\gamma$, so the signs and statistical significance reported below do not depend on the calibration; only the intercept $\boldsymbol{\beta}_{x0}$ varies non-trivially with γ.

The estimated supply structure, read through this lens, is sparse and concentrated. Only two of the three risks exhibit systematic state dependence: the supply and price of hedging-risk-premium risk vary with the slope of the curve, and those of monetary-policy risk with its level and slope. Risk-bearing-capacity risk shows no systematic state dependence, and curvature has no explanatory power for the time-variation of the supply of any of the three shocks.

The supply of hedging-risk-premium risk depends on a single factor. Its slope loading is positive and significant at the 10% level, while the intercept, level, and curvature coefficients are small or imprecisely estimated. Recall that a higher slope factor corresponds to a flatter, or even inverted, yield curve (see Figure 1). The positive loading therefore implies that both the supply of and the price of hedging-risk-premium risk rise when the curve flattens or inverts. A flat or inverted curve is itself among the most reliable predictors of recessions (see, e.g., Estrella and Hardouvelis, 1991; Estrella and Mishkin, 1998), and the market therefore demands greater compensation for bearing hedging-risk-premium risk ahead of economic downturns.

The supply of risk-bearing-capacity risk, on the other hand, shows no clear state dependence. None of the coefficients in its row is statistically distinguishable from zero, including the intercept, so neither the supply of nor the price of this risk varies systematically with the shape of the curve.

The supply of monetary-policy risk, in contrast, exhibits strong state dependence. Its intercept is positive and significant at the 10% level, indicating a positive average supply of this risk. More importantly, the loading on the level factor is negative and significant at the 1% level, while the loading on the slope factor is positive and significant at the 5% level. The curvature loading, by contrast, is not statistically distinguishable from zero. This configuration implies that both the supply of and the price of monetary-policy risk rise as the level of interest rates falls, or the yield curve flattens or inverts. To the extent that the level of interest rates tracks the business cycle, low in recessions and higher in expansions, the compensation for monetary-policy risk is countercyclical, rising when the economy weakens and falling as it strengthens. The positive slope loading, mirroring that of hedging-risk-premium risk, reinforces this countercyclicality, since a flatter or inverted curve tends to foreshadow recessions.

Read together, the two risks whose compensation varies with the state both carry it countercyclically. The price of hedging-risk-premium risk rises ahead of recessions and that of monetary-policy risk both ahead of and during them, consistent with the general prediction that the compensation for risk is highest in bad times (see, e.g., Fama and French, 1989; Campbell and Cochrane, 1999).

6 Variance Decompositions

We now construct variance decompositions to gauge the relative contributions of the hedging-risk-premium, risk-bearing-capacity, and monetary-policy shocks to forecast variances. These show the proportion of the forecast variance attributable to each shock and are closely related to the impulse-response functions presented in the previous section. Table 3 summarizes these results and shows a sharp segmentation of yield-curve risk. Movements at the long end are overwhelmingly a hedging-risk-premium phenomenon. By contrast, short-rate variability is dominated on impact by monetary-policy shocks and at medium horizons by risk-bearing-capacity shocks.

Nominal short-term rate i_t. Consistent with its interpretation as a monetary-policy shock, this shock accounts for half of the one-quarter-ahead forecast variance of the nominal short-term rate (49.47%), with the risk-bearing-capacity and risk-premium shocks explaining the remainder (35.98% and 14.56%, respectively). As the forecast horizon increases, the explanatory power of the risk-bearing-capacity shock becomes dominant (59.69% and 63.45% at the one- and ten-year forecast horizons, respectively), the risk-premium shock becomes a more important driver of the short-term interest rate (19.52% and 32.12% at the one- and ten-year forecast horizons, respectively), and the explanatory power of the monetary-policy shock declines steadily, becoming small in the long run (20.79% and 4.42% at the one- and ten-year forecast horizons, respectively). This pattern is consistent with (i) monetary-policy shocks that move the policy rate on impact but have little persistence, and (ii) hedging-risk-premium and risk-bearing-capacity shocks that propagate into medium- and long-run rate variability.

Inflation π_t and output growth g_t. The risk-bearing-capacity shock accounts for an overwhelming proportion of the short- and medium-term volatility of inflation (over 80% at both horizons), with the hedging-risk-premium shock explaining almost the remainder and the role of the monetary-policy shock being negligible. At the ten-year forecast horizon, the risk-bearing-capacity shock remains the main driver of the inflation forecast variance (70.73%). Still, the role of the hedging-risk-premium shock increases, accounting for close to 30% of this variance (28.69%).

Similar to the inflation variance decompositions, the risk-bearing-capacity shock accounts for the majority of the one-quarter-ahead variance in output growth (56.27%). Still, its share declines as the forecast horizon increases (51.90% and 40.96% at the one- and ten-year forecast horizons, respectively). Conversely, the contribution of the hedging-risk-premium shock increases steadily with the forecast horizon (34.92% and 41.75% at the one-quarter and one-year forecast horizons, respectively), overtaking the contribution of the risk-bearing-capacity shock at the ten-year forecast horizon (56.06%). Again, consistent with the low persistence of the monetary-policy shock, the contribution of this shock is small (8.81% at the one-quarter horizon and 2.98% at the ten-year forecast horizon).

Two-year nominal yield $y_t^{(2y)}$. The proportion of the forecast variance of the two-year nominal yield is a near even split between the hedging-risk-premium and risk-bearing-capacity shocks at all horizons (47.40% vs. 50.70% at the one-quarter horizon, and 52.64% vs. 46.95% at the ten-year horizon). Once again, the monetary-policy shock has a negligible contribution to the forecast variance.

This symmetry reflects the medium-run nature of the two-year segment of the yield curve: close enough to the short end of the yield curve that its expectations component is sensitive to the factors driving the medium-term dynamics of the short-term nominal rate (largely driven by risk-bearing-capacity shocks as mentioned earlier), yet risky enough that its term-premium component loads on the hedging-risk-premium shock. Indeed, our results suggest that the risk-bearing-capacity shock accounts for roughly two-thirds of the forecast variance in the expectations component of the two-year yield at short and medium horizons (69.45% and 71.96%, respectively), declining slightly to 63.70% at the ten-year horizon, with most of the remainder explained by the hedging-risk-premium shock. The forecast variance of the term-premium component of the two-year yield, on the other hand, is almost entirely driven by the hedging-risk-premium shock (89.57% and 91.66% at the one-quarter and ten-year forecast horizons, respectively).

Ten-year nominal yield $y_t^{(10y)}$. The forecast variance of the ten-year nominal yield is overwhelmingly driven by hedging-risk-premium shocks at all horizons. At the one-quarter horizon, hedging-risk-premium shocks account for nearly all variation (96.31%), with the risk-bearing-capacity shock explaining the small remainder (3.69%) and the monetary-policy shock having no discernible effect. This pattern persists at medium horizons. Although the contribution of risk-bearing-capacity shocks rises slightly at the ten-year horizon (13.82%), the hedging-risk-premium shock remains dominant (85.71%). In contrast, monetary-policy shocks continue to play no meaningful role.

This dominance reflects the long-run nature of the ten-year segment of the yield curve, in which movements are driven primarily by the term premium rather than by near-term monetary-policy expectations. Indeed, the hedging-risk-premium shock explains the large majority of the forecast variance in the ten-year term premium at both short and long horizons (86.03% and 88.19% at the one-quarter and ten-year horizons, respectively). In contrast, the expectations component is driven mostly by the risk-bearing-capacity shock at all horizons (roughly 62% at short and medium horizons), with the hedging-risk-premium shock gaining ground at the long end but not overtaking it (46.22% versus 53.54% at the ten-year horizon).

7 Implied Monetary Policy Rule

The nominal short-term interest rate impulse responses to the hedging-risk-premium and risk-bearing-capacity shocks suggest a systematic response of the Federal Reserve to movements in inflation and output growth. In this section, we make this connection explicit by inferring the Federal Reserve's implied monetary-policy rule over our sample and interpreting the monetary-policy shock as the innovation to this rule.

7.1 Taylor-rule specification

Similar to BCZZ, we assume that there is a central bank that sets a target for its monetary policy using a nominal short-term interest rate feedback rule. Specifically, we assume that the target for the short-term nominal interest rate, i_t^R, depends on the h-period-ahead expected inflation, $\mathrm{E}_t\pi_{t+h}$, and the h-period-ahead output growth, $\mathrm{E}_t g_{t+h}$:

$$i_t^R = \psi_0 + \psi_\pi \mathrm{E}_t \pi_{t+h} + \psi_g \mathrm{E}_t g_{t+h}, \tag{7.1}$$

where ψ_0, ψ_π, and ψ_g are policy parameters. When $h > 0$, equation (7.1) captures a forward-looking Taylor rule as in Clarida, Galí, and Gertler (1998).[23]

Following BCZZ, we further assume that the implementation of this rule is subject to discretion in that the actual observed short-term nominal interest rate, i_t, is the sum of the target rate, i_t^R, and a policy discretion term, u_t:

$$i_t = i_t^R + u_t = \psi_0 + \psi_\pi \mathrm{E}_t \pi_{t+h} + \psi_g \mathrm{E}_t g_{t+h} + u_t, \tag{7.2}$$

where we assume that the discretion term is a linear function of the state variables:

$$u_t = \boldsymbol{\psi}_x' \mathbf{x}_t, \tag{7.3}$$

and where $\boldsymbol{\psi}_x$ is an unrestricted vector of unknown parameters. As noted by BCZZ, this framework nests, under appropriate restrictions on the parameters of this model, (a) the case in which the policy discretion term u_t is *iid* noise, (b) u_t is a stationary exogenous Gaussian AR(1) process, or (c) u_t depends on all or a subset of the state variables in $\mathbf{x}_t$.

7.2 Identification and estimation of the implied policy rule

As with BCZZ, introducing a monetary-policy rule into our term-structure model raises yet another identification problem (in addition to identifying the portfolio-balance model parameters and the structural shocks).

Specifically, note that by matching coefficients in equations (2.4) and (7.2) we have the $M + 1$ cross-equation restrictions:

$$\boldsymbol{\delta}_x' = \psi_\pi \mathbf{p}_x' \boldsymbol{\Phi}_{xx}^h + \psi_g \mathbf{g}_x' \boldsymbol{\Phi}_{xx}^h + \boldsymbol{\psi}_x', \tag{7.4}$$

$$\delta_{x0} = \psi_0 + \psi_\pi \left[p_{x0} + \mathbf{p}_x' (\mathbf{I} - \boldsymbol{\Phi}_{xx})^{-1} (\mathbf{I} - \boldsymbol{\Phi}_{xx}^h) \boldsymbol{\Phi}_{x0} \right] + \psi_g \left[g_{x0} + \mathbf{g}_x' (\mathbf{I} - \boldsymbol{\Phi}_{xx})^{-1} (\mathbf{I} - \boldsymbol{\Phi}_{xx}^h) \boldsymbol{\Phi}_{x0} \right]. \tag{7.5}$$

[23]Note that Taylor's (1993) original rule used the output gap instead of output growth. For this reason, and as is standard in the macro-finance literature, we slightly abuse the conventional terminology and continue to refer to the monetary-policy rule in equation (7.1) as a Taylor rule.

Again, we can formally assess the identification of the monetary-policy rule's parameters by comparing the number of restrictions imposed on the short-term nominal rate process by this rule with the number of new parameters introduced. Specifically, the total number of restrictions implied by equations (7.4) and (7.5) is $M + 1$. In contrast, the new parameters introduced by the Taylor rule are ψ_0, ψ_π, ψ_g, and $\boldsymbol{\psi}_x$. This yields $M + 3$ free parameters. Therefore, we have that the number of free parameters in the monetary-policy rule exceeds the number of restrictions implied by equations (7.4) and (7.5). Consequently, and as discussed by BCZZ, the Taylor rule is generally underidentified without additional assumptions.

We identify the parameters of the Taylor rule in equation (7.1) by interpreting the monetary-policy shock as the innovation to the discretionary term, u_t:

$$u_{t+1} - \mathrm{E}_t u_{t+1} = \sigma_u \mathbf{e}_3' \boldsymbol{\eta}_{t+1}, \tag{7.6}$$

where, since we have that the third shock in $\boldsymbol{\eta}_t$ corresponds to the monetary-policy shock identified above, $\mathbf{e}_3$ is an $(M \times 1)$ vector of zeros with a one in the third position. Note that, while the literature on the identification of monetary-policy shocks usually estimates monetary-policy shocks from the discretionary monetary-policy term implied by a pre-specified monetary-policy rule (see Ramey, 2016, for a review of the literature), here we take the opposite direction: we try to estimate the monetary-policy rule that would be consistent with a pre-specified monetary-policy shock (i.e., the one we estimated in Section 5 above).

Substituting the expression for $\boldsymbol{\eta}_t$ in equation (2.1) in (7.6) we have that

$$u_{t+1} - \mathrm{E}_t u_{t+1} = \underbrace{\sigma_u \mathbf{e}_3' \boldsymbol{\Sigma}_x^{-1} \mathbf{x}_{t+1}}_{u_{t+1}} - \underbrace{\sigma_u \mathbf{e}_3' \boldsymbol{\Sigma}_x^{-1} \left(\boldsymbol{\Phi}_{x0} + \boldsymbol{\Phi}_{xx} \mathbf{x}_t\right)}_{\mathrm{E}_t u_{t+1}}. \tag{7.7}$$

Thus, equating coefficients between equations (7.3) and (7.7), we have that $\boldsymbol{\psi}_x' = \sigma_u \mathbf{e}_3' \boldsymbol{\Sigma}_x^{-1}$.

Further, substituting this expression for u_t, as well as those for inflation, π_t, and output growth, g_t, in equations (2.2) and (2.3) into the expression for the short-term nominal rate implied by the Taylor rule in equation (7.2), we obtain

$$\begin{aligned} i_t = &\left\{\psi_0 + \psi_\pi \left[p_{x0} + \mathbf{p}_x'(\mathbf{I} - \mathbf{\Phi}_{xx})^{-1}(\mathbf{I} - \mathbf{\Phi}_{xx}^h)\mathbf{\Phi}_{x0}\right] + \psi_g \left[g_{x0} + \mathbf{g}_x'(\mathbf{I} - \mathbf{\Phi}_{xx})^{-1}(\mathbf{I} - \mathbf{\Phi}_{xx}^h)\mathbf{\Phi}_{x0}\right]\right\} \\ &+ \left(\psi_\pi \mathbf{p}_x' \mathbf{\Phi}_{xx}^h + \psi_g \mathbf{g}_x' \mathbf{\Phi}_{xx}^h + \sigma_u \mathbf{e}_3' \mathbf{\Sigma}_x^{-1}\right) \mathbf{x}_t. \end{aligned} \tag{7.8}$$

Finally, matching coefficients for the loadings on $\mathbf{x}_t$ with those in the expression for the nominal short-rate, i_t, in equation (2.4) delivers the following set of linear equations:

$$\left[(\mathbf{\Phi}_{xx}^h)'\mathbf{p}_x \quad (\mathbf{\Phi}_{xx}^h)'\mathbf{g}_x \quad (\mathbf{\Sigma}_x^{-1})'\mathbf{e}_3\right] \begin{pmatrix} \psi_\pi \\ \psi_g \\ \sigma_u \end{pmatrix} = \boldsymbol{\delta}_x. \tag{7.9}$$

Thus, we can plug our estimates of the portfolio-balance parameters obtained above into equation (7.9) and solve for ψ_π, ψ_g, and σ_u to obtain estimates of these coefficients. Note that recovering these three coefficients requires the $(M \times 3)$ matrix in equation (7.9) to have full column rank. In our $M = 3$ specification the system is square, so this amounts to requiring that this matrix be non-singular. Estimates of ψ_0 and $\boldsymbol{\psi}_x$, on the other hand, follow from[24]

$$\begin{aligned} \psi_0 = \delta_{x0} &- \psi_\pi \left[p_{x0} + \mathbf{p}_x'(\mathbf{I} - \mathbf{\Phi}_{xx})^{-1}(\mathbf{I} - \mathbf{\Phi}_{xx}^h)\mathbf{\Phi}_{x0}\right] \\ &- \psi_g \left[g_{x0} + \mathbf{g}_x'(\mathbf{I} - \mathbf{\Phi}_{xx})^{-1}(\mathbf{I} - \mathbf{\Phi}_{xx}^h)\mathbf{\Phi}_{x0}\right], \end{aligned} \tag{7.10}$$

$$\boldsymbol{\psi}_x' = \sigma_u \mathbf{e}_3' \mathbf{\Sigma}_x^{-1}. \tag{7.11}$$

Panel a of Table 4 presents the estimates of the Taylor rule coefficients using this approach for $h = 0$ (contemporaneous rule), while panel b presents the results for $h = 4$ (one-year ahead forward-looking rule). Asymptotic standard errors are calculated using the Delta method. The coefficients of the Taylor rule are, however, very imprecisely estimated. The point

[24] Importantly, we note that the model fit remains unchanged from that presented above for the portfolio-balance model since this identification scheme does not affect δ_{x0} and $\boldsymbol{\delta}_x$.

estimate of the inflation coefficient is less than one in the contemporaneous rule (0.55) and greater than one in the forward-looking rule (1.67), a pattern that would suggest a systematic monetary-policy component that "looks through" short-term fluctuations in inflation while responding more than proportionally to changes in one-year-ahead inflation expectations. Note, however, that we cannot reject the hypothesis that the inflation coefficient equals one in either specification ($t = -0.33$ and $t = 0.48$, respectively), so we read this pattern as suggestive rather than conclusive.

8 Final Remarks

This paper provides a tractable way to estimate and structurally identify portfolio-balance models of the yield curve using GDTSM tools. We show that, under stationary physical factor dynamics and sufficiently low arbitrageur risk aversion, the portfolio-balance equilibrium is unique, stable, and observationally equivalent to a GDTSM. This result delivers a one-to-one mapping that recovers portfolio-balance parameters from standard GDTSM likelihood estimates. With a supply-factor structure and a "quantity" orthogonality restriction, the mapping also identifies a structural impact matrix and economically interpretable shocks, which we label hedging-risk-premium, risk-bearing-capacity, and monetary-policy shocks, and which we use to study impulse responses, variance decompositions, and the monetary-policy rule implied by the joint yield–macro dynamics.

An area that deserves further investigation is the role of the ZLB for interest rates in the estimation of portfolio-balance models of the yield curve. As shown in King (2019), we would expect the impact of a bond-supply shock to be attenuated when interest rates are near the ZLB, due to the reduction in interest-rate volatility associated with remaining at the ZLB for longer. In his model, the short-term nominal interest rate is modelled as the maximum of a Gaussian shadow short rate and zero: an approach in line with a strand of the literature on empirical yield-curve modelling which extends traditional GDTSMs to deal with the ZLB on interest rates by assuming a shadow rate process for the nominal short-term interest rate (see, e.g., Kim and Singleton, 2012; Christensen and Rudebusch, 2015; Wu and Xia, 2016; among others). Our results suggest that there may be a similar mapping between shadow-rate GDTSMs and portfolio-balance models, which could be exploited to estimate shadow-rate portfolio-balance models. We leave this for further research.

It would also be interesting to extend our framework to incorporate balance-sheet costs faced by arbitrageurs, as emphasized in recent portfolio-balance models of the term structure (see, e.g., He, Nagel, and Song, 2022; Greenwood, Hanson, and Vayanos, 2024; and Hanson, Malkhozov, and Venter, 2024). Motivated by the financial regulations introduced in the aftermath of the Global Financial Crisis, these models maintain the assumption of constant arbitrageur risk aversion but introduce balance-sheet constraints that further limit arbitrageurs' willingness to absorb bond-supply shocks, even in riskless trades. These costs create wedges between arbitrageurs' shadow prices of risk and market prices of risk, and can materially alter the transmission of supply shocks along the yield curve. Extending our estimation and identification strategy to this setting would enable us to quantify balance-sheet constraints and distinguish risk-bearing-capacity shocks from regulatory or funding-driven balance-sheet shocks. Doing so would enhance the economic interpretation of portfolio-balance forces and provide a unified empirical framework linking yield curve dynamics to intermediary balance-sheet conditions.

References

[1] Adrian, T., R. K. Crump, and E. Moench. 2013. "Pricing the Term Structure with Linear Regressions." *Journal of Financial Economics*, 110 (1): 110–38.

[2] Ang, A., and M. Piazzesi. 2003. "A No-Arbitrage Vector Autoregression of Term Structure Dynamics with Macroeconomic and Latent Variables." *Journal of Monetary Economics*, 50 (4): 745–787

[3] Angeletos, G. M. 2002. "Fiscal Policy with Noncontingent Debt and the Optimal Maturity Structure." *Quarterly Journal of Economics*, 117 (3): 1105–1131.

[4] Backus, D. K., M. Chernov, S. E. Zin, and I. Zviadadze. 2022. "Monetary Policy Risk: Rules versus Discretion." *The Review of Financial Studies*, 35 (5): 2308-2344.

[5] Backus, D. K., S. Foresi, and C. I. Telmer. 2001. "Affine Term Structure Models and the Forward Premium Anomaly." *Journal of Finance*, 56 (1): 279–304.

[6] Bajari, P., H. Hong, and S. P. Ryan. 2010. "Identification and Estimation of a Discrete Game of Complete Information." *Econometrica*, 78 (5): 1529–68.

[7] Bauer, M. D., and G. D. Rudebusch. 2014. "The Signaling Channel for Federal Reserve Bond Purchases." *International Journal of Central Banking*, 10 (3): 233-289.

[8] Bhandari, A., D. Evans, M. Golosov, and T. J. Sargent. 2017. "Fiscal Policy and Debt Management with Incomplete Markets." *Quarterly Journal of Economics*, 132 (2): 617–663.

[9] Blanchard, O. J., and D. Quah. 1989. "The Dynamic Effects of Aggregate Demand and Supply Disturbances." *American Economic Review*, 79 (4), 655–673.

[10] Bordo, M. D., J. H. Cochrane, and J. B. Taylor (eds.). 2023. *How Monetary Policy Got Behind the Curve—and How to Get Back*. Hoover Institution Press. Stanford, CA.

[11] Bordo, M. D., J. H. Cochrane, and J. B. Taylor (eds.). 2024. *Getting Monetary Policy Back on Track*. Hoover Institution Press. Stanford, CA.

[12] Calvet, L. E., A. J. Fisher, and L. Wu. 2018. "Staying on Top of the Curve: A Cascade Model of the Term Structure Dynamics." *Journal of Financial and Quantitative Analysis*, 53 (2): 937–963.

[13] Campbell, J. Y., and J. H. Cochrane. 1999. "By Force of Habit: A Consumption-Based Explanation of Aggregate Stock Market Behavior." *Journal of Political Economy*, 107 (2): 205–251.

[14] Campbell, J. Y. and L. M. Viceira. 2002. *Strategic Asset Allocation*. Oxford University Press. Oxford, United Kingdom.

[15] Carpenter, S., J. Ihrig, E. Klee, D. Quinn, and A. Boote. 2015. "The Federal Reserve's Balance Sheet and Earnings: A Primer and Projections." *International Journal of Central Banking*, 11 (2): 237–283.

[16] Christensen, J. H. E., and G. D. Rudebusch. 2012. "The Response of Interest Rates to US and UK Quantitative Easing." *The Economic Journal* 122(564): F385–414.

[17] Christensen, J. H. E., and G. D. Rudebusch. 2015. "Estimating Shadow-Rate Term Structure Models with Near-Zero Yields." *Journal of Financial Econometrics* 13(2): 226–259.

[18] Christiano L. J., M. Eichenbaum, and C. L. Evans. 1999. "Monetary policy shocks: What have we learned and to what end?" *Handbook of Macroeconomics* Vol 1A: 65-148.

[19] Cieslak, A., and H. Pang. 2021. "Common Shocks in Stocks and Bonds." *Journal of Financial Economics* 142 (2): 880–904.

[20] Clarida, R., J. Galí, and M. Gertler. 1998. "Monetary Policy Rules in Practice: Some International Evidence." *European Economic Review*, 42 (6): 1033–1067.

[21] Costain J., G. Nuño, and C. Thomas. 2025. "The term structure of interest rates in a heterogeneous monetary union." *Journal of Finance*, 80 (4): 2389–2434.

[22] Dai, Q., and K. J. Singleton. 2000. "Specification Analysis of Affine Term Structure Models." *Journal of Finance* 55 (5): 1943–78.

[23] Diez de los Rios, A. 2015. "A New Linear Estimator for Gaussian Dynamic Term Structure Models." *Journal of Business and Economic Statistics*, 33 (2): 282-295.

[24] Diez de los Rios, A. 2025. "A Portfolio-Balance Model of Inflation and Yield Curve Determination." *The Review of Asset Pricing Studies*, 15 (2): 121-161.

[25] El-Erian, M. A. 2022. "Fed and ECB Still Behind the Inflation Curve." *Financial Times*, February 7, 2022.

[26] Estrella, A., and G. A. Hardouvelis. 1991. "The Term Structure as a Predictor of Real Economic Activity." *Journal of Finance*, 46 (2): 555–576.

[27] Estrella, A., and F. S. Mishkin. 1998. "Predicting U.S. Recessions: Financial Variables as Leading Indicators." *Review of Economics and Statistics*, 80 (1): 45–61.

[28] Fama, E. F., and K. R. French. 1989. "Business Conditions and Expected Returns on Stocks and Bonds." *Journal of Financial Economics*, 25 (1): 23–49.

[29] Fisher, F. M., 1966. *The Identification Problem in Econometrics*. McGraw-Hill, New York.

[30] Gagnon, J., M. Raskin, J. Remache, and B. Sack. 2011. "The Financial Market Effects of the Federal Reserve's Large-Scale Asset Purchases." *International Journal of Central Banking* 7 (1): 3–43.

[31] Gertler, M., and P. Karadi. 2011. "A Model of Unconventional Monetary Policy." *Journal of Monetary Economics* 58 (1): 17–34.

[32] Gourinchas P.O., W.D. Ray, and D. Vayanos. 2025. "A preferred-habitat model of term premia, exchange rates, and monetary policy spillovers." *American Economic Review* 115, 3788-3824

[33] Greenwood, R., S. G. Hanson and G. Y. Liao. 2018. "Asset Price Dynamics in Partially Segmented Markets." *Review of Financial Studies,* 31: 3307-3343.

[34] Greenwood, R., S. G. Hanson, J. S. Rudolph and L. H. Summers. 2016. "The Optimal Maturity of Government Debt." In: Wessel D. (Ed.), *The $13 Trillion Question: How America Manages Its Debt*. Brookings Institution Press, Washington DC, 1-42.

[35] Greenwood, R., S. G. Hanson, J.C. Stein, A. Sunderam. 2023. "A quantity-driven theory of term premia and exchange rates." *Quarterly Journal of Economics*. 138(4): 2327–89.

[36] Greenwood, R., S. G. Hanson and D. Vayanos. 2015. "Forward Guidance in the Yield Curve: Short Rates versus Bond Supply." NBER Working Paper No. 21750.

[37] Greenwood, R., S. G. Hanson and D. Vayanos. 2024. "Supply and Demand and the Term Structure of Interest Rates." *Annual Review of Financial Economics* 16: 115–51.

[38] Greenwood, R. and D. Vayanos. 2014. "Bond Supply and Excess Bond Returns." *Review of Financial Studies*, 27 (3): 663-713.

[39] Guibaud, S., Y. Nosbusch, and D. Vayanos. 2013. "Bond Market Clienteles, the Yield Curve, and the Optimal Maturity Structure of Government Debt." *Review of Financial Studies*, 26 (8): 1914–1961.

[40] Gürkaynak, R. S., B. Sack, and J. H. Wright. 2007. "The U.S. Treasury Yield Curve: 1961 to the Present." *Journal of Monetary Economics* 54 (8) : 2291–304.

[41] Hamilton, J. D., and J. C. Wu. 2012a. "Identification and Estimation of Gaussian Affine Term Structure Models." *Journal of Econometrics*, 168 (2): 315–31.

[42] Hamilton, J. D., and J. C. Wu. 2012b. "The Effectiveness of Alternative Monetary Policy Tools in a Zero Lower Bound Environment." *Journal of Money, Credit and Banking*, 44 (S1): 3–46.

[43] Hanson S. G., D.O. Lucca, J.H. Wright. 2021. "Rate-amplifying demand and the excess sensitivity of long-term rates." *Quarterly Journal of Economics* 136(3): 1719–81.

[44] Hanson, S. G., A. Malkhozov, and G. Venter. 2024. "Demand-and-Supply Imbalance Risk and Long-Term Swap Spreads." *Journal of Financial Economics.* 154, 103814.

[45] He Z., S. Nagel, and Z. Song. 2022. "Treasury inconvenience yields during the COVID-19 crisis." *Journal of Financial Economics*, 143(1): 57–79.

[46] Hernández de Cos, P. 2025. "Fiscal threats in a changing global financial system." Lecture delivered at the London School of Economics, November 27. Bank for International Settlements.

[47] Hofmann, B., C. Manea, and B. Mojon. 2024. "Targeted Taylor rules: monetary policy responses to demand- and supply-driven inflation." BIS Quarterly Review.

[48] Huberman, G., S. Kandel, and R. F. Stambaugh. 1987. "Mimicking Portfolios and Exact Arbitrage Pricing." *Journal of Finance*, 42 (1): 1–9.

[49] Jansen, K. A. E., W. Li, and L. Schmid. 2025. "Granular Treasury Demand with Arbitrageurs." NBER Working Paper No. 33243.

[50] Jappelli R., L. Pelizzon, M.G. Subrahmanyam. 2023. "Quantitative easing, the repo market, and the term structure of interest rates". SAFE Working Paper Series 395.

[51] Joslin, S., A. Le, and K. J. Singleton. 2013. "Why Gaussian Macro-Finance Term Structure Models Are (Nearly) Unconstrained Factor-VARs." *Journal of Financial Economics* 109 (3): 604–22.

[52] Joslin, S., M. Priebsch, and K. J. Singleton. 2014. "Risk Premiums in Dynamic Term Structure Models with Unspanned Macro Risks." *Journal of Finance* 69, (3): 1197–233.

[53] Joslin, S., K. J. Singleton, and H. Zhu. 2011. "A New Perspective on Gaussian Dynamic Term Structure Models." *The Review of Financial Studies* 24: 926–70.

[54] Kaminska, I. and G. Zinna. 2020. "Official Demand for U.S. Debt: Implications for U.S. Real Rates." *Journal of Money, Credit and Banking* 52(2-3): 323-364.

[55] Kim D. H., K.J. Singleton. 2012. "Term Structure Models and the Zero Bound: An Empirical Investigation of Japanese Yields." *Journal of Econometrics* 170: 32-49.

[56] King, T. B. 2019. "Expectation and Duration at the Effective Lower Bound." *Journal of Financial Economics*, 134 (3): 736–760.

[57] Koijen, R. and M. Yogo. 2019. "A demand system approach to asset pricing". *Journal of Political Economy*, 127(4): 1475–1515.

[58] Li, C., and M. Wei. 2013. "Term Structure Modeling with Supply Factors and the Federal Reserve's Large-Scale Asset Purchase Programs," *International Journal of Central Banking*, 9 (1), 3-39.

[59] Litterman, R., and J. A. Scheinkman. 1991. "Common Factors Affecting Bond Returns," *Journal of Fixed Income*, 1, 54–61.

[60] Miran, S. and N. Roubini. 2024. "ATI: Activist Treasury Issuance and the Tug-of-War Over Monetary Policy." Hudson Bay Capital.

[61] Modigliani F., and R. Sutch. 1966. "Innovations in interest rate policy." *American Economic Review*. 56(1-2): 178–97.

[62] Potter, S. 2013. "The Implementation of Current Asset Purchases." Speech at the Forecasters Club of New York, New York City, 27 March.

[63] Ramey, V. A. 2016. "Macroeconomic Shocks and Their Propagation." In Handbook of Macroeconomics, edited by John B. Taylor and Harald Uhlig, vol. 2. Elsevier.

[64] Ray, W. 2019. "Monetary Policy and the Limits to Arbitrage: Insights from a New Keynesian Preferred Habitat Model." Mimeo.

[65] Ray, W., M. Droste, and Y. Gorodnichenko. 2024. "Unbundling Quantitative Easing: Taking a Cue from Treasury Auctions." *Journal of Political Economy*, 132 (9): 3115–3172.

[66] Rothenberg, T. J. 1971. "Identification in parametric models". *Econometrica* 39: 577–591.

[67] Stein, J. C. 2012. "Evaluating Large-Scale Asset Purchases." Speech at the Brookings Institute, Washington D.C., 11 October.

[68] Taylor, J. B. 1993. “Discretion versus policy rules in practice.” *Carnegie-Rochester Conference Series on Public Policy*, 39: 195-214.

[69] Tobin J. 1958. “Liquidity preference as behavior towards risk.” *Review of Economic Studies.* 25(2): 65–86.

[70] Tobin J. 1969. “A general equilibrium approach to monetary theory.” *Journal of Money, Credit and Banking*. 1(1): 15–29.

[71] Vayanos, D. and J. Vila. 2009. “A Preferred-Habitat Model of the Term Structure of Interest Rates.” NBER Working Paper No. 15487.

[72] Vayanos, D. and J. Vila. 2021. “A Preferred-Habitat Model of the Term Structure of Interest Rates.” *Econometrica,* 89 (1): 77-112.

[73] Williams, J. C. 2011. “Unconventional Monetary Policy: Lessons from the Past Three Years.” FRBSF Economic Letter 31.

[74] Williams, J. C. 2014. “Monetary Policy at the Zero Lower Bound: Putting Theory into Practice.” Speech at Brookings Institute, Washington D.C., 16 January.

[75] Wu, J.C. and F.D. Xia. 2016. “Measuring the Macroeconomic Impact of Monetary Policy at the Zero Lower Bound.” *Journal of Money, Credit and Banking*, 48 (2-3): 253-291.

[76] Yellen, J. L. 2011a. “The Federal Reserve’s Asset Purchase Program.” Speech at the Brimmer Policy Forum, Allied Social Science Associations Annual Meeting, Denver, Colorado, 8 January.

[77] Yellen, J. L. 2011b. “Unconventional Monetary Policy and Central Bank Communications.” Speech at the U.S. Monetary Policy Forum, New York, New York City, 25 February.

[78] Zellner, A. 1962. “An Efficient Method of Estimating Seemingly Unrelated Regressions and Tests for Aggregation Bias.” *Journal of the American Statistical Association*, 57 (298): 348–368.

Table 1. Estimates of the GDTSM

(a) Physical dynamics of the state variables

$100 \times \mathbf{\Phi}_{x0}$	$\mathbf{\Phi}_{xx}$			$10^4 \times \mathbf{\Omega}_{xx}$		
0.1622	0.9748***	0.0233	-0.2528	0.1716***		
(0.1130)	(0.0175)	(0.0703)	(0.3021)	(0.0166)		
0.0475	-0.0008	0.9382***	-0.4520***	-0.0244***	0.0345***	
(0.0506)	(0.0078)	(0.0315)	(0.1354)	(0.0041)	(0.0030)	
0.0635***	0.0049	0.0168	0.7006***	-0.0153***	0.0012	0.0061***
(0.0213)	(0.0033)	(0.0132)	(0.0569)	(0.0028)	(0.0012)	(0.0007)

(b) Risk-neutral dynamics of the state variables

$100 \times k_{\infty}^{\mathbb{Q}\$}$	$\boldsymbol{\phi}_{zz}^{\mathbb{Q}}$		
0.0167***	0.9975***	0.8839***	0.7832***
(0.0007)	(0.0002)	(0.0024)	(0.0042)

(c) Inflation

$100 \times p_{x0}$	$\mathbf{p}_x'$		
0.6128***	0.0816***	0.1208**	-0.4715**
(0.0822)	(0.0127)	(0.0511)	(0.2168)

(d) Growth

$100 \times g_{x0}$	$\mathbf{g}_x'$		
0.5264***	0.0661***	0.0184	-0.4431
(0.1558)	(0.0241)	(0.0968)	(0.4107)

Maximum likelihood estimates for a sample period of 1986Q1 to 2025Q2. The dynamics are given by $\mathbf{x}_{t+1} = \mathbf{\Phi}_{x0} + \mathbf{\Phi}_{xx}\mathbf{x}_t + \mathbf{\Sigma}_x\boldsymbol{\eta}_{t+1}$, where $\boldsymbol{\eta}_{t+1} \sim iid\, N(0, \mathbf{I}_M)$. Bond (log) prices are given by $b_t^{(n)} = -b_{x0}^{(n)} - \mathbf{b}_x^{(n)'}\mathbf{x}_t$ where $\mathbf{b}_x^{(n)'} = \mathbf{b}_x^{(n-1)'}\mathbf{\Phi}_{xx}^{\mathbb{Q}} + \mathbf{b}_x^{(1)'}$, $b_{x0}^{(n)} = b_{x0}^{(n-1)} + b_{x0}^{(1)} + \mathbf{b}_x^{(n-1)'}\mathbf{\Phi}_{x0}^{\mathbb{Q}\$} - \frac{1}{2}\mathbf{b}_x^{(n-1)'}\mathbf{\Omega}_{xx}\mathbf{b}_x^{(n-1)}$, $\mathbf{\Omega}_{xx} = \mathbf{\Sigma}_x\mathbf{\Sigma}_x'$. Here, $\mathbf{b}_x^{(1)} = \boldsymbol{\delta}_x$ and $\mathbf{\Phi}_{x0}^{\mathbb{Q}\$} = \mathbf{\Phi}_{x0}^{\mathbb{Q}} - \mathbf{\Omega}_{xx}\mathbf{p}_x$. The eigenvalues of $\mathbf{\Phi}_{xx}$ are 0.9690, 0.9006, and 0.7440. Asymptotic standard errors are in parentheses. ***, **, and * indicate a parameter estimate statistically different from zero at the 1%, 5%, and 10% levels, respectively.

Table 2. Estimates of the portfolio-balance model

(a) Structural impact matrix

$100 \times \boldsymbol{\Sigma}_x$		
0.3608***	0.1912***	0.0704***
(0.0223)	(0.0122)	(0.0040)
-0.1357***	0.0993***	0.0788***
(0.0091)	(0.0085)	(0.0045)
-0.0220***	-0.0565***	0.0490***
(0.0061)	(0.0051)	(0.0028)

(b) Nominal bond supply factors

$\boldsymbol{\beta}_{x0}$	$\boldsymbol{\beta}_x$		
0.0131	-0.1823	1.9573*	1.6577
(0.0171)	(0.2633)	(1.0626)	(4.5577)
0.0019	-0.3471	0.5911	3.2493
(0.0171)	(0.2644)	(1.0731)	(4.5650)
0.0310*	-1.1282***	2.1864**	3.0176
(0.0175)	(0.2766)	(1.0976)	(4.6612)

Estimates derived from the maximum-likelihood estimates of the GDTSM (Table 1); the risk-aversion parameter γ is calibrated as described in Section 5.1. In panel (b), the rows correspond to the hedging-risk-premium, risk-bearing-capacity, and monetary-policy factors, and the columns of $\boldsymbol{\beta}_x$ correspond to the level, slope, and curvature factors. Asymptotic standard errors are in parentheses. ***, **, and * indicate a parameter estimate statistically different from zero at the 1%, 5%, and 10% levels, respectively.

Table 3. Variance decompositions

		Shock		
		Hedging risk premium	Risk-bearing capacity	Monetary policy
i_t	1Q	14.56%	35.98%	49.47%
	4Q	19.52%	59.69%	20.79%
	40Q	32.12%	63.45%	4.42%
π_t	1Q	15.46%	82.80%	1.74%
	4Q	17.70%	81.07%	1.22%
	40Q	28.69%	70.73%	0.58%
g_t	1Q	34.92%	56.27%	8.81%
	4Q	41.75%	51.90%	6.35%
	40Q	56.06%	40.96%	2.98%
$y_t^{(2y)}$	1Q	47.40%	50.70%	1.90%
	4Q	47.31%	51.60%	1.09%
	40Q	52.64%	46.95%	0.41%
$exp_t^{(2y)}$	1Q	23.19%	69.45%	7.36%
	4Q	24.61%	71.96%	3.43%
	40Q	35.35%	63.70%	0.96%
$tp_t^{(2y)}$	1Q	89.57%	0.00%	10.43%
	4Q	91.97%	2.52%	5.52%
	40Q	91.66%	5.94%	2.39%
$y_t^{(10y)}$	1Q	96.31%	3.69%	0.00%
	4Q	96.07%	3.81%	0.12%
	40Q	85.71%	13.82%	0.47%
$exp_t^{(10y)}$	1Q	36.64%	62.31%	1.06%
	4Q	37.67%	61.73%	0.60%
	40Q	46.22%	53.54%	0.25%
$tp_t^{(10y)}$	1Q	86.03%	13.12%	0.85%
	4Q	84.78%	14.90%	0.32%
	40Q	88.19%	10.97%	0.84%

Forecast-error variance decompositions for the sample period 1986Q1 to 2025Q2. Each entry is the percentage of the h-quarter-ahead forecast-error variance of the row variable attributable to each of the three orthonormal structural shocks, computed as $\sum_{k=0}^{h-1} \psi_{j,k}^2 \big/ \sum_i \sum_{k=0}^{h-1} \psi_{i,k}^2$, where $\psi_{j,k}$ is the response of the variable at horizon k to structural shock j, for horizons $h = 1$, 4, and 40 quarters. i_t is the short rate, π_t inflation, and g_t output growth; $y_t^{(n)}$, $exp_t^{(n)}$, and $tp_t^{(n)}$ denote the n-maturity yield and its expectations and term-premium components.

Table 4. Estimates of the monetary policy rule

(a) Contemporaneous rule

$100 \times \psi_0$	ψ_π	ψ_g	$\boldsymbol{\psi}_x'$			$100 \times \sigma_u$
-0.8952***	0.5450	1.0068	0.1998***	0.3280***	1.2526***	0.1013***
(0.2809)	(1.3699)	(1.5199)	(0.0410)	(0.0840)	(0.2582)	(0.0216)

(b) Forward-looking rule

$100 \times \psi_0$	ψ_π	ψ_g	$\boldsymbol{\psi}_x'$			$100 \times \sigma_u$
-1.2570***	1.6713	0.5120	0.1728***	0.2836***	1.0833***	0.0876***
(0.3693)	(1.4086)	(1.8197)	(0.0256)	(0.0512)	(0.1486)	(0.0124)

Estimates derived from the maximum-likelihood estimates of the GDTSM (Table 1); sample period 1986Q1 to 2025Q2. The nominal short-term interest rate is set according to the policy rule given by $i_t = \psi_0 + \psi_\pi \mathrm{E}_t \pi_{t+h} + \psi_g \mathrm{E}_t g_{t+h} + u_t$, for $h = 0$ (contemporaneous rule) and $h = 4$ (forward-looking rule). The discretionary monetary policy term satisfies $u_t = \boldsymbol{\psi}_x' \mathbf{x}_t$. Asymptotic standard errors are in parentheses. ***, **, and * indicate a parameter estimate statistically different from zero at the 1%, 5%, and 10% levels, respectively.

Figure 1. Loadings of the first three principal components of U.S. government zero-coupon bond yields

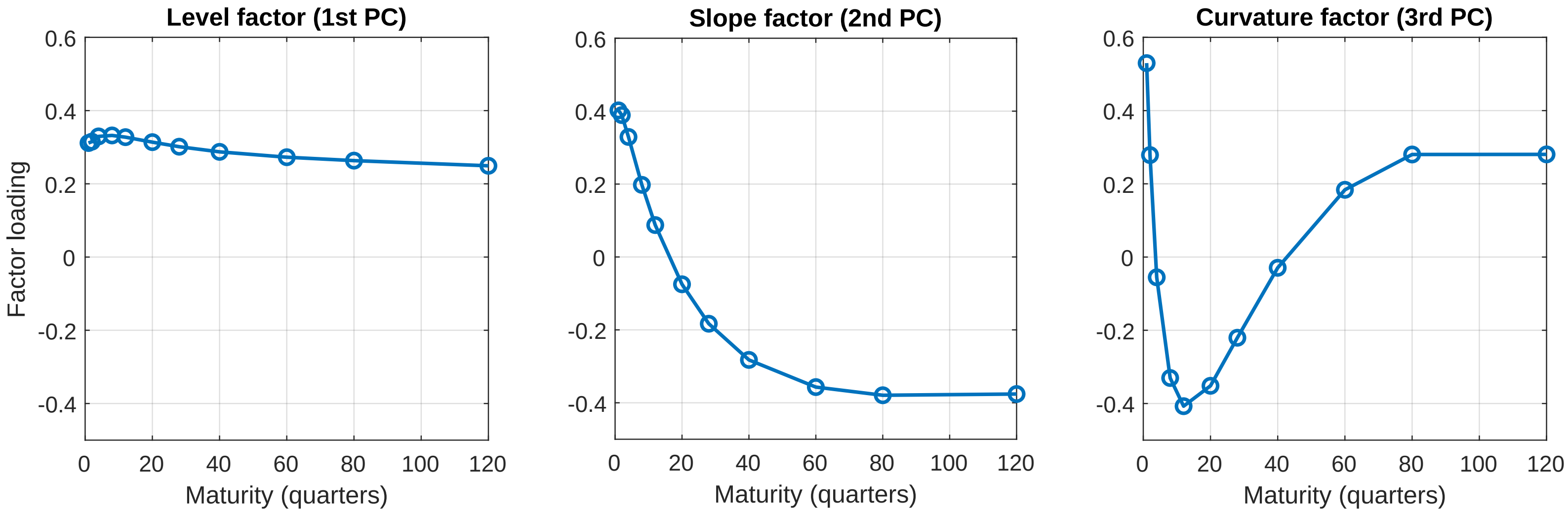

Sample: 1986Q1 to 2025Q2.

Figure 2. Estimated structural shocks

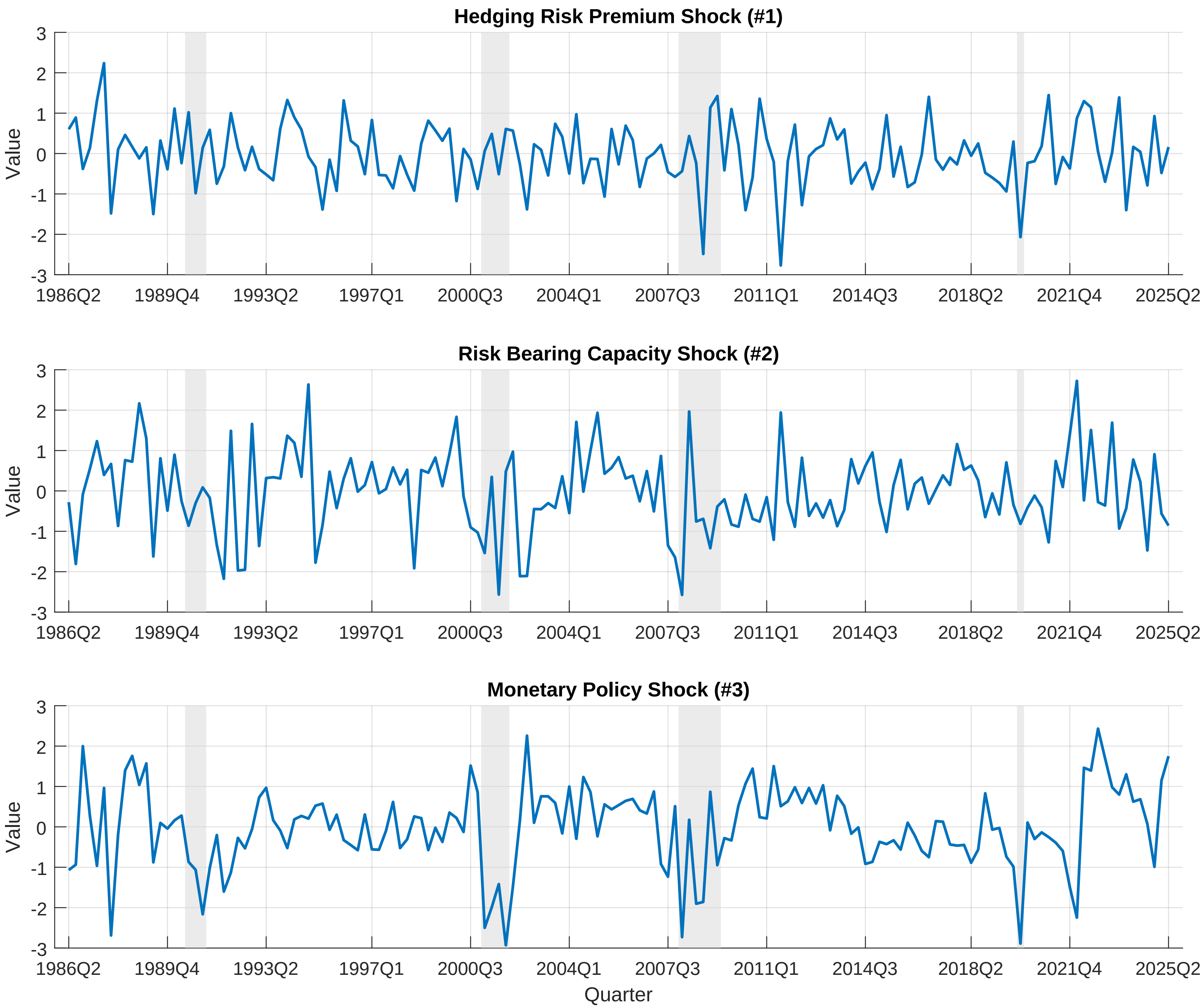

Shaded areas denote NBER recessions; the shocks are standardized to unit variance. Sample: 1986Q1 to 2025Q2.

Figure 3. Impulse responses for hedging-risk-premium shock (#1)

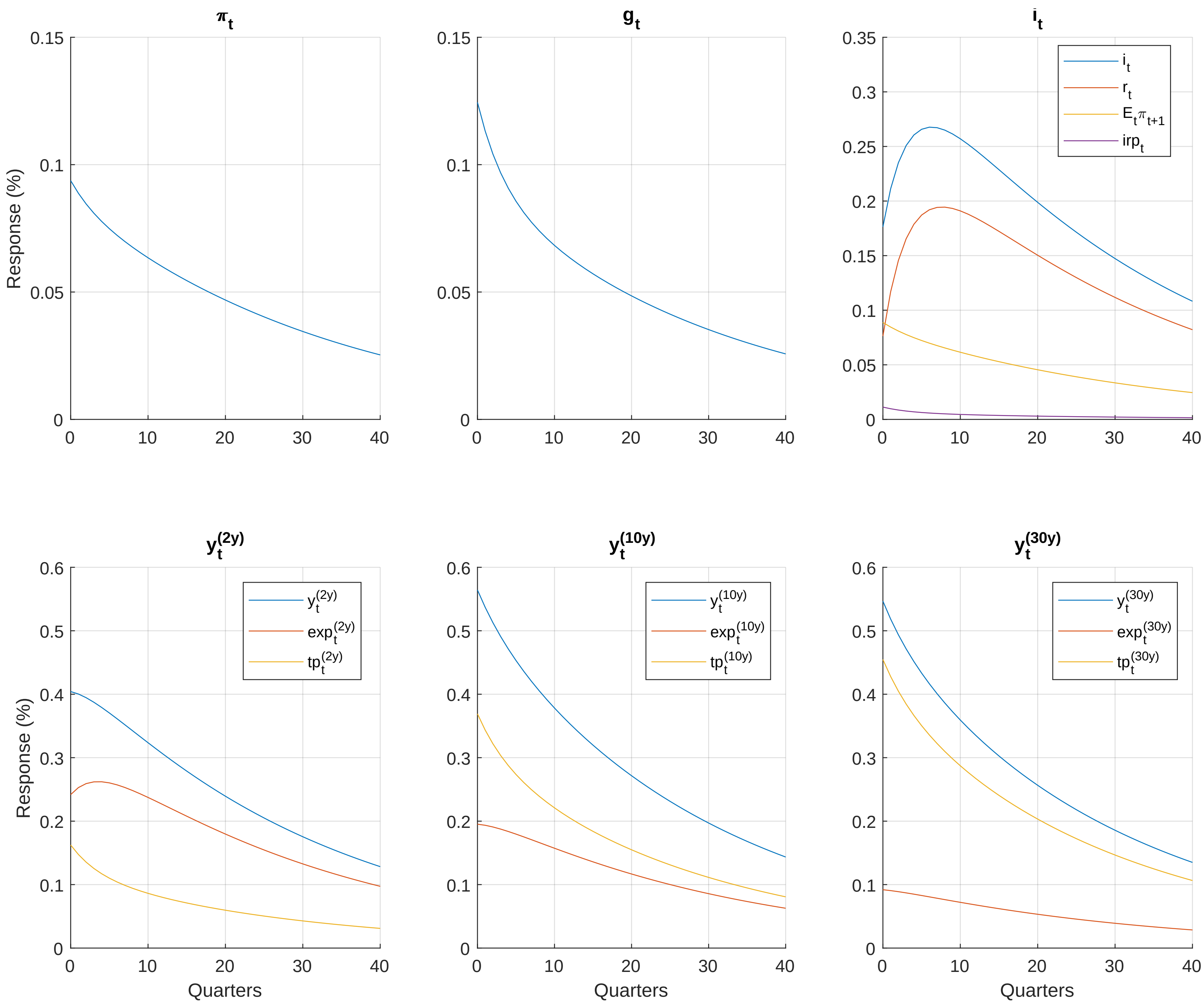

Figure 4. Impulse responses for risk-bearing-capacity shock (#2)

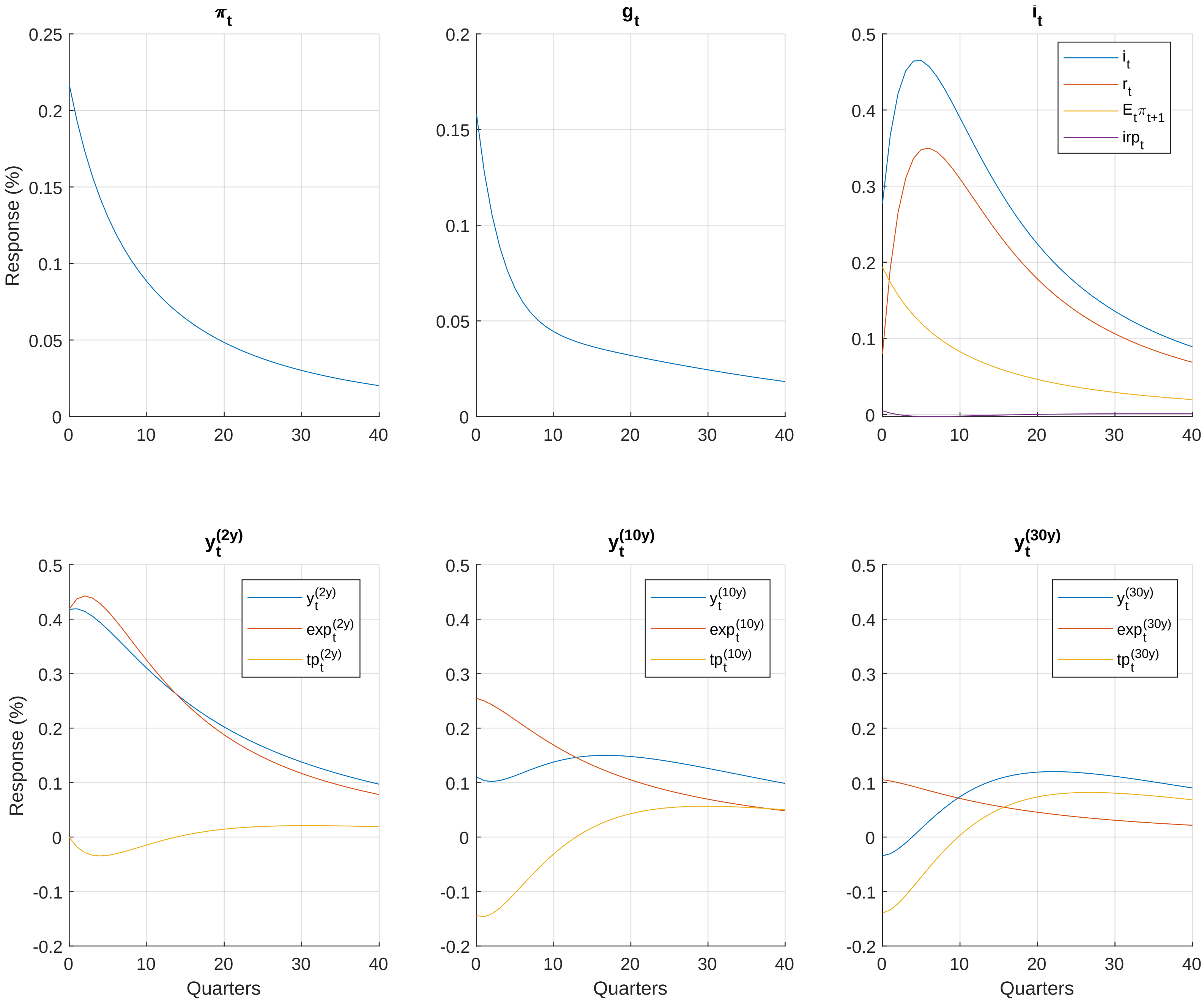

Figure 5. Impulse responses for monetary-policy shock (#3)

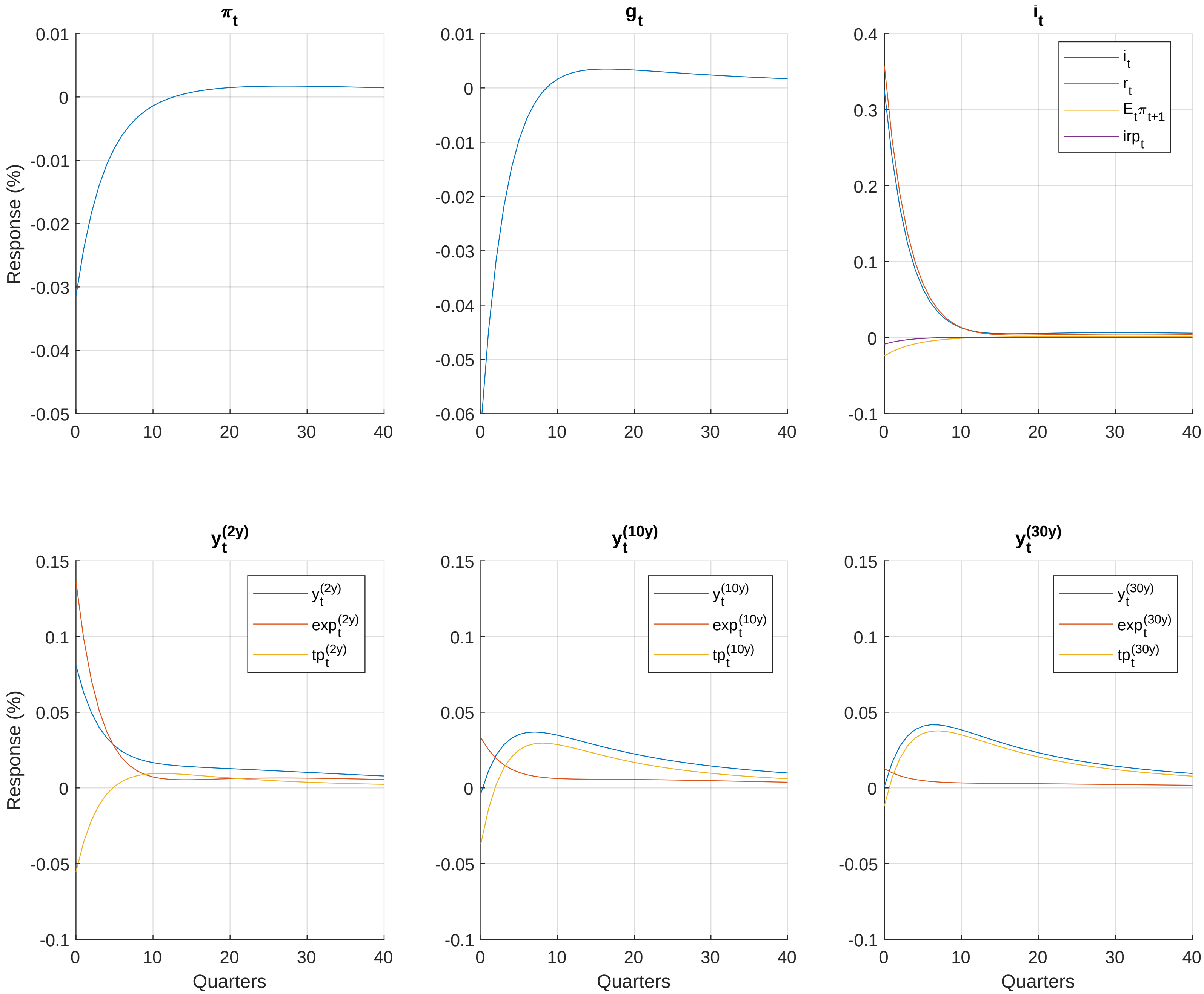

Appendix

A Invariant transformations of portfolio-balance models of the term structure of interest rates

As noted by Dai and Singleton (2000), Gaussian dynamic term structure models (GDTSMs) are invariant under affine transformations of the factors. In this appendix, we extend this invariance argument to portfolio-balance models, as this is an important property that we will require below to both (i) prove the existence of a unique equilibrium in the portfolio-balance model and (ii) estimate the model.

For this, start by assuming, as in the main body of the paper, the following structure for the portfolio-balance model:

$$\mathbf{x}_{t+1} = \mathbf{\Phi}_{x0} + \mathbf{\Phi}_{xx}\mathbf{x}_t + \mathbf{\Sigma}_x \boldsymbol{\eta}_{t+1}, \tag{A.1}$$

$$\mathbf{x}_{t+1} = \mathbf{\Phi}^{\mathbb{Q}}_{x0} + \mathbf{\Phi}^{\mathbb{Q}}_{xx}\mathbf{x}_t + \mathbf{\Sigma}_x \boldsymbol{\eta}^{\mathbb{Q}}_{t+1}, \tag{A.2}$$

$$i_t = \delta_{x0} + \boldsymbol{\delta}'_x \mathbf{x}_t, \tag{A.3}$$

$$\pi_t = p_{x0} + \mathbf{p}'_x \mathbf{x}_t, \tag{A.4}$$

$$g_t = g_{x0} + \mathbf{g}'_x \mathbf{x}_t, \tag{A.5}$$

$$s^{(n)}_t = s^{(n)}_{x0} + \mathbf{s}^{(n)\prime}_x \mathbf{x}_t, \qquad \text{for } n = 2, \dots, N, \tag{A.6}$$

where $\mathbf{x}_t$ is an $(M \times 1)$-vector of state variables, both $\boldsymbol{\eta}_{t+1}$ and $\boldsymbol{\eta}^{\mathbb{Q}}_{t+1}$ are *iid* $N(0, \mathbf{I})$, and $\mathbf{\Omega}_{xx} = \mathbf{\Sigma}_x \mathbf{\Sigma}'_x$.

Consider now, as in Dai and Singleton (2000), the following affine transformation to our state variables:

$$\mathbf{z}_t = \mathbf{c} + \mathbf{D}\mathbf{x}_t, \tag{A.7}$$

where $\mathbf{c}$ is a $(M \times 1)$-vector and $\mathbf{D}$ is a $(M \times M)$ non-singular matrix. To show the invariance of our portfolio-balance model under this affine transformation of the factors, we start by finding the dynamics of the new rotated factors under both the physical, $\mathbb{P}$, and risk-neutral, $\mathbb{Q}$, distributions.

Dynamics under $\mathbb{P}$ and $\mathbb{Q}$. Specifically, we have that the dynamics of $\mathbf{z}_t$ remain a VAR(1) under both the physical and risk-neutral distributions:

$$\mathbf{z}_{t+1} = \boldsymbol{\Phi}_{z0} + \boldsymbol{\Phi}_{zz}\mathbf{z}_t + \boldsymbol{\Sigma}_z\boldsymbol{\eta}_{t+1}, \tag{A.8}$$

$$\mathbf{z}_{t+1} = \boldsymbol{\Phi}^{\mathbb{Q}}_{z0} + \boldsymbol{\Phi}^{\mathbb{Q}}_{zz}\mathbf{z}_t + \boldsymbol{\Sigma}_z\boldsymbol{\eta}^{\mathbb{Q}}_{t+1}, \tag{A.9}$$

with

$$\boldsymbol{\Phi}_{zz} = \mathbf{D}\boldsymbol{\Phi}_{xx}\mathbf{D}^{-1}, \qquad \boldsymbol{\Phi}_{z0} = (\mathbf{I} - \boldsymbol{\Phi}_{zz})\mathbf{c} + \mathbf{D}\boldsymbol{\Phi}_{x0}, \tag{A.10}$$

$$\boldsymbol{\Phi}^{\mathbb{Q}}_{zz} = \mathbf{D}\boldsymbol{\Phi}^{\mathbb{Q}}_{xx}\mathbf{D}^{-1}, \qquad \boldsymbol{\Phi}^{\mathbb{Q}}_{z0} = (\mathbf{I} - \boldsymbol{\Phi}^{\mathbb{Q}}_{zz})\mathbf{c} + \mathbf{D}\boldsymbol{\Phi}^{\mathbb{Q}}_{x0}, \tag{A.11}$$

$$\boldsymbol{\Sigma}_z = \mathbf{D}\boldsymbol{\Sigma}_x, \qquad \boldsymbol{\Omega}_{zz} = \mathbf{D}\boldsymbol{\Omega}_{xx}\mathbf{D}'. \tag{A.12}$$

Specifically, using $\mathbf{x}_t = \mathbf{D}^{-1}(\mathbf{z}_t - \mathbf{c})$, the $\mathbb{P}$-dynamics satisfy

$$\begin{aligned} \mathbf{z}_{t+1} &= \mathbf{c} + \mathbf{D}(\boldsymbol{\Phi}_{x0} + \boldsymbol{\Phi}_{xx}\mathbf{x}_t + \boldsymbol{\Sigma}_x\boldsymbol{\eta}_{t+1}) \\ &= \underbrace{(\mathbf{I} - \mathbf{D}\boldsymbol{\Phi}_{xx}\mathbf{D}^{-1})\mathbf{c} + \mathbf{D}\boldsymbol{\Phi}_{x0}}_{\boldsymbol{\Phi}_{z0}} + \underbrace{\mathbf{D}\boldsymbol{\Phi}_{xx}\mathbf{D}^{-1}}_{\boldsymbol{\Phi}_{zz}}\mathbf{z}_t + \underbrace{\mathbf{D}\boldsymbol{\Sigma}_x}_{\boldsymbol{\Sigma}_z}\boldsymbol{\eta}_{t+1}, \end{aligned} \tag{A.13}$$

which is equation (A.8), and exactly the same algebra under $\mathbb{Q}$ yields (A.9).

Affine variables. For any variable that is affine in $\mathbf{x}_t$, say $v_t = v_{x0} + \mathbf{v}'_x\mathbf{x}_t$, substituting $\mathbf{x}_t = \mathbf{D}^{-1}(\mathbf{z}_t - \mathbf{c})$ yields

$$v_t = \underbrace{v_{x0} - \mathbf{v}'_x\mathbf{D}^{-1}\mathbf{c}}_{v_{z0}} + \underbrace{\mathbf{v}'_x\mathbf{D}^{-1}}_{\mathbf{v}'_z}\mathbf{z}_t. \tag{A.14}$$

Therefore, we have that i_t, π_t, g_t, and $s_t^{(n)}$ can be rewritten as the following affine functions of $\mathbf{z}_t$

$$\boldsymbol{\delta}_z' = \boldsymbol{\delta}_x'\mathbf{D}^{-1}, \qquad \delta_{z0} = \delta_{x0} - \boldsymbol{\delta}_z'\mathbf{c}, \tag{A.15}$$

$$\mathbf{p}_z' = \mathbf{p}_x'\mathbf{D}^{-1}, \qquad p_{z0} = p_{x0} - \mathbf{p}_z'\mathbf{c}, \tag{A.16}$$

$$\mathbf{g}_z' = \mathbf{g}_x'\mathbf{D}^{-1}, \qquad g_{z0} = g_{x0} - \mathbf{g}_z'\mathbf{c}, \tag{A.17}$$

$$\mathbf{s}_z^{(n)\prime} = \mathbf{s}_x^{(n)\prime}\mathbf{D}^{-1}, \qquad s_{z0}^{(n)} = s_{x0}^{(n)} - \mathbf{s}_z^{(n)\prime}\mathbf{c}. \tag{A.18}$$

Bond prices recursions. Remember that we have that the log bond prices are affine in $\mathbf{x}_t$:

$$b_t^{(n)} = -b_{x0}^{(n)} - \mathbf{b}_x^{(n)\prime}\mathbf{x}_t \qquad n = 1, \dots, N, \tag{A.19}$$

which can thus be expressed as affine functions of $\mathbf{z}_t$:

$$b_t^{(n)} = -\underbrace{\left[b_{x0}^{(n)} - \mathbf{b}_x^{(n)\prime}\mathbf{D}^{-1}\mathbf{c}\right]}_{b_{z0}^{(n)}} - \underbrace{\left[\mathbf{b}_x^{(n)\prime}\mathbf{D}^{-1}\right]}_{\mathbf{b}_z^{(n)\prime}}\mathbf{z}_t, \tag{A.20}$$

with

$$\mathbf{b}_z^{(n)\prime} = \mathbf{b}_x^{(n)\prime}\mathbf{D}^{-1}, \tag{A.21}$$

$$b_{z0}^{(n)} = b_{x0}^{(n)} - \mathbf{b}_x^{(n)\prime}\mathbf{D}^{-1}\mathbf{c}. \tag{A.22}$$

Substituting the expression for the recursion of the bond loadings in equation (2.23) in the main text into equation (A.21) we have

$$\begin{aligned}
\mathbf{b}_z^{(n)\prime} &= \left[\mathbf{b}_x^{(n-1)\prime}\boldsymbol{\Phi}_{xx}^{\mathbb{Q}} + \boldsymbol{\delta}_x'\right]\mathbf{D}^{-1} \\
&= \mathbf{b}_z^{(n-1)\prime}\underbrace{\left(\mathbf{D}\boldsymbol{\Phi}_{xx}^{\mathbb{Q}}\mathbf{D}^{-1}\right)}_{\boldsymbol{\Phi}_{zz}^{\mathbb{Q}}} + \underbrace{\boldsymbol{\delta}_x'\mathbf{D}^{-1}}_{\boldsymbol{\delta}_z'} \\
&= \mathbf{b}_z^{(n-1)\prime}\boldsymbol{\Phi}_{zz}^{\mathbb{Q}} + \boldsymbol{\delta}_z'.
\end{aligned} \tag{A.23}$$

Consequently, we have that the structure of the bond loading recursion is preserved under affine transformations.

On the other hand, substituting the recursion of the bond constant in equation (2.24) in the main text into equation (A.22) we have

$$\begin{aligned}
b_{z0}^{(n)} &= b_{x0}^{(n-1)} + \mathbf{b}_x^{(n-1)\prime}\left(\boldsymbol{\Phi}_{x0}^{\mathbb{Q}} - \boldsymbol{\Omega}_{xx}\mathbf{p}_x\right) - \frac{1}{2}\mathbf{b}_x^{(n-1)\prime}\boldsymbol{\Omega}_{xx}\mathbf{b}_x^{(n-1)} + \delta_{x0} - \mathbf{b}_x^{(n)\prime}\mathbf{D}^{-1}\mathbf{c} \\
&= b_{z0}^{(n-1)} + \mathbf{b}_z^{(n-1)\prime}\left(\mathbf{D}\boldsymbol{\Phi}_{x0}^{\mathbb{Q}} - \mathbf{D}\boldsymbol{\Omega}_{xx}\mathbf{D}'\mathbf{p}_z\right) - \frac{1}{2}\mathbf{b}_z^{(n-1)\prime}\mathbf{D}\boldsymbol{\Omega}_{xx}\mathbf{D}'\mathbf{b}_z^{(n-1)} + \delta_{x0} \\
&+ \left[\mathbf{b}_z^{(n-1)\prime} - \mathbf{b}_z^{(n)\prime}\right]\mathbf{c} \\
&= b_{z0}^{(n-1)} + \mathbf{b}_z^{(n-1)\prime}\left(\boldsymbol{\Phi}_{z0}^{\mathbb{Q}} - \boldsymbol{\Omega}_{zz}\mathbf{p}_z\right) - \frac{1}{2}\mathbf{b}_z^{(n-1)\prime}\boldsymbol{\Omega}_{zz}\mathbf{b}_z^{(n-1)} + \delta_{z0},
\end{aligned} \tag{A.24}$$

where, for the last equality, we have used that (i) $\mathbf{D}\boldsymbol{\Phi}_{x0}^{\mathbb{Q}} = \boldsymbol{\Phi}_{z0}^{\mathbb{Q}} - (\mathbf{I} - \boldsymbol{\Phi}_{zz}^{\mathbb{Q}})\mathbf{c}$ (equation A.11), (ii) $\boldsymbol{\Omega}_{zz} = \mathbf{D}\boldsymbol{\Omega}_{xx}\mathbf{D}'$ (equation A.12), (iii) $\delta_{x0} = \delta_{z0} + \boldsymbol{\delta}_z'\mathbf{c}$ (equation A.15), (iv) $\mathbf{p}_x' = \mathbf{p}_z'\mathbf{D}$ (equation A.16), and (v) $\mathbf{b}_z^{(n)\prime} = \mathbf{b}_z^{(n-1)\prime}\boldsymbol{\Phi}_{zz}^{\mathbb{Q}} + \boldsymbol{\delta}_z'$ (equation A.23). Therefore, we have, once again that the structure of the bond constant recursion is preserved under affine transformations.

Short real rate. Since the real short-term rate is affine in $\mathbf{x}_t$, we have that

$$r_t = \underbrace{\left[\rho_{x0} - \boldsymbol{\rho}_x'\mathbf{D}^{-1}\mathbf{c}\right]}_{\rho_{z0}} + \underbrace{\left[\boldsymbol{\rho}_x'\mathbf{D}^{-1}\right]}_{\boldsymbol{\rho}_z'}\mathbf{z}_t \tag{A.25}$$

with

$$\boldsymbol{\rho}_z' = \boldsymbol{\rho}_x'\mathbf{D}^{-1}, \qquad \rho_{z0} = \rho_{x0} - \boldsymbol{\rho}_z'\mathbf{c}. \tag{A.26}$$

Substituting the expressions for the loadings and constant of the real short-term rate in equations (2.21) and (2.22), we have:

$$\begin{aligned}
\boldsymbol{\rho}_z' &= \left(\boldsymbol{\delta}_x' - \mathbf{p}_x'\boldsymbol{\Phi}_{xx}^{\mathbb{Q}}\right)\mathbf{D}^{-1} \\
&= \boldsymbol{\delta}_x'\mathbf{D}^{-1} - (\mathbf{p}_x'\mathbf{D}^{-1})(\mathbf{D}\boldsymbol{\Phi}_{xx}^{\mathbb{Q}}\mathbf{D}^{-1}) \\
&= \boldsymbol{\delta}_z' - \mathbf{p}_z'\boldsymbol{\Phi}_{zz}^{\mathbb{Q}},
\end{aligned} \tag{A.27}$$

and

$$\begin{aligned}
\rho_{z0} &= \delta_{x0} - p_{x0} - \mathbf{p}_x'\boldsymbol{\Phi}_{x0}^{\mathbb{Q}} + \frac{1}{2}\mathbf{p}_x'\boldsymbol{\Omega}_{xx}\mathbf{p}_x - \boldsymbol{\rho}_z'\mathbf{c} \\
&= \delta_{z0} - p_{z0} - \mathbf{p}_z'\left[\boldsymbol{\Phi}_{z0}^{\mathbb{Q}} - \left(\mathbf{I} - \boldsymbol{\Phi}_{zz}^{\mathbb{Q}}\right)\mathbf{c}\right] + \frac{1}{2}\mathbf{p}_z'\boldsymbol{\Omega}_{zz}\mathbf{p}_z + \left[\boldsymbol{\delta}_z' - \mathbf{p}_z' - \boldsymbol{\rho}_z'\right]\mathbf{c} \\
&= \delta_{z0} - p_{z0} - \mathbf{p}_z'\boldsymbol{\Phi}_{z0}^{\mathbb{Q}} + \frac{1}{2}\mathbf{p}_z'\boldsymbol{\Omega}_{zz}\mathbf{p}_z.
\end{aligned} \tag{A.28}$$

Therefore, the structure of the real short-rate constant and loadings is also preserved under affine transformations of the factors.

Risk-neutral parameters. We finally need to verify that the equilibrium relationship between the parameters describing the dynamics of the factors under the risk-neutral measure and those driving the supply of bonds that the arbitrageur needs to absorb (equations 2.25 and 2.26) is still satisfied under affine transformations. Specifically, we need to prove that the rotated risk-neutral parameters satisfy:

$$\mathbf{\Phi}_{zz}^{\mathbb{Q}} = \mathbf{\Phi}_{zz} + \gamma \mathbf{\Omega}_{zz} \sum_{j=2}^{N} \left[\mathbf{b}_z^{(j-1)} \mathbf{s}_z^{(j)\prime} \right], \tag{A.29}$$

$$\mathbf{\Phi}_{z0}^{\mathbb{Q}} = \mathbf{\Phi}_{z0} + \gamma \mathbf{\Omega}_{zz} \left\{ \mathbf{p}_z + \sum_{j=2}^{N} \left[\mathbf{b}_z^{(j-1)} s_{z0}^{(j)} \right] \right\}, \tag{A.30}$$

Focusing on the autocorrelation matrix of the factors under the risk neutral measure first, we have that substituting equation (2.25) into (A.11) delivers

$$\begin{aligned}
\mathbf{\Phi}_{zz}^{\mathbb{Q}} &= \mathbf{D} \left\{ \mathbf{\Phi}_{xx} + \gamma \mathbf{\Omega}_{xx} \sum_{j=2}^{N} \left[\mathbf{b}_x^{(j-1)} \mathbf{s}_x^{(j)\prime} \right] \right\} \mathbf{D}^{-1} \\
&= \mathbf{D} \mathbf{\Phi}_{xx} \mathbf{D}^{-1} + \gamma \mathbf{D} \mathbf{\Omega}_{xx} \mathbf{D}' \sum_{j=2}^{N} \left[\mathbf{b}_z^{(j-1)} \mathbf{s}_z^{(j)\prime} \mathbf{D} \right] \mathbf{D}^{-1} \\
&= \mathbf{\Phi}_{zz} + \gamma \mathbf{\Omega}_{zz} \sum_{j=2}^{N} \left[\mathbf{b}_z^{(j-1)} \mathbf{s}_z^{(j)\prime} \right],
\end{aligned} \tag{A.31}$$

which delivers equation (A.29) as required.

On the other hand, using (2.26) we have

$$\begin{aligned}
\mathbf{\Phi}_{z0}^{\mathbb{Q}} &= (\mathbf{I} - \mathbf{\Phi}_{zz}^{\mathbb{Q}}) \mathbf{c} + \mathbf{D} \mathbf{\Phi}_{x0}^{\mathbb{Q}} \\
&= (\mathbf{I} - \mathbf{\Phi}_{zz}^{\mathbb{Q}}) \mathbf{c} + \mathbf{D} \left(\mathbf{\Phi}_{x0} + \gamma \mathbf{\Omega}_{xx} \left\{ \mathbf{p}_x + \sum_{j=2}^{N} \left[\mathbf{b}_x^{(j-1)} s_{x0}^{(j)} \right] \right\} \right) \\
&= (\mathbf{\Phi}_{zz} - \mathbf{\Phi}_{zz}^{\mathbb{Q}}) \mathbf{c} + \mathbf{\Phi}_{z0} + \gamma \mathbf{\Omega}_{zz} \left(\mathbf{p}_z + \sum_{j=2}^{N} \left\{ \mathbf{b}_z^{(j-1)} \left[s_{z0}^{(j)} + \mathbf{s}_z^{(j)\prime} \mathbf{c} \right] \right\} \right) \\
&= \mathbf{\Phi}_{z0} + \gamma \mathbf{\Omega}_{zz} \left\{ \mathbf{p}_z + \sum_{j=2}^{N} \left[\mathbf{b}_z^{(j-1)} s_{z0}^{(j)} \right] \right\},
\end{aligned} \tag{A.32}$$

which coincides with equation (A.30).

B Proofs

B.1 Proof of Lemma 1

Note that equation (2.16) implies that the conditional covariance between the excess real returns from investing in two nominal bonds with different maturities n and j is

$$\mathrm{Cov}_t\left[rx_{t+1}^{(n)}, rx_{t+1}^{(j)}\right] = \left[\mathbf{p}_x + \mathbf{b}_x^{(n-1)}\right]' \boldsymbol{\Omega}_{xx}\left[\mathbf{p}_x + \mathbf{b}_x^{(j-1)}\right]. \tag{A.1}$$

Using this expression and $\boldsymbol{\Omega}_{xx} = \boldsymbol{\Sigma}_x \boldsymbol{\Sigma}_x'$, we have that the right-hand side of (2.14) can be written as

$$\begin{aligned}\gamma \sum_{j=1}^{N} \mathrm{Cov}_t\left[rx_{t+1}^{(n)}, rx_{t+1}^{(j)}\right] d_t^{(j)} &= \gamma\left[\mathbf{p}_x + \mathbf{b}_x^{(n-1)}\right]' \boldsymbol{\Sigma}_x \boldsymbol{\Sigma}_x' \sum_{j=1}^{N}\left[\mathbf{p}_x + \mathbf{b}_x^{(j-1)}\right] d_t^{(j)} \\ &= \left\{-\left[\mathbf{p}_x + \mathbf{b}_x^{(n-1)}\right]' \boldsymbol{\Sigma}_x\right\} \times \underbrace{\gamma \boldsymbol{\Sigma}_x' \sum_{j=1}^{N}\left\{-\left[\mathbf{p}_x + \mathbf{b}_x^{(j-1)}\right] d_t^{(j)}\right\}}_{\boldsymbol{\lambda}_{x,t}},\end{aligned} \tag{A.2}$$

which delivers equations (2.17) and (2.18).

B.2 Proof of Theorem 1

Evaluating the arbitrageurs' FOC at the bond market clearing conditions in equations (2.19) and (2.20) we have that:

$$\begin{aligned}&\mathrm{E}_t rx_{t+1}^{(n)} + \frac{1}{2}\mathrm{Var}_t\left[rx_{t+1}^{(n)}\right] = \\ &\qquad \gamma \mathrm{Cov}_t\left[rx_{t+1}^{(n)}, rx_{t+1}^{(1)}\right]\left[1 - \sum_{j=2}^{N} s_t^{(j)}\right] + \gamma \sum_{j=2}^{N} \mathrm{Cov}_t\left[rx_{t+1}^{(n)}, rx_{t+1}^{(j)}\right] s_t^{(j)} = \\ &\qquad \gamma \mathrm{Cov}_t\left[rx_{t+1}^{(n)}, rx_{t+1}^{(1)}\right] + \gamma \sum_{j=2}^{N} \mathrm{Cov}_t\left[rx_{t+1}^{(n)}, (rx_{t+1}^{(j)} - rx_{t+1}^{(1)})\right] s_t^{(j)},\end{aligned} \tag{A.3}$$

where again, $\widetilde{rx}_{t+1}^{(n)} \equiv rx_{t+1}^{(n)} - rx_{t+1}^{(1)}$.

Note that the left-hand side of this equation satisfies:

$$\begin{aligned}
\mathrm{E}_t rx_{t+1}^{(n)} + \frac{1}{2}\mathrm{Var}_t\left[rx_{t+1}^{(n)}\right] = &\left\{b_{x0}^{(n)} - \left[p_{x0} + b_{x0}^{(n-1)}\right] - \left[\mathbf{p}_x + \mathbf{b}_x^{(n-1)}\right]' \boldsymbol{\Phi}_{x0} - \rho_{x0}\right\} \\
&+ \left\{\mathbf{b}_x^{(n)\prime} - \left[\mathbf{p}_x + \mathbf{b}_x^{(n-1)}\right]' \boldsymbol{\Phi}_{xx} - \boldsymbol{\rho}_x'\right\} \mathbf{x}_t \\
&+ \frac{1}{2}\left[\mathbf{p}_x + \mathbf{b}_x^{(n-1)}\right]' \boldsymbol{\Omega}_{xx}\left[\mathbf{p}_x + \mathbf{b}_x^{(n-1)}\right].
\end{aligned} \tag{A.4}$$

On the other hand, substituting the expression for the supply of bonds, $s_t^{(n)} = s_{x0}^{(n)} + \mathbf{s}_x^{(n)\prime}\mathbf{x}_t$, on the right-hand side of (A.3) we obtain

$$\begin{aligned}
&\gamma \mathrm{Cov}_t\left[rx_{t+1}^{(n)}, rx_{t+1}^{(1)}\right] + \gamma\sum_{j=2}^{N}\mathrm{Cov}_t\left[rx_{t+1}^{(n)}, \widetilde{rx}_{t+1}^{(j)}\right] s_t^{(j)} = \\
&\quad = \gamma\left[\mathbf{p}_x + \mathbf{b}_x^{(n-1)}\right]' \boldsymbol{\Omega}_{xx}\mathbf{p}_x + \gamma\left[\mathbf{p}_x + \mathbf{b}_x^{(n-1)}\right]' \boldsymbol{\Omega}_{xx}\sum_{j=2}^{N}\mathbf{b}_x^{(j-1)}\left[s_{x0}^{(j)} + \mathbf{s}_x^{(j)\prime}\mathbf{x}_t\right]
\end{aligned} \tag{A.5}$$

Nominal bond prices. Collecting terms for $\mathbf{x}_t$ in equation (A.4) and matching coefficients with equation (A.5), we arrive at the following recursions for the loadings of the equilibrium (log) prices of the nominal bonds

$$\mathbf{b}_x^{(n)\prime} = \left[\mathbf{p}_x + \mathbf{b}_x^{(n-1)}\right]' \boldsymbol{\Phi}_{xx}^{\mathbb{Q}} + \boldsymbol{\rho}_x', \tag{A.6}$$

where $\boldsymbol{\Phi}_{xx}^{\mathbb{Q}} = \boldsymbol{\Phi}_{xx} + \gamma\boldsymbol{\Omega}_{xx}\sum_{j=2}^{N}\left[\mathbf{b}_x^{(j-1)}\mathbf{s}_x^{(j)\prime}\right]$ as defined in equation (2.25) in the main text.

Further, by evaluating equation (A.6) at $n = 1$, we obtain that

$$\boldsymbol{\delta}_x' = \mathbf{p}_x'\boldsymbol{\Phi}_{xx}^{\mathbb{Q}} + \boldsymbol{\rho}_x', \tag{A.7}$$

which (i) allows us to write equation (A.6) as $\mathbf{b}_x^{(n)\prime} = \mathbf{b}_x^{(n-1)\prime}\boldsymbol{\Phi}_{xx}^{\mathbb{Q}} + \boldsymbol{\delta}_x'$, which is equation (2.23) in the main text, and (ii) delivers the expression for the loadings on the real short rate in equation (2.21) once we solve for $\boldsymbol{\rho}_x$.

Similarly, by collecting and matching terms for the constant in both equations (A.4) and (A.5), we arrive at the following recursion for the constant of the equilibrium (log) prices of the nominal bonds:

$$b_{x0}^{(n)} = p_{x0} + b_{x0}^{(n-1)} + \left[\mathbf{p}_x + \mathbf{b}_x^{(n-1)}\right]' \boldsymbol{\Phi}_{x0}^{\mathbb{Q}} - \tfrac{1}{2}\left[\mathbf{p}_x + \mathbf{b}_x^{(n-1)}\right]' \boldsymbol{\Omega}_{xx}\left[\mathbf{p}_x + \mathbf{b}_x^{(n-1)}\right] + \rho_{x0}, \tag{A.8}$$

where $\mathbf{\Phi}^{\mathbb{Q}}_{x0} = \mathbf{\Phi}_{x0} + \gamma \mathbf{\Omega}_{xx} \left\{ \mathbf{p}_x + \sum_{j=2}^{N} \left[\mathbf{b}_x^{(j-1)} s_{x0}^{(j)} \right] \right\}$ as defined in equation (2.26) in the main text.

Evaluating equation (A.8) at $n = 1$ as above

$$\delta_{x0} = p_{x0} + \mathbf{p}_x' \mathbf{\Phi}^{\mathbb{Q}}_{x0} - \frac{1}{2} \mathbf{p}_x' \mathbf{\Omega}_{xx} \mathbf{p}_x + \rho_{x0}, \tag{A.9}$$

and, using this expression to re-arrange equation (A.8), we find that $b_{x0}^{(n)} = b_{x0}^{(n-1)} + \mathbf{b}_x^{(n-1)'} (\mathbf{\Phi}^{\mathbb{Q}}_{x0} - \mathbf{\Omega}_{xx} \mathbf{p}_x) - \frac{1}{2} \mathbf{b}_x^{(n-1)'} \mathbf{\Omega}_{xx} \mathbf{b}_x^{(n-1)} + \delta_{x0}$, which coincides with equation (2.24) in Theorem 1. Similarly, solving for ρ_{x0} above delivers the expression for the constant of the real short-rate in equation (2.22) in the text.

B.2.1 Proof of existence and uniqueness of a solution

Fixed-point mapping for $\mathbf{\Phi}^{\mathbb{Q}}_{xx}$. To complete the proof of the theorem, we need to show that equation (2.25) has a unique solution for γ below a threshold $\overline{\gamma}$ and that all the eigenvalues of $\mathbf{\Phi}^{\mathbb{Q}}_{xx}$ lie inside the unit circle in the complex plane. For this purpose, define the following mapping

$$\mathbf{T}(\mathbf{\Phi}^{\mathbb{Q}}_{xx}) = \mathbf{\Phi}_{xx} + \gamma \mathbf{\Omega}_{xx} \sum_{j=2}^{N} \left[\mathbf{b}_x^{(j-1)} (\mathbf{\Phi}^{\mathbb{Q}}_{xx}) \mathbf{s}_x^{(j)'} \right], \tag{A.10}$$

where $\mathbf{b}_x^{(n)'} (\mathbf{\Phi}^{\mathbb{Q}}_{xx}) = \boldsymbol{\delta}_x' \sum_{k=0}^{n-1} (\mathbf{\Phi}^{\mathbb{Q}}_{xx})^k$, and note that solving the equation $\mathbf{T}(\mathbf{\Phi}^{\mathbb{Q}}_{xx}) = \mathbf{\Phi}^{\mathbb{Q}}_{xx}$ is equivalent to finding a fixed point of the mapping $\mathbf{T}$.

Banach contraction mapping theorem. To prove the existence and uniqueness of the solution to equation (A.10), i.e., the existence of a unique fixed point, we will invoke the Banach contraction mapping theorem. Specifically, let (X, d) be a *complete metric space*, where $d : X \times X \to [0, \infty)$ is a *metric*, that satisfies that, for all $x, y, z \in X$,

1. $d(x, y) = 0$ if and only if $x = y$,

2. $d(x, y) = d(y, x)$ (symmetry),

3. $d(x,z) \leq d(x,y) + d(y,z)$ (triangle inequality);

and *completeness* means that every Cauchy sequence (x_n) in X (that is, sequences satisfying $d(x_m, x_n) \to 0$ as $m, n \to \infty$) converges to some limit $x \in X$.

Let $T : X \to X$ be a *contraction mapping*, i.e., there exists a constant $0 < q < 1$ such that

$$d[T(x), T(y)] \leq q\, d(x,y) \quad \text{for all } x, y \in X. \tag{A.11}$$

Then T admits a unique fixed point $x^\star \in X$ such that $T(x^\star) = x^\star$, and for any initial point $x_0 \in X$, the *Picard iteration* $x_{n+1} = T(x_n)$ converges to $x^\star$.

Matrix norm choice. In order to prove the existence and uniqueness of the solution to equation (A.10), we will work on the closed ball

$$\mathcal{B}_\rho = \left\{ \mathbf{\Phi}^{\mathbb{Q}}_{xx} : \|\mathbf{\Phi}^{\mathbb{Q}}_{xx}\| \leq \rho \right\}, \qquad \text{with} \quad 0 \leq \rho < 1, \tag{A.12}$$

equipped with the metric $d(\mathbf{X}, \mathbf{Y}) = \|\mathbf{X} - \mathbf{Y}\|$ induced by the spectral norm. Specifically, let $\mathbf{A} \in \mathbb{R}^{n \times n}$ be a real square matrix and let $\|\mathbf{v}\|$ be the Euclidean norm of a vector $\mathbf{v} \in \mathbb{R}^n$:

$$\|\mathbf{v}\| \equiv \sqrt{\mathbf{v}'\mathbf{v}} \tag{A.13}$$

Then, the spectral norm of the matrix $\mathbf{A}$ is defined as the operator norm induced by the Euclidean vector norm:

$$\|\mathbf{A}\| \equiv \sup_{\mathbf{v} \neq 0} \frac{\|\mathbf{A}\mathbf{v}\|}{\|\mathbf{v}\|} = \sqrt{\lambda_{\max}(\mathbf{A}'\mathbf{A})}, \tag{A.14}$$

where $\lambda_{\max}(\cdot)$ denotes the largest eigenvalue of a matrix. Importantly, the spectral norm of a matrix has two important properties that we will use below: (i) the spectral norm of a matrix is *submultiplicative* ($\|\mathbf{AB}\| \leq \|\mathbf{A}\|\,\|\mathbf{B}\|$), and (ii) it dominates the spectral radius of a matrix (i.e., its largest eigenvalue). Specifically, using the definition of the spectral radius of a real square matrix $\mathbf{A} \in \mathbb{R}^{M \times M}$

$$\varrho(\mathbf{A}) \equiv \max_i |\lambda_i(\mathbf{A})|, \tag{A.15}$$

where $\lambda_i(\mathbf{A})$ are the eigenvalues of $\mathbf{A}$, we have that $\varrho(\mathbf{A}) \leq \|\mathbf{A}\| < 1$. Consequently, since any fixed point in $\mathcal{B}_\rho$ satisfies $\|\mathbf{\Phi}_{xx}^{\mathbb{Q}}\| \leq \rho < 1$, then we have $\varrho(\mathbf{\Phi}_{xx}^{\mathbb{Q}}) < 1$, which implies that any candidate for a solution of (A.10) will satisfy that the dynamics under the $\mathbb{Q}$-measure are stationary.

Since $\mathbb{R}^{M\times M}$ endowed with $\|\cdot\|$ is complete (finite-dimensional normed spaces are Banach), any closed subset, such as $\mathcal{B}_\rho$, is complete under the subspace metric. Therefore, $(\mathcal{B}_\rho, \|\cdot\|)$ is a complete metric space, which is the setting required by Banach's theorem. Specifically, to invoke Banach's contraction mapping theorem for (A.10) on $(\mathcal{B}_\rho, \|\cdot\|)$ we will need to establish:

1. *Self-map property:* find the set of $\gamma \geq 0$ such that $\mathbf{\Phi}_{xx}^{\mathbb{Q}}$ remains in the closed ball, i.e., $\mathbf{T}(\mathcal{B}_\rho) \subseteq \mathcal{B}_\rho$.

2. *Contraction property:* find the set of $\gamma \geq 0$ making $\mathbf{T}(\mathcal{B}_\rho)$ a contraction on $\mathcal{B}_\rho$.

Three useful lemmas. Before establishing the set of values for γ that satisfy both the self-map and contraction properties, we first establish three lemmas that will be useful below. Specifically, for $\|\mathbf{A}\| \leq \rho < 1$, define $\mathbf{S}_n(\mathbf{A}) \equiv \sum_{k=0}^{n-1} \mathbf{A}^k$

Lemma 2. *Let* $\mathbf{A}$ *be a real square matrix that has a spectral radius* $\varrho(\mathbf{A}) < 1$*, and let* $\mathbf{P} \succ \mathbf{0}$ *be the unique symmetric positive definite matrix that solves the discrete Lyapunov equation*

$$\mathbf{A}'\mathbf{P}\mathbf{A} = \mathbf{P} - \mathbf{Q}, \tag{A.16}$$

for a given symmetric positive definite matrix $\mathbf{Q} \succ \mathbf{0}$*. Define* $\tilde{\mathbf{A}} = \mathbf{P}^{1/2}\mathbf{A}\mathbf{P}^{-1/2}$*, where* $\mathbf{P}^{1/2}$ *is the symmetric square root of* $\mathbf{P}$ *such that* $\mathbf{P} = \mathbf{P}^{1/2}\mathbf{P}^{1/2}$*. Then*

$$\|\tilde{\mathbf{A}}\| = \sqrt{1 - \lambda_{\min}(\mathbf{P}^{-1/2}\mathbf{Q}\mathbf{P}^{-1/2})} < 1, \tag{A.17}$$

where $\lambda_{\min}(\cdot)$ *denotes the smallest eigenvalue of a matrix.*

Proof. Using the definition of the spectral norm of a real matrix $\mathbf{M}$ as in equation (A.14) we have that:

$$\|\mathbf{M}\|^2 = \sup_{\mathbf{v}\neq 0} \frac{\|\mathbf{M}\mathbf{v}\|^2}{\|\mathbf{v}\|^2} = \sup_{\mathbf{v}\neq 0} \frac{\mathbf{v}'(\mathbf{M}'\mathbf{M})\mathbf{v}}{\mathbf{v}'\mathbf{v}}, \tag{A.18}$$

that is, the square of the spectral norm of a matrix coincides with the supremum of the following Rayleigh quotient

$$R(\mathbf{v}) = \frac{\mathbf{v}'(\mathbf{M}'\mathbf{M})\mathbf{v}}{\mathbf{v}'\mathbf{v}} \tag{A.19}$$

The Rayleigh-Ritz theorem states that, for any symmetric matrix $\mathbf{S}$, the Rayleigh quotients for $\mathbf{v} \neq 0$ are bounded by the smallest and largest eigenvalues of $\mathbf{S}$:

$$\lambda_{\min}(\mathbf{S}) \leq \frac{\mathbf{v}'\mathbf{S}\mathbf{v}}{\mathbf{v}'\mathbf{v}} \leq \lambda_{\max}(\mathbf{S}), \tag{A.20}$$

where equality is achieved when $\mathbf{v}$ is equal to the eigenvector corresponding to $\lambda_{\min}(\mathbf{S})$ and $\lambda_{\max}(\mathbf{S})$. Consequently, we have that taking square roots and applying the Rayleigh-Ritz theorem to the case that $\mathbf{S} = \mathbf{M}'\mathbf{M}$ is symmetric, delivers

$$\|\mathbf{M}\| = \sqrt{\lambda_{\max}(\mathbf{M}'\mathbf{M})}, \tag{A.21}$$

which coincides with the definition of the spectral norm of a matrix in equation (A.14) above.

Now conjugating the Lyapunov equation (A.16) by $\mathbf{P}^{-1/2}$, we have that

$$\tilde{\mathbf{A}}'\tilde{\mathbf{A}} = \mathbf{P}^{-1/2}(\mathbf{A}'\mathbf{P}\mathbf{A})\mathbf{P}^{-1/2} = \mathbf{P}^{-1/2}(\mathbf{P} - \mathbf{Q})\mathbf{P}^{-1/2} = \mathbf{I} - \mathbf{B}, \tag{A.22}$$

where we have defined

$$\mathbf{B} = \mathbf{P}^{-1/2}\mathbf{Q}\mathbf{P}^{-1/2}. \tag{A.23}$$

Then, using equation (A.22) to compute the spectral norm of $\tilde{\mathbf{A}}$ we have that ,

$$\|\tilde{\mathbf{A}}\| = \sqrt{\lambda_{\max}(\tilde{\mathbf{A}}'\tilde{\mathbf{A}})} = \sqrt{\lambda_{\max}(\mathbf{I} - \mathbf{B})} \tag{A.24}$$

Since $\mathbf{Q} \succ \mathbf{0}$ and $\mathbf{P} \succ \mathbf{0}$, the matrix $\mathbf{B}$ is also symmetric and positive definite, which implies that all its eigenvalues are real and positive. Moreover, since $\mathbf{P} - \mathbf{Q} \succeq \mathbf{0}$, we have that $\mathbf{I} - \mathbf{B} = \tilde{\mathbf{A}}'\tilde{\mathbf{A}} \succeq \mathbf{0}$ (cf. equation A.22 above) which implies that all the eigenvalues of $\mathbf{B}$ are bounded above by 1. Consequently,

$$0 < \lambda_{\min}(\mathbf{B}) \leq \lambda_{\max}(\mathbf{B}) \leq 1. \tag{A.25}$$

Moreover, if we denote by $\sigma(\mathbf{B})$ the set of all the eigenvalues of $\mathbf{B}$ (i.e., the spectrum of the matrix $\mathbf{B}$), then $\sigma(\mathbf{I} - \mathbf{B}) = \{1 - \lambda : \lambda \in \sigma(\mathbf{B})\}$. To prove this, we use that $\mathbf{Bx} = \lambda\mathbf{x}$ (i.e., the definition of an eigenvalue) implies that $(\mathbf{I} - \mathbf{B})\mathbf{x} = (1 - \lambda)\mathbf{x}$. Consequently, since all the eigenvalues of $\mathbf{B}$ are real and bounded between 0 and 1, we have that the largest eigenvalue of $\mathbf{I} - \mathbf{B}$ coincides with one minus the smallest eigenvalue of $\mathbf{B}$:

$$\|\tilde{\mathbf{A}}\| = \sqrt{\lambda_{\max}(\mathbf{I} - \mathbf{B})} = \sqrt{1 - \lambda_{\min}(\mathbf{B})} < 1, \tag{A.26}$$

where the strict inequality follows from $\lambda_{\min}(\mathbf{B}) > 0$. □

Lemma 3. *If $\|\mathbf{A}\| \leq \rho < 1$, then*

$$\|\mathbf{S}_n(\mathbf{A})\| \leq \sum_{k=0}^{n-1} \|\mathbf{A}\|^k \leq \frac{1}{1 - \rho}. \tag{A.27}$$

Proof. The submultiplicativity of the spectral norm gives $\|\mathbf{A}^k\| \leq \|\mathbf{A}\|^k \leq \rho^k$. Then, summing from $k = 0$ to $n - 1$ yields equation (A.27). □

Lemma 4. *If $\|\mathbf{A}\| \leq \rho < 1$ and $\|\mathbf{B}\| \leq \rho < 1$, then*

$$\|\mathbf{S}_n(\mathbf{A}) - \mathbf{S}_n(\mathbf{B})\| \leq \frac{1}{(1 - \rho)^2}\|\mathbf{A} - \mathbf{B}\|. \tag{A.28}$$

Proof. Using the telescoping factorization

$$\mathbf{A}^k - \mathbf{B}^k = \sum_{m=0}^{k-1} \mathbf{A}^{k-1-m}(\mathbf{A} - \mathbf{B})\mathbf{B}^m, \tag{A.29}$$

and the submultiplicativity property of the spectral norm, we get

$$\begin{aligned}\|\mathbf{A}^k - \mathbf{B}^k\| &\leq \sum_{m=0}^{k-1} \|\mathbf{A}^{k-1-m}\|\|\mathbf{A} - \mathbf{B}\|\|\mathbf{B}^m\| \\ &\leq \sum_{m=0}^{k-1} \rho^{k-1-m}\|\mathbf{A} - \mathbf{B}\|\rho^m \\ &= k\rho^{k-1}\|\mathbf{A} - \mathbf{B}\|.\end{aligned} \tag{A.30}$$

Therefore

$$
\begin{aligned}
\|\mathbf{S}_n(\mathbf{A}) - \mathbf{S}_n(\mathbf{B})\| &\le \left(\sum_{k=1}^{n-1} k\rho^{k-1}\right) \|\mathbf{A} - \mathbf{B}\| \\
&\le \left(\sum_{k=1}^{\infty} k\rho^{k-1}\right) \|\mathbf{A} - \mathbf{B}\| \\
&= \frac{1}{(1-\rho)^2} \|\mathbf{A} - \mathbf{B}\|,
\end{aligned}
\tag{A.31}
$$

since $\sum_{k=1}^{\infty} k\rho^{k-1} = \frac{1}{(1-\rho)^2}$ for $0 \le \rho < 1$. □

Self-map property. As noted above, we need to find the set of $\gamma \ge 0$ such that $\mathbf{\Phi}_{xx}^{\mathbb{Q}}$ remains in the closed ball, i.e., $\|\mathbf{\Phi}_{xx}^{\mathbb{Q}}\| \le \rho$. Specifically, note that:

$$
\begin{aligned}
\|\mathbf{T}(\mathbf{\Phi}_{xx}^{\mathbb{Q}})\| &\le \|\mathbf{\Phi}_{xx}\| + \gamma \ \|\mathbf{\Omega}_{xx}\| \|\boldsymbol{\delta}_x\| \sum_{j=2}^{N} \left\|\mathbf{S}_{j-1}(\mathbf{\Phi}_{xx}^{\mathbb{Q}})\right\| \|\mathbf{s}_x^{(j)}\| \\
&\le \|\mathbf{\Phi}_{xx}\| + \frac{\gamma}{1-\rho} \|\mathbf{\Omega}_{xx}\| \|\boldsymbol{\delta}_x\| \left(\sum_{j=2}^{N} \|\mathbf{s}_x^{(j)}\|\right),
\end{aligned}
\tag{A.32}
$$

where we have used Lemma 3.

Thus, to ensure that $\mathbf{T}(\mathcal{B}_\rho) \subseteq \mathcal{B}_\rho$, we need that

$$
\|\mathbf{\Phi}_{xx}\| + \frac{\gamma}{1-\rho} \|\mathbf{\Omega}_{xx}\| \|\boldsymbol{\delta}_x\| \left(\sum_{j=2}^{N} \|\mathbf{s}_x^{(j)}\|\right) \le \rho,
\tag{A.33}
$$

which requires both that $\|\mathbf{\Phi}_{xx}\| \le \rho$ and that

$$
0 \le \gamma \le \frac{(\rho - \|\mathbf{\Phi}_{xx}\|)(1-\rho)}{\|\mathbf{\Omega}_{xx}\| \|\boldsymbol{\delta}_x\| \sum_{j=2}^{N} \|\mathbf{s}_x^{(j)}\|}.
\tag{A.34}
$$

While, as stated above, the spectral norm of a matrix dominates its spectral radius, the opposite of this statement is not generally true. However, since we have assumed that the dynamics of the factors are stationary under the physical measure, $\mathbb{P}$, we have that $\varrho(\mathbf{\Phi}_{xx}) < 1$. Consequently, we can use Lemma 2 to find a set of rotated factors $\mathbf{z} = \mathbf{P}^{1/2}\mathbf{x}$, where $\mathbf{P}$ satisfies equation (A.16) with $\mathbf{A} = \mathbf{\Phi}_{xx}$ and a suitably chosen symmetric positive definite matrix $\mathbf{Q}$ (for example, the identity matrix), such that the autocorrelation matrix of the new rotated factors, $\mathbf{\Phi}_{zz} = \mathbf{P}^{1/2}\mathbf{\Phi}_{xx}\mathbf{P}^{-1/2}$, satisfies $\|\mathbf{\Phi}_{zz}\| < \rho < 1$ (as required for $\mathbf{T}(\mathcal{B}_\rho) \subseteq \mathcal{B}_\rho$).[25] Therefore, we can assume without loss of generality, that $\|\mathbf{\Phi}_{xx}\| < \rho < 1$, since we can always rotate the factors so that their autocorrelation matrix satisfies this condition.

Contraction property. We now turn to find the values of $\gamma \geq 0$ such that $\mathbf{T}$ is a contraction on $\mathcal{B}_\rho$. Specifically, let $\mathbf{\Phi}^{\mathbb{Q}}_{xx}, \widetilde{\mathbf{\Phi}}^{\mathbb{Q}}_{xx} \in \mathcal{B}_\rho$, then we have

$$\begin{aligned}\|\mathbf{T}(\mathbf{\Phi}^{\mathbb{Q}}_{xx}) - \mathbf{T}(\widetilde{\mathbf{\Phi}}^{\mathbb{Q}}_{xx})\| &\leq \gamma\|\mathbf{\Omega}_{xx}\| \left\| \sum_{j=2}^{N} \left\{ \left[\mathbf{b}_x^{(j-1)}(\mathbf{\Phi}^{\mathbb{Q}}_{xx}) - \mathbf{b}_x^{(j-1)}(\widetilde{\mathbf{\Phi}}^{\mathbb{Q}}_{xx}) \right] \mathbf{s}_x^{(j)\prime} \right\} \right\| \\ &\leq \gamma\|\mathbf{\Omega}_{xx}\| \left\| \sum_{j=2}^{N} \left\{ \left[\mathbf{S}_{j-1}(\mathbf{\Phi}^{\mathbb{Q}}_{xx})' - \mathbf{S}_{j-1}(\widetilde{\mathbf{\Phi}}^{\mathbb{Q}}_{xx})' \right] \boldsymbol{\delta}_x \mathbf{s}_x^{(j)\prime} \right\} \right\|,\end{aligned} \tag{A.35}$$

where we have used that $\mathbf{b}_x^{(n)\prime}(\mathbf{\Phi}^{\mathbb{Q}}_{xx}) = \boldsymbol{\delta}_x' \sum_{k=0}^{n-1}(\mathbf{\Phi}^{\mathbb{Q}}_{xx})^k = \boldsymbol{\delta}_x'\mathbf{S}_n(\mathbf{\Phi}^{\mathbb{Q}}_{xx})$. Then, applying Lemma 4, we have that

$$\begin{aligned}\|\mathbf{T}(\mathbf{\Phi}^{\mathbb{Q}}_{xx}) - \mathbf{T}(\widetilde{\mathbf{\Phi}}^{\mathbb{Q}}_{xx})\| &\leq \gamma\|\mathbf{\Omega}_{xx}\|\|\boldsymbol{\delta}_x\| \sum_{j=2}^{N} \left[\left\| \mathbf{S}_{j-1}(\mathbf{\Phi}^{\mathbb{Q}}_{xx}) - \mathbf{S}_{j-1}(\widetilde{\mathbf{\Phi}}^{\mathbb{Q}}_{xx}) \right\| \left\| \mathbf{s}_x^{(j)} \right\| \right] \\ &\leq \frac{\gamma}{(1-\rho)^2}\|\mathbf{\Omega}_{xx}\|\|\boldsymbol{\delta}_x\| \left[\sum_{j=2}^{N} \left\| \mathbf{s}_x^{(j)} \right\| \right] \|\mathbf{\Phi}^{\mathbb{Q}}_{xx} - \widetilde{\mathbf{\Phi}}^{\mathbb{Q}}_{xx}\|\end{aligned} \tag{A.36}$$

Thus $\mathbf{T}(\cdot)$ is a contraction if

$$0 \leq \frac{\gamma}{(1-\rho)^2}\|\mathbf{\Omega}_{xx}\|\|\boldsymbol{\delta}_x\| \left(\sum_{j=2}^{N} \left\| \mathbf{s}_x^{(j)} \right\| \right) < 1 \tag{A.37}$$

which imposes the following bounds on the relative risk aversion parameter:

$$0 \leq \gamma < \frac{(1-\rho)^2}{\|\mathbf{\Omega}_{xx}\|\|\boldsymbol{\delta}_x\| \sum_{j=2}^{N} \|\mathbf{s}_x^{(j)}\|}. \tag{A.38}$$

[25] Importantly, it can be shown that $\|\tilde{\mathbf{A}}\| = \|\mathbf{A}\|_{\mathbf{P}}$ where $\|\cdot\|_{\mathbf{P}}$ is the matrix (operator) norm induced by the (non-Euclidean) weighted vector norm $\|\mathbf{v}\|_{\mathbf{P}} = \sqrt{\mathbf{v}'\mathbf{P}\mathbf{v}}$. Therefore, by working with the rotated set of factors, $\mathbf{z} = \mathbf{P}^{1/2}\mathbf{x}$, we are essentially working with a different matrix norm, which is guaranteed to exist under the assumption that $\varrho(\mathbf{\Phi}_{xx}) < 1$, under which $\|\mathbf{\Phi}_{xx}\|_{\mathbf{P}} < 1$.

Relative risk aversion bound. Note that both equations (A.34) and (A.38) must hold in order for equation (A.10) to have a unique solution. Choosing $\rho^\star = \frac{1}{2}(1 + \|\mathbf{\Phi}_{xx}\|)$, which is guaranteed to satisfy $\rho^\star < 1$ given that $\|\mathbf{\Phi}_{xx}\| < 1$, makes both bounds collapse to

$$0 \leq \gamma < \overline{\gamma} \;\equiv\; \frac{(1 - \|\mathbf{\Phi}_{xx}\|)^2}{4\|\mathbf{\Omega}_{xx}\|\|\boldsymbol{\delta}_x\| \sum_{j=2}^N \|\mathbf{s}_x^{(j)}\|}. \tag{A.39}$$

B.3 Proof of Theorem 2

Prices of risk. Evaluating the arbitrageurs' prices of risk in equation (2.18) at the market clearing conditions in equations (2.19) and (2.20), we have that

$$\boldsymbol{\lambda}_{x,t} = -\gamma \mathbf{\Sigma}_x' \left\{ \mathbf{p}_x \sum_{j=1}^N d_t^{(j)} + \sum_{j=2}^N \mathbf{b}_x^{(j-1)} d_t^{(j)} \right\} = -\gamma \mathbf{\Sigma}_x' \left\{ \mathbf{p}_x + \sum_{j=2}^N \mathbf{b}_x^{(j-1)} s_t^{(j)} \right\}, \tag{A.40}$$

where the first equality uses the initial condition $\mathbf{b}_x^{(0)} = \mathbf{0}$, and the second uses Walras's law, $\sum_{j=1}^N d_t^{(j)} = 1$, together with $d_t^{(j)} = s_t^{(j)}$ for $j = 2, \ldots, N$. Note that the prices of risk are affine in the state variables, since the supply of nominal bonds is affine in $\mathbf{x}_t$. Specifically, substituting $s_t^{(j)} = s_{x0}^{(j)} + \mathbf{s}_x^{(j)\prime} \mathbf{x}_t$ into equation (A.40), we have that

$$\boldsymbol{\lambda}_{x,t} = -\gamma \mathbf{\Sigma}_x' \left\{ \mathbf{p}_x + \sum_{j=2}^N \left[\mathbf{b}_x^{(j-1)} s_{x0}^{(j)} \right] \right\} - \gamma \mathbf{\Sigma}_x' \sum_{j=2}^N \left[\mathbf{b}_x^{(j-1)} \mathbf{s}_x^{(j)\prime} \right] \mathbf{x}_t, \tag{A.41}$$

which delivers equation (2.29) in the main text.

Inflation. Following a similar argument to Backus, Foresi, and Telmer (2001), we have that, in complete markets, inflation must satisfy

$$\pi_{t+1} = \log M_{t+1} - \log M_{t+1}^{\$}. \tag{A.42}$$

Substituting the expressions for the real and nominal SDFs in equations (2.28) and (2.27) into this equation yields:

$$\pi_{t+1} = i_t - r_t + \frac{1}{2} \boldsymbol{\lambda}_{x,t}^{\$\prime} \boldsymbol{\lambda}_{x,t}^{\$} - \frac{1}{2} \boldsymbol{\lambda}_{x,t}' \boldsymbol{\lambda}_{x,t} + \left(\boldsymbol{\lambda}_{x,t}^{\$} - \boldsymbol{\lambda}_{x,t} \right)' \boldsymbol{\eta}_{t+1}. \tag{A.43}$$

By rearranging terms, using $\boldsymbol{\lambda}^{\$}_{x,t} - \boldsymbol{\lambda}_{x,t} = \boldsymbol{\Sigma}'_x \mathbf{p}_x$, and that $\boldsymbol{\lambda}^{\$\prime}_{x,t}\boldsymbol{\lambda}^{\$}_{x,t} = \boldsymbol{\lambda}'_{x,t}\boldsymbol{\lambda}_{x,t} + \mathbf{p}'_x\boldsymbol{\Omega}_{xx}\mathbf{p}_x + 2\mathbf{p}'_x\boldsymbol{\Sigma}_x\boldsymbol{\lambda}_{x,t}$, we find

$$\pi_{t+1} = (\delta_{x0} - \rho_{x0}) + (\boldsymbol{\delta}_x - \boldsymbol{\rho}_x)'\mathbf{x}_t + \frac{1}{2}\mathbf{p}'_x\boldsymbol{\Omega}_{xx}\mathbf{p}_x + \mathbf{p}'_x\boldsymbol{\Sigma}_x\boldsymbol{\lambda}_{x,t} + \mathbf{p}'_x\boldsymbol{\Sigma}_x\boldsymbol{\eta}_{t+1}. \tag{A.44}$$

Substituting $\boldsymbol{\eta}_{t+1} = \boldsymbol{\Sigma}_x^{-1}\left(\mathbf{x}_{t+1} - \boldsymbol{\Phi}_{x0} - \boldsymbol{\Phi}_{xx}\mathbf{x}_t\right)$ from equation (2.1) and $\boldsymbol{\lambda}_{x,t}$ from equation (2.29), we have that

$$\pi_{t+1} = (\delta_{x0} - \rho_{x0}) + (\boldsymbol{\delta}_x - \boldsymbol{\rho}_x)'\mathbf{x}_t + \frac{1}{2}\mathbf{p}'_x\boldsymbol{\Omega}_{xx}\mathbf{p}_x - \mathbf{p}'_x\boldsymbol{\Phi}^{\mathbb{Q}}_{x0} - \mathbf{p}'_x\boldsymbol{\Phi}^{\mathbb{Q}}_{xx}\mathbf{x}_t + \mathbf{p}'_x\mathbf{x}_{t+1}. \tag{A.45}$$

For $\pi_{t+1} = p_{x0} + \mathbf{p}'_x\mathbf{x}_{t+1}$ to be true, all terms for $\mathbf{x}_t$ must be zero, and the constant term must be equal to p_{x0}. Thus, collecting all the terms for $\mathbf{x}_t$ and equating to zero, we find

$$\boldsymbol{\rho}'_x = \boldsymbol{\delta}'_x - \mathbf{p}'_x\boldsymbol{\Phi}^{\mathbb{Q}}_{xx}, \tag{A.46}$$

which is equation (2.21).

Similarly, collecting all the terms for the constants, we have that:

$$\delta_{x0} - \rho_{x0} + \frac{1}{2}\mathbf{p}'_x\boldsymbol{\Omega}_{xx}\mathbf{p}_x - \mathbf{p}'_x\boldsymbol{\Phi}^{\mathbb{Q}}_{x0} = p_{x0}, \tag{A.47}$$

which delivers equation (2.22) once we solve for ρ_{x0}.

Nominal bond prices. To price zero-coupon nominal bonds using the nominal SDF in equation (2.28), we have:

$$B^{(n)}_t = \mathrm{E}_t\left[M^{\$}_{t+1}B^{(n-1)}_{t+1}\right]. \tag{A.48}$$

Substituting the expression for the SDF in equation (2.28), and the conjecture for the log price of the nominal bonds, we have that the RHS of (A.48) satisfies:

$$\begin{aligned}&\mathrm{E}_t\left[M^{\$}_{t+1}B^{(n-1)}_{t+1}\right] = \\ &\quad= \mathrm{E}_t\left\{\exp\left[-\delta_{x0} - \boldsymbol{\delta}'_x\mathbf{x}_t - \frac{1}{2}\boldsymbol{\lambda}^{\$\prime}_{x,t}\boldsymbol{\lambda}^{\$}_{x,t} - \boldsymbol{\lambda}^{\$\prime}_{x,t}\boldsymbol{\eta}_{t+1} - b^{(n-1)}_{x0} - \mathbf{b}^{(n-1)\prime}_x\mathbf{x}_{t+1}\right]\right\},\end{aligned} \tag{A.49}$$

which upon substitution of the expressions for $\mathbf{x}_{t+1}$ in equation (2.1), and $\boldsymbol{\lambda}^{\$}_{x,t}$ in equation (2.32) gives:

$$\begin{aligned} \mathrm{E}_t\left[M^{\$}_{t+1}B^{(n-1)}_{t+1}\right] = \mathrm{E}_t\Bigg(\exp\Bigg\{ & - \delta_{x0} - b^{(n-1)}_{x0} - \mathbf{b}^{(n-1)\prime}_{x}\boldsymbol{\Phi}_{x0} \\ - \left[\boldsymbol{\delta}'_x + \mathbf{b}^{(n-1)\prime}_{x}\boldsymbol{\Phi}_{xx}\right]\mathbf{x}_t - \frac{1}{2}\boldsymbol{\lambda}^{\$\prime}_{x,t}\boldsymbol{\lambda}^{\$}_{x,t} & - \left[\boldsymbol{\lambda}^{\$\prime}_{x,t} + \mathbf{b}^{(n-1)\prime}_{x}\boldsymbol{\Sigma}_x\right]\boldsymbol{\eta}_{t+1}\Bigg\}\Bigg). \end{aligned} \tag{A.50}$$

Using the properties of the log-normal distribution, we have that

$$\begin{aligned} & \mathrm{E}_t\left(\exp\left\{-\left[\boldsymbol{\lambda}^{\$\prime}_{x,t} + \mathbf{b}^{(n-1)\prime}_{x}\boldsymbol{\Sigma}_x\right]\boldsymbol{\eta}_{t+1}\right\}\right) = \\ & \exp\left[\frac{1}{2}\boldsymbol{\lambda}^{\$\prime}_{x,t}\boldsymbol{\lambda}^{\$}_{x,t} + \frac{1}{2}\mathbf{b}^{(n-1)\prime}_{x}\boldsymbol{\Omega}_{xx}\mathbf{b}^{(n-1)}_{x} + \mathbf{b}^{(n-1)\prime}_{x}\boldsymbol{\Sigma}_x\boldsymbol{\lambda}^{\$}_{x,t}\right]. \end{aligned} \tag{A.51}$$

Substituting this expression into equation (A.50) and rearranging, we have that taking logs on both sides of equation (A.48) delivers:

$$\begin{aligned} -b^{(n)}_{x0} - \mathbf{b}^{(n)\prime}_{x}\mathbf{x}_t = & -\delta_{x0} - b^{(n-1)}_{x0} - \mathbf{b}^{(n-1)\prime}_{x}\boldsymbol{\Phi}^{\mathbb{Q}\$}_{x0} \\ & - \left[\boldsymbol{\delta}_x + \mathbf{b}^{(n-1)\prime}_{x}\boldsymbol{\Phi}^{\mathbb{Q}}_{xx}\right]'\mathbf{x}_t + \frac{1}{2}\mathbf{b}^{(n-1)\prime}_{x}\boldsymbol{\Omega}_{xx}\mathbf{b}^{(n-1)}_{x}, \end{aligned} \tag{A.52}$$

where we have used that $\boldsymbol{\lambda}^{\$}_{x,t} = \boldsymbol{\Sigma}^{-1}_x(\boldsymbol{\Phi}_{x0} - \boldsymbol{\Phi}^{\mathbb{Q}\$}_{x0}) + \boldsymbol{\Sigma}^{-1}_x(\boldsymbol{\Phi}_{xx} - \boldsymbol{\Phi}^{\mathbb{Q}}_{xx})\mathbf{x}_t$. Collecting terms on both sides of equation (A.52) delivers the recursions for the pricing of nominal bonds in equations (2.23) and (2.24) in the main text.

B.4 Proof of Proposition 1

Imposing the factor–mimicking choice for supply loadings, namely $\mathbf{s}^{(n)}_{\beta} = \boldsymbol{\omega}^{(n)}$, we have that

$$\boldsymbol{\Omega}_{xx}\sum_{j=2}^{N}\mathbf{b}^{(j-1)}_{x}\mathbf{s}^{(j)\prime}_{\beta} = \boldsymbol{\Omega}_{xx}\sum_{j=2}^{N}\mathbf{b}^{(j-1)}_{x}\boldsymbol{\omega}^{(j)\prime} \tag{A.53}$$

$$= \boldsymbol{\Omega}_{xx}\left[-\sum_{j=2}^{N}\mathbf{b}^{(j-1)}_{x}\mathbf{b}^{(j-1)\prime}_{x}\right]\left[\sum_{k=2}^{N}\mathbf{b}^{(k-1)}_{x}\mathbf{b}^{(k-1)\prime}_{x}\right]^{-1}(\boldsymbol{\Sigma}^{-1}_x)' \tag{A.54}$$

$$= -\boldsymbol{\Omega}_{xx}(\boldsymbol{\Sigma}'_x)^{-1} \tag{A.55}$$

$$= -\boldsymbol{\Sigma}_x. \tag{A.56}$$

Further, plugging equation (A.56) into equation (3.4), we have

$$\boldsymbol{\Phi}^{\mathbb{Q}}_{xx} = \boldsymbol{\Phi}_{xx} - \gamma\boldsymbol{\Sigma}_x\boldsymbol{\beta}_x, \tag{A.57}$$

which, once we solve for $\boldsymbol{\beta}_x$ delivers

$$\boldsymbol{\beta}_x = \frac{1}{\gamma}\boldsymbol{\Sigma}_x^{-1}(\boldsymbol{\Phi}_{xx} - \boldsymbol{\Phi}_{xx}^{\mathbb{Q}}) = \frac{1}{\gamma}\boldsymbol{\lambda}_x. \tag{A.58}$$

Similarly, we can plug equation (A.56) into equation (3.3), and use that $s_{\beta 0}^{(j)} = 0$ from equation (3.8), to obtain

$$\boldsymbol{\Phi}_{x0}^{\mathbb{Q}} = \boldsymbol{\Phi}_{x0} + \gamma\boldsymbol{\Omega}_{xx}\mathbf{p}_x - \gamma\boldsymbol{\Sigma}_x\boldsymbol{\beta}_{x0}, \tag{A.59}$$

and solving for $\boldsymbol{\beta}_{x0}$

$$\boldsymbol{\beta}_{x0} = \frac{1}{\gamma}\boldsymbol{\Sigma}_x^{-1}(\boldsymbol{\Phi}_{x0} - \boldsymbol{\Phi}_{x0}^{\mathbb{Q}}) + \boldsymbol{\Sigma}_x'\mathbf{p}_x = \frac{1}{\gamma}\boldsymbol{\lambda}_{x0} + \boldsymbol{\Sigma}_x'\mathbf{p}_x. \tag{A.60}$$

B.5 Proof of Proposition 2

Define the across-maturity stacks

$$\mathbf{b}_x \equiv \begin{bmatrix} \mathbf{b}_x^{(1)\prime} \\ \vdots \\ \mathbf{b}_x^{(N-1)\prime} \end{bmatrix}, \quad \mathbf{s}_x \equiv \begin{bmatrix} \mathbf{s}_x^{(2)\prime} \\ \vdots \\ \mathbf{s}_x^{(N)\prime} \end{bmatrix}, \quad \mathbf{s}_{x0} \equiv \begin{bmatrix} s_{x0}^{(2)} \\ \vdots \\ s_{x0}^{(N)} \end{bmatrix}, \quad \boldsymbol{\omega} \equiv \begin{bmatrix} \boldsymbol{\omega}^{(2)\prime} \\ \vdots \\ \boldsymbol{\omega}^{(N)\prime} \end{bmatrix}, \tag{A.61}$$

each with $N-1$ rows, where $\mathbf{s}_x^{(n)}$ and $s_{x0}^{(n)}$ are the loading and intercept of the reduced-form supply $s_t^{(n)} = s_{x0}^{(n)} + \mathbf{s}_x^{(n)\prime}\mathbf{x}_t$. The matrix $\mathbf{B} = \sum_{n=2}^N \mathbf{b}_x^{(n-1)}\mathbf{b}_x^{(n-1)\prime}$ is then the Gram matrix $\mathbf{B} = \mathbf{b}_x'\mathbf{b}_x$, positive definite provided that $N-1 \geq M$ and the loadings $\left\{\mathbf{b}_x^{(n-1)}\right\}_{n=2}^N$ span $\mathbb{R}^M$, as discussed in Section 3. The risk-neutral mapping in equations (2.25) and (2.26) depends on the supply schedule only through the two aggregates $\mathbf{b}_x'\mathbf{s}_x = \sum_{j=2}^N \mathbf{b}_x^{(j-1)}\mathbf{s}_x^{(j)\prime}$ and $\mathbf{b}_x'\mathbf{s}_{x0} = \sum_{j=2}^N \mathbf{b}_x^{(j-1)}s_{x0}^{(j)}$:

$$\boldsymbol{\Phi}_{xx}^{\mathbb{Q}} = \boldsymbol{\Phi}_{xx} + \gamma\boldsymbol{\Omega}_{xx}\left(\mathbf{b}_x'\mathbf{s}_x\right), \qquad \boldsymbol{\Phi}_{x0}^{\mathbb{Q}} = \boldsymbol{\Phi}_{x0} + \gamma\boldsymbol{\Omega}_{xx}\left(\mathbf{p}_x + \mathbf{b}_x'\mathbf{s}_{x0}\right). \tag{A.62}$$

By equation (2.29), the associated prices of risk are $\boldsymbol{\lambda}_x = \boldsymbol{\Sigma}_x^{-1}(\boldsymbol{\Phi}_{xx} - \boldsymbol{\Phi}_{xx}^{\mathbb{Q}}) = -\gamma\boldsymbol{\Sigma}_x'(\mathbf{b}_x'\mathbf{s}_x)$ and $\boldsymbol{\lambda}_{x0} = \boldsymbol{\Sigma}_x^{-1}(\boldsymbol{\Phi}_{x0} - \boldsymbol{\Phi}_{x0}^{\mathbb{Q}}) = -\gamma\boldsymbol{\Sigma}_x'(\mathbf{p}_x + \mathbf{b}_x'\mathbf{s}_{x0})$, where the second equalities use equation (A.62) and $\boldsymbol{\Omega}_{xx} = \boldsymbol{\Sigma}_x\boldsymbol{\Sigma}_x'$.

Part (i): observational equivalence. Two affine supply schedules support the same equilibrium if and only if they imply the same aggregates $\mathbf{b}_x'\mathbf{s}_x$ and $\mathbf{b}_x'\mathbf{s}_{x0}$. Sufficiency follows from equation (A.62): equal aggregates yield the same $\mathbf{\Phi}_{xx}^{\mathbb{Q}}$ and $\mathbf{\Phi}_{x0}^{\mathbb{Q}}$, and the bond-price recursions, the real short-rate coefficients, and the prices of risk depend on the schedule only through them. For necessity, if two schedules $(\mathbf{s}_{A,x}, \mathbf{s}_{A,x0})$ and $(\mathbf{s}_{B,x}, \mathbf{s}_{B,x0})$ support the same equilibrium, the first equation in (A.62) gives $\gamma\mathbf{\Omega}_{xx}(\mathbf{b}_x'\mathbf{s}_{A,x}) = \mathbf{\Phi}_{xx}^{\mathbb{Q}} - \mathbf{\Phi}_{xx} = \gamma\mathbf{\Omega}_{xx}(\mathbf{b}_x'\mathbf{s}_{B,x})$, and since $\gamma > 0$ and $\mathbf{\Omega}_{xx}$ is non-singular, $\mathbf{b}_x'\mathbf{s}_{A,x} = \mathbf{b}_x'\mathbf{s}_{B,x}$. The second equation delivers $\mathbf{b}_x'\mathbf{s}_{A,x0} = \mathbf{b}_x'\mathbf{s}_{B,x0}$. Because $-\gamma\mathbf{\Sigma}_x'$ is invertible, equality of these aggregates is equivalent to equality of the prices of risk $\boldsymbol{\lambda}_x$ and $\boldsymbol{\lambda}_{x0}$.

Part (ii): unique factor-mimicking representative. Stacking the factor-mimicking weights $\boldsymbol{\omega}^{(n)} = -\mathbf{\Sigma}_x^{-1}\mathbf{B}^{-1}\mathbf{b}_x^{(n-1)}$ of equation (3.5) and using the symmetry of $\mathbf{B}$, we have that

$$\boldsymbol{\omega} = -\mathbf{b}_x\mathbf{B}^{-1}\left(\mathbf{\Sigma}_x'\right)^{-1}, \qquad \text{so that} \qquad \mathbf{b}_x'\boldsymbol{\omega} = -\left(\mathbf{\Sigma}_x'\right)^{-1}, \tag{A.63}$$

the second equality being equation (A.56) after premultiplication by $\mathbf{\Omega}_{xx}^{-1}$. A factor-mimicking schedule satisfies both equation (3.7) and the risk-free asset weight $s_{\beta 0}^{(n)} = 0$ of equation (3.8), so that its loadings are $\boldsymbol{\beta}_x'\boldsymbol{\omega}^{(n)}$, that is, $\boldsymbol{\omega}\boldsymbol{\beta}_x$ in stacked form, and its aggregate is $\mathbf{b}_x'\boldsymbol{\omega}\boldsymbol{\beta}_x = -(\mathbf{\Sigma}_x')^{-1}\boldsymbol{\beta}_x$. Matching the aggregate that identifies the equivalence class in part (i) pins the coordinate uniquely,

$$-\left(\mathbf{\Sigma}_x'\right)^{-1}\boldsymbol{\beta}_x = \mathbf{b}_x'\mathbf{s}_x \quad \Longleftrightarrow \quad \boldsymbol{\beta}_x = -\mathbf{\Sigma}_x'\left(\mathbf{b}_x'\mathbf{s}_x\right) = \tfrac{1}{\gamma}\boldsymbol{\lambda}_x, \tag{A.64}$$

and, using the risk-free asset weight, the representative's intercept is $s_{x0}^{(n)} = \boldsymbol{\omega}^{(n)\prime}\boldsymbol{\beta}_{x0}$, so that matching the corresponding aggregate pins the constant, $\boldsymbol{\beta}_{x0} = -\mathbf{\Sigma}_x'(\mathbf{b}_x'\mathbf{s}_{x0}) = \frac{1}{\gamma}\boldsymbol{\lambda}_{x0} + \mathbf{\Sigma}_x'\mathbf{p}_x$. Each equivalence class therefore contains exactly one factor-mimicking schedule, and its coordinates coincide with the recovery formulas of Proposition 1; recovering the supply factors and selecting the canonical representative are the same operation.

Part (iii): projection form. Substituting equation (A.64) into the representative's loadings $\boldsymbol{\omega\beta}_x$ and using equation (A.63),

$$\boldsymbol{\omega\beta}_x = -\mathbf{b}_x\mathbf{B}^{-1}\left(\boldsymbol{\Sigma}_x'\right)^{-1}\left[-\boldsymbol{\Sigma}_x'\left(\mathbf{b}_x'\mathbf{s}_x\right)\right] = \mathbf{b}_x\mathbf{B}^{-1}\mathbf{b}_x'\mathbf{s}_x, \tag{A.65}$$

and likewise $\boldsymbol{\omega\beta}_{x0} = \mathbf{b}_x\mathbf{B}^{-1}\mathbf{b}_x'\mathbf{s}_{x0}$. The matrix $\mathbf{b}_x\mathbf{B}^{-1}\mathbf{b}_x' = \mathbf{b}_x(\mathbf{b}_x'\mathbf{b}_x)^{-1}\mathbf{b}_x'$ is the orthogonal projector onto the column span of $\mathbf{b}_x$, so the representative is the projection of any class member onto that span. The residual $\mathbf{s}_x^{\perp} = \mathbf{s}_x - \boldsymbol{\omega\beta}_x$ satisfies $\mathbf{b}_x'\mathbf{s}_x^{\perp} = \mathbf{b}_x'\mathbf{s}_x - \mathbf{B}\mathbf{B}^{-1}(\mathbf{b}_x'\mathbf{s}_x) = \mathbf{0}$, so it leaves the aggregates in equation (A.62) unchanged, and with them the prices of risk and every bond price. It does change the quantities of bonds that arbitrageurs hold, and it is not identified from yields.

B.6 Proof of Proposition 3

To consider the effects of an unanticipated change $\Delta s_{x0}^{(n)}$ in the intercept of the supply of the nominal n-period bond available to the arbitrageur, as given in equation (5.1), we start by conjecturing that the real short-term rate and the nominal bond prices are affine in the pricing factors $\mathbf{x}_t$ and the term $\Delta\overline{\beta}\phi_\beta^t$:

$$r_t = \rho_{x0} + \boldsymbol{\rho}_x'\mathbf{x}_t + \rho_\beta\Delta\overline{\beta}\phi_\beta^t, \tag{A.66}$$

$$b_t^{(n)} = -b_{x0}^{(n)} - \mathbf{b}_x^{(n)\prime}\mathbf{x}_t - b_\beta^{(n)}\Delta\overline{\beta}\phi_\beta^t, \qquad \text{for } n = 1, \ldots, N. \tag{A.67}$$

Following a similar approach to that in the proof of Theorem 1 above, we find that the coefficients for the real short-term rate and nominal bond prices for the constant and $\mathbf{x}_t$ remain unchanged with respect to the general case, while the nominal bond price coefficients for the QE factor satisfy:

$$b_\beta^{(n)} = b_\beta^{(n-1)}\phi_\beta + \rho_\beta + \gamma\left[\mathbf{b}_x^{(n-1)} + \mathbf{p}_x\right]'\boldsymbol{\Omega}_{xx}\sum_{j=1}^{N}\left[\mathbf{b}_x^{(j-1)} + \mathbf{p}_x\right]s_\beta^{(j)}. \tag{A.68}$$

Note that $b_\beta^{(1)} = 0$, since the central bank controls the supply of short-term nominal bonds so that the nominal short-term interest rate remains consistent with equation (2.4), which does not depend on the QE factor. Evaluating equation (A.68) at $n = 1$, and using the initial conditions $b_\beta^{(0)} = 0$ and $\mathbf{b}_x^{(0)} = \mathbf{0}$, we have that

$$\rho_\beta = -\gamma \mathbf{p}_x' \mathbf{\Omega}_{xx} \sum_{j=1}^{N} \left[\mathbf{b}_x^{(j-1)} + \mathbf{p}_x \right] s_\beta^{(j)}, \tag{A.69}$$

which, once we substitute this expression for ρ_β into equation (A.68) delivers equation (5.3) in the main text.

C Estimation details

We now provide additional details on the estimation of the GDTSM underlying our analysis. Specifically, for the purpose of estimating the model, it is particularly useful to resort to its state-space representation of the observed variables (i.e., the nominal bond yields and inflation).

In a general state-space representation, there is a transition equation that describes the dynamic evolution of the state factors over time and a measurement equation that relates the observed data to the state factor. In our case, the VAR dynamics in (2.1) can be interpreted as the transition equation, while the processes for inflation and output growth in equations (2.2) and (2.3), respectively, and the conjecture for the bond yields in equation (2.10) are the measurement equations linking the observed data to the underlying state factor.

Let us denote $\widetilde{y}_t^{(n)}$, $\widetilde{\pi}_t$, and $\widetilde{g}_t$ as the observed yields, observed inflation, and observed output growth, respectively, and which we assume are all subject to measurement error. The vector $\mathbf{y}_t = \left[y_t^{(1)}, ... y_t^{(N)} \right]'$, on the other hand, comprises the model-implied yields that stack the affine mapping in equation (2.10) for the maturities used in the estimation of the model. Correspondingly, $\widetilde{\mathbf{y}}_t$ represents the vector of observed yields. Let $\mathbf{u}_{y,t}$ be a zero-mean, normally distributed bond yield measurement error that is iid across time, independent of the innovations to the pricing factor, $\boldsymbol{\varepsilon}_{x,t}$, and that has a covariance matrix $\mathbf{\Sigma}_{u_y u_y}$. Additionally, we assume that $u_{\pi,t}$ and $u_{g,t}$, the inflation and growth measurement errors, respectively, are both normally distributed and *iid* across time, independent of the bond yield measurement errors, the innovations to the pricing factors and from each other. Let the variances of $u_{\pi,t}$ and $u_{g,t}$ be denoted by $\sigma^2_{u_\pi}$ and $\sigma^2_{u_g}$, respectively.

Given this notation, the measurement equations of the state-space representation of the canonical GDTSM proposed by JSZ satisfy:

$$\widetilde{\pi}_t = p_{z0} + \mathbf{p}_z'\mathbf{z}_t + u_{\pi,t}, \tag{A.1}$$

$$\widetilde{g}_t = g_{z0} + \mathbf{g}_z'\mathbf{z}_t + u_{g,t}, \tag{A.2}$$

$$\widetilde{\mathbf{y}}_t = \mathbf{a}_{z0} + \mathbf{a}_z\mathbf{z}_t + \mathbf{u}_{y,t}, \tag{A.3}$$

where, given the canonical representation of our GDTSM adopted in the paper, $\mathbf{a}_z$ is a nonlinear function of $\boldsymbol{\phi}^{\mathbb{Q}}_{zz}$ (the eigenvalues of $\boldsymbol{\Phi}^{\mathbb{Q}}_{zz}$), and $\mathbf{a}_{z0}$ is a nonlinear function of $k^{\mathbb{Q}\$}_{\infty}$, $\boldsymbol{\phi}^{\mathbb{Q}}_{zz}$, and $\boldsymbol{\Omega}_{zz}$. The transition equation is, on the other hand, given by

$$\mathbf{z}_{t+1} = \boldsymbol{\Phi}_{z0} + \boldsymbol{\Phi}_{zz}\mathbf{z}_t + \boldsymbol{\varepsilon}_{z,t+1}, \tag{A.4}$$

where $\boldsymbol{\varepsilon}_{z,t+1} \sim iid\, N(0, \boldsymbol{\Omega}_{zz})$.

Given the latent nature of the pricing factors, estimation could, in principle, be achieved via Kalman filtering. Instead, we follow JSZ in (i) working with bond state variables that are linear combinations (i.e., portfolios) of the yields themselves, $\mathbf{x}_t = \mathbf{W}'\widetilde{\mathbf{y}}_t$, where $\mathbf{W}$ is a full-rank matrix of weights, and in (ii) further assuming that $\mathbf{x}_t$ is observed perfectly, i.e., $\mathbf{W}'\mathbf{u}_{y,t} = \mathbf{0}$.

These assumptions allow us to rotate our set of latent factors, $\mathbf{x}_t$, into a set of observed factors and, in turn, factorize the joint likelihood function of the observed variables into the marginal component of the (observed) linear combination of yields, $\mathbf{x}_t$, and the conditional components corresponding to all the individual yields and inflation, given $\mathbf{x}_t$. Specifically, we have that the vector of observable pricing factors, $\mathbf{x}_t$, is simply an affine (invariant) transformation of the original latent factors, $\mathbf{z}_t$:

$$\mathbf{x}_t = \mathbf{W}'\widetilde{\mathbf{y}}_t = \mathbf{W}'\mathbf{a}_{z0} + (\mathbf{W}'\mathbf{a}_z)\mathbf{z}_t + \mathbf{W}'\mathbf{u}_{y,t} = \mathbf{c} + \mathbf{D}\mathbf{z}_t, \tag{A.5}$$

where $\mathbf{c} = \mathbf{W}'\mathbf{a}_{z0}$ and $\mathbf{D} = \mathbf{W}'\mathbf{a}_z$.

Consequently, by applying the properties of affine transformations for GDTSMs (see appendix A) we have that JSZ canonical representation can be recast as the following alternative state-space model with measurement equations given by

$$\widetilde{\pi}_t = p_{x0} + \mathbf{p}_x'\mathbf{x}_t + u_{\pi,t}, \tag{A.6}$$

$$\widetilde{g}_t = g_{x0} + \mathbf{g}_x'\mathbf{x}_t + u_{g,t}, \tag{A.7}$$

$$\mathbf{x}_t^{\perp} = \mathbf{a}_{x0}^{\perp} + \mathbf{a}_x^{\perp}\mathbf{x}_t + \mathbf{W}_{\perp}'\mathbf{u}_{y,t}, \tag{A.8}$$

and transition equation given by:

$$\mathbf{x}_{t+1} = \mathbf{\Phi}_{x0} + \mathbf{\Phi}_{xx}\mathbf{x}_t + \boldsymbol{\varepsilon}_{x,t+1}, \tag{A.9}$$

where $\mathbf{x}_t^{\perp} = \mathbf{W}_{\perp}'\widetilde{\mathbf{y}}_t$, $\mathbf{W}_{\perp}'$ is a basis for the orthogonal component of the row span of $\mathbf{W}'$, $\boldsymbol{\varepsilon}_{x,t+1} \sim iid\, N(0, \mathbf{\Omega}_{xx})$, and:

$$\mathbf{p}_x' = \mathbf{p}_z'\mathbf{D}^{-1}, \qquad p_{x0} = p_{z0} - \mathbf{p}_x'\mathbf{c}, \tag{A.10}$$

$$\mathbf{g}_x' = \mathbf{g}_z'\mathbf{D}^{-1}, \qquad g_{x0} = g_{z0} - \mathbf{g}_x'\mathbf{c}, \tag{A.11}$$

$$\mathbf{\Phi}_{xx} = \mathbf{D}\mathbf{\Phi}_{zz}\mathbf{D}^{-1}, \qquad \mathbf{\Phi}_{x0} = (\mathbf{I} - \mathbf{\Phi}_{xx})\mathbf{c} + \mathbf{D}\mathbf{\Phi}_{z0}, \tag{A.12}$$

$$\mathbf{\Omega}_{xx} = \mathbf{D}\mathbf{\Omega}_{zz}\mathbf{D}', \tag{A.13}$$

$$\mathbf{a}_x^{\perp} = \mathbf{W}_{\perp}'\mathbf{a}_z\mathbf{D}^{-1}, \qquad \mathbf{a}_{x0}^{\perp} = \mathbf{W}_{\perp}'\left(\mathbf{a}_{z0} - \mathbf{a}_z\mathbf{D}^{-1}\mathbf{c}\right). \tag{A.14}$$

Note that focusing on $\mathbf{x}_t^{\perp} = \mathbf{W}_{\perp}'\widetilde{\mathbf{y}}_t$ in the measurement equation of this (rotated) model eliminates the redundant measurement equations for $\mathbf{x}_t$, given that these are perfectly observed.

Importantly, and despite this rotation into observable pricing factors, $\mathbf{a}_x^{\perp}$ remains a nonlinear function of $\boldsymbol{\phi}_{zz}^{\mathbb{Q}}$ only, while $\mathbf{a}_{x0}^{\perp}$ is a nonlinear function of $k_{\infty}^{\mathbb{Q}\$}$, $\boldsymbol{\phi}_{zz}^{\mathbb{Q}}$, and $\boldsymbol{\Omega}_{zz}$. On the other hand, neither the inflation coefficients, p_{x0} and $\mathbf{p}_x'$, the output growth coefficients, g_{x0} and $\mathbf{g}_x'$, nor the coefficients of the conditional mean of the (observable) factors, $\boldsymbol{\Phi}_{x0}$ and $\boldsymbol{\Phi}_{xx}$, enter into the functional forms of the cross-sectional bond yield parameters.

This separation between cross-sectional and physical dynamics combined with the assumption that the VAR dynamics remain unrestricted allows us to adapt JSZ's proposed two-step maximum likelihood estimator to our case. In the first step, we estimate p_{x0}, $\mathbf{p}_x$, g_{x0}, and $\mathbf{g}_x$ via ordinary least squares (OLS) regressions of the observed inflation and output growth on a constant and $\mathbf{x}_t$. This approach recovers the ML estimates of these parameters given our assumption that $u_{\pi,t}$ and $u_{g,t}$ are normally distributed, iid across time, independent of the bond yield measurement errors, the innovations to the pricing factors, and independent of each other. Moreover, and similarly to JSZ, we recover the estimates of $\boldsymbol{\Phi}_{x0}$ and $\boldsymbol{\Phi}_{xx}$ by OLS given that, since the VAR dynamics are unrestricted, OLS recovers the ML estimates of the conditional mean parameters (Zellner, 1962).

In the second step, we estimate the remaining parameters of the model ($k_{\infty}^{\mathbb{Q}\$}$, $\boldsymbol{\phi}_{zz}^{\mathbb{Q}}$, and $\boldsymbol{\Omega}_{xx}$) via numerical maximization of the likelihood function taking as given the estimates obtained in the first step.[26] Finally, we note that we use this estimate of $\boldsymbol{\Omega}_{xx}$ to obtain an estimate of $\boldsymbol{\Sigma}_x$, while the latent-factor covariance is the derived object, recovered as $\hat{\boldsymbol{\Omega}}_{zz} = \hat{\mathbf{D}}^{-1}\hat{\boldsymbol{\Omega}}_{xx}(\hat{\mathbf{D}}')^{-1}$.

In order to satisfy the identification restriction of Hamilton and Wu (2012b) that the real eigenvalues be ordered, we assume that the eigenvalues of $\boldsymbol{\Phi}_{zz}^{\mathbb{Q}}$ collected in $\boldsymbol{\phi}_{zz}^{\mathbb{Q}}$ follow a

[26] We further assume that $\boldsymbol{\Sigma}_{u_y u_y} = \sigma_{u_y}^2 \times \mathbf{W}_{\perp}\mathbf{W}_{\perp}'$. This guarantees that $\mathbf{W}'\boldsymbol{\Sigma}_{u_y u_y}\mathbf{W} = \mathbf{0}$ and allows us to concentrate $\sigma_{u_y}^2$ from the likelihood function through $\hat{\sigma}_{u_y}^2 = \sum_{t=1}^{T}\sum_n \left[\widetilde{y}_t^{(n)} - y_t^{(n)}\right]^2 / (T \times (\widetilde{N} - M))$ where T is the length of the sample, $\widetilde{N}$ the number of observed yields, and M is the number of factors.

power-law relation,

$$\phi^{\mathbb{Q}}_{zz,i} = \overline{\phi}^{\mathbb{Q}}_{zz}\,\varphi^{\,i-1}, \qquad i = 1, \ldots, M, \tag{A.15}$$

where $\overline{\phi}^{\mathbb{Q}}_{zz}$ is the largest eigenvalue of $\mathbf{\Phi}^{\mathbb{Q}}_{zz}$ and the power-scaling coefficient $0 < \varphi < 1$ controls the spacing between eigenvalues (see Calvet, Fisher, and Wu, 2018, for an application of power-law structures to term-structure modelling). Since $0 < \varphi < 1$, this relation orders the eigenvalues by construction and reduces the M risk-neutral eigenvalues to the two parameters $(\overline{\phi}^{\mathbb{Q}}_{zz}, \varphi)$; the eigenvalues and standard errors reported in panel b of Table 1 are the corresponding delta-method transforms. Because higher-order eigenvalues are difficult to estimate precisely, the power-law structure improves the robustness of the estimation while still fitting the cross-section with an RMSPE below ten basis points; this benefit becomes especially valuable in specifications with more than two factors.

Standard errors for all estimated and derived quantities are obtained by the delta method from the inverse of the observed information matrix of the full joint likelihood of yields, inflation, and output growth, evaluated at the two-step estimates, which coincide with the joint maximum-likelihood estimates given the separation result, treating the portfolio-weight matrix $\mathbf{W}$ as fixed.